Sec 1

THE SPECTRUM OF CYCLOPENTANONE

THE SPECTRUM OF
CYCLOPENTANONE

By

HELEN ELAINE HOWARD-LOCK, B.Sc.

A Thesis
Submitted to the Faculty of Graduate Studies
in Partial Fulfilment of the Requirements
for the Degree
Doctor of Philosophy

McMaster University
September, 1968

DOCTOR OF PHILOSOPHY (1968)
(Chemical Physics)

McMaster University
Hamilton, Ontario

TITLE; The Spectrum of Cyclopentanone

AUTHOR: Helen Elaine Howard-Lock; B.Sc. (McMaster University)

SUPERVISOR; Dr. Gerald W. King

NUMBER OF PAGES: (xiii), 223

SCOPE AND CONTENTS:

The infrared, Raman and ultraviolet spectra of cyclopentanone, cyclopentanone -$\alpha,\alpha,\alpha',\alpha'$-$d_4$ and cyclopentanone-d_8 have been studied. The high resolution ultraviolet absorption spectra of the three isotopic species have been analysed in detail. The electronic transition has been identified as a singlet-singlet transition associated with $\underline{n}\rightarrow\pi^*$ orbital electron promotion. The vibrational and rotational structures accompanying this electronic transition have been analysed and the results are in agreement with theoretical predictions. The geometry of the molecule in both ground and excited states has been calculated. In the excited state conformation, the oxygen atom is bent out of the plane of the three adjacent carbon atoms; there is a potential barrier of 705 cm^{-1} with respect to the oxygen out-of-plane bending vibration in the upper state.

to all the members of my family, both
near and far, whose love and self-sacrifice
have made this work possible

" ... dream of things that have not been done,
and say, why not."

quoted by Senator Robert F. Kennedy
June 5, 1968

"Now, no scientist has ever seen an electron.
'Electron' is simply the name for a consistent
set of things that happen in certain circumstances."

Warren Weaver
in "Can a Scientist Believe in God?",
Reader's Digest, May, 1968.

ACKNOWLEDGEMENTS

I wish to thank my supervisor, Dr. Gerald W. King, for providing me with the opportunity of working in his research group, and for his continuing advice and encouragement during this work.

I thank the following persons: my research colleagues, Dr. W. J. Balfour, Mr. E. J. Finn, Dr. J. L. Hencher, Dr. V. A. Job, Mr. K. G. Kidd, Mr. J. O. P. McBride, Mr. R. McLean, Dr. E. H. Pinnington, Dr. A. W. Richardson, Mr. S. P. So, K. I. Srikameswaran, Dr. J. Tyrrel and Mr. C. H. Warren for stimulating discussions and experimental assistance; Dr. D. C. Moule, for many valuable suggestions; Mr. John Bradford, for valuable technical assistance, Dr. R. F. W. Bader, Dr. I. D. Brown, Dr. C. Calvo, Dr. M. Ingleby, Dr. C. J. L. Lock, Mrs. E. Marseglia, Dr. D. B. MacLean, Dr. J. J. McCullough and Dr. C. V. Stager, for advice and helpful discussions.

I am grateful to Mrs. R. Foster for her skillful typing of this manuscript.

Finally, I wish to acknowledge generous financial assistance from the National Research Council of Canada (1964-1968).

TABLE OF CONTENTS

LIST OF TABLES

LIST OF ILLUSTRATIONS

CHAPTER 1

INTRODUCTION

1.1 Theory

The total internal energy of an isolated molecule is conserved. A stationary state of the molecule, of energy E, may be represented by a wave function ψ, which is an eigenfunction of the time-independent wave equation:

$$H\psi = E\psi \tag{1.1}$$

In equation (1.1), H is the quantum mechanical Hamiltonian operator which, if electronic and nuclear spin terms are excluded, can be written as the sum of kinetic and potential energy operators for the nuclei and electrons:

$$H = -\sum_{\alpha} \frac{\hbar^2}{2M_{\alpha}} \nabla_{\alpha}^2 - \sum_{i} \frac{\hbar^2}{2m} \nabla_{i}^2 + V_{NN} + V_{NE} + V_{EE} \tag{1.2}$$

The first term on the right is the kinetic energy operator for the nuclei (mass M_{α}), the second term is the kinetic energy operator of the electrons (mass m) and the remaining terms V_{NN}, V_{NE} and V_{EE} represent the potential energy operators for the electrostatic interactions between all pairs of particles (nuclei, N and electrons, E).

The complete quantum mechanical Hamiltonian operator for a molecule is too complex for solution of equation (1.1). Born and Oppenheimer[1] have shown that the motions of a molecule can be separated into three types -- electronic, vibrational, and rotational. By expanding the Hamiltonian in a power series[a] in terms of a parameter, κ, and solving the wave equation by the methods of perturbation theory, these authors showed that the energies E_{el}, E_v and E_r corresponding to the three types of motion have different magnitudes[b], given by

$$E_r \simeq \kappa^2 E_v \simeq \kappa^4 E_{el} \qquad (1.3)$$

In the classical description, the nuclei, because of their heavier mass, move much more slowly than the electrons. The nuclei may be treated as fixed for the purpose of calculating the energies of the electrons. In quantum mechanics, the separation of the electron and nuclear motions implies that the wave functions may be written in the product form

$$\psi = \psi_{el}\ \psi_n \qquad (1.4)$$

The product wavefunction[c] represents a good approximation to an eigenfunction of H . If the first term in the Hamiltonian of equation (1.2) is set equal to zero, the energy of the electrons for a given fixed set of nuclear positions can be obtained by solving the wave equation:

---

[a] The method has been discussed by many authors; for example, Liehr[2], Messiah[3], p. 783, and Tinkham[4], pp. 210-213.

[b] κ is $(m/M)^{\frac{1}{4}}$ where m is the mass of the electron and M is the average nuclear mass; κ is typically of the order 0.1.

[c] This is commonly known as the zero-order Born-Oppenheimer approximation to the eigenfunction. See, for example, King[5], pp. 113-115, Herzberg[6], p. 148 and Herzberg[7], p. 129.

$$[- \sum_i \frac{\hbar^2}{2m} \nabla_i^2 + V_{NN} + V_{NE} + V_{EE}]\psi_{el} = E\psi_{el} \qquad (1.5)$$

In equation (1.5), the wave function ψ_{el} depends only on the coordinates associated with the electrons. The coordinates of the nuclei came into the wave function as parameters because of the term V_{NE}. The term V_{NN}, which represents the electrostatic repulsion between a pair of nuclei, does not affect ψ_{el} but adds directly to the eigenvalue, so that

$$E_{el} = E - V_{NN} \qquad (1.6)$$

Equation (1.5) then becomes

$$[- \sum_i \frac{\hbar^2}{2m} \nabla_i^2 + V_{NE} + V_{EE}]\psi_{el} = E_{el}\psi_{el} \qquad (1.7)$$

where the eigenvalues E_{el} are the energies of different electronic states.

ψ_n of equation (1.4) is a solution of

$$[- \sum_\alpha \frac{\hbar^2}{2M_\alpha} \nabla_\alpha^2 + V_{NN}]\psi_n = [E - E_{el}]\psi_n \qquad (1.8)$$

This is the wave equation for the nuclei moving in the potential field $E_{el} + V_{NN}$. The minimum value of $E_{el} + V_{NN}$ for a given stable electronic state is defined as the electronic energy, E_e of the state. The vibrational levels have energy E_v relative to E_e.

Classically, because of the large difference in the frequencies of vibrational and rotational motions, these motions may be treated independently of each other. In quantum mechanics, the nuclear wave function may be written

$$\psi_n = \psi_v \psi_r \tag{1.9}$$

In each vibrational level of each electronic state the molecule may be regarded as rotating with a moment of inertia given by an average geometrical configuration. As a first approximation, the molecule is treated as a rigid body for the interpretation of the rotational levels. As a result of the separation of the wave function ψ into a product of components $\psi_{el}\psi_v\psi_r$, the total internal energy of the molecule is given by the sum of components

$$E = E_e + E_v + E_r \tag{1.10}$$

1.2 Spectroscopic Transitions

The electronic, vibrational and rotational energies can assume only certain values -- the eigenvalues of the corresponding wave equations. A transition from one discrete state to another in a molecule is accomplished by absorption or emission of radiation; that is, the energy content of one molecule is changed by exactly the energy of one photon, (absorbed or emitted). The relationship between the energy of a photon (in ergs), its wavelength (λ in cm.) and its frequency (ν' in sec^{-1}), is given by

$$E = h\nu' = \frac{hc}{\lambda} \tag{1.11}$$

where h is Planck's constant and c is the velocity of light in vacuum. Another quantity, the wave number, is more generally used in spectroscopy as a measure of energy. The wavenumber, ν, is the reciprocal of the vacuum wavelength of the photon and is commonly quoted in reciprocal centimetres:

$$\nu = \frac{1}{\lambda_{vac}} \, (\mathrm{cm}^{-1}) \tag{1.12}$$

Conversion to other units[d] gives:

$$1\,\mathrm{ev} = 8065.8\ \mathrm{cm}^{-1} = 1.6021\ 10^{-12}\,\mathrm{ergs\ molecule}^{-1} = 23.06\ \mathrm{kcal\ mole}^{-1}.$$

Thermal energy may be related to temperature by means of the Boltzmann constant; that is, $E_{thermal} = kT$. At 300^{o}K, $kT = 208.5\ \mathrm{cm}^{-1} = 0.0259\ \mathrm{ev} = 0.596\ \mathrm{kcal\ mole}^{-1}$.

Transitions between the rotational energy states associated with one vibrational state (usually the lowest vibrational level of the electronic ground state) produce spectra in the microwave region (0.1 - 10 cm^{-1}). From the frequencies of the rotational spectrum, the three moments of inertia of a molecule, I_a, I_b, and I_c, about three mutually perpendicular axes a, b and c can be determined. The geometrical parameters of a model (representing the molecule) can be varied until the calculated moments of inertia agree with the values found from the spectra, and so the geometrical structure of the molecule can be determined. If there are more than three molecular parameters, the microwave spectra of isotopically substituted species of the molecule provides additional information -- three moments of inertia per species.

Transitions between different vibrational states of the ground (lowest) electronic state produce spectra in the region 100-4000 cm^{-1}

---

[d] Values of the fundamental constants from reference (8).

which are observed by infrared and Raman spectroscopy. From these spectra the fundamental frequencies of vibration in the ground electronic state can be obtained. Each vibrational transition is accompanied by changes in rotational energies so that the vibrational bands which are observed have rotational fine structure. Sometimes molecular structures for each vibrational level can be calculated from the moments of inertia if the rotational fine structure is resolved. In large molecules, with large moments of inertia, the rotational fine structure is seldom resolved, since the spacing of the rotational lines depends inversely on the moments of inertia. Often qualitative predictions about the equilibrium molecular geometry can be made directly from the vibrational spectrum, since which transitions are allowed, and the rotational contours of the resulting bands, depend on the symmetry of the molecule.

Transitions between different electronic states usually give rise to spectra in the visible or ultraviolet regions (10,000 - 100,000 cm^{-1}). In general, an electronic transition is composed of vibrational bands, each band accompanied by rotational fine structure. From vibrational analysis of the electronic band spectrum, the fundamental frequencies of the molecule in the electronically excited state can be obtained; from rotational analysis, accurate molecular dimensions can be determined.

At normal temperatures ($\sim$ 300^{o}K) most molecules are in the electronic ground state, and in electronic absorption spectra, transitions occur from the ground state to an excited state. Since the electronic spectrum depends on both the ground and excited states, knowledge of the structure of the molecule in the ground state, and the related vibrational frequencies, is helpful in the analysis of the electronic spectrum. This knowledge is obtained from microwave, infrared and Raman spectral studies.

Although the energy difference between any pair of states can be calculated, the spectroscopic transition between the states cannot always be observed. The probability of an electric dipole transition between an upper state represented by a wave function ψ' and a lower state represented by a wavefunction ψ'' is proportional to the square of the transition moment, R. R is given by the equation

$$R = \int \psi'^{*} \mu \ \psi'' \, d\tau \qquad (1.13)$$

where μ is the electric dipole operator and $d\tau$ is an element of the coordinate space of which ψ is a function. The probabilities of magnetic dipole and electric quadruple transitions may be calculated from similar expressions, but they are usually much smaller ($\sim 10^{-5}$ and 10^{-7} of the electric dipole transition probability, respectively), and they will be ignored in this work. Restrictions on the value of R are imposed by symmetry, and the application of group theory makes it possible to predict which transitions are allowed.

1.3 Previous Spectroscopic and Structural Studies of Cyclopentanone

In this section and the following one, certain papers will be mentioned only briefly in order that the bibliography be complete. The significant results which are not reviewed here will be discussed in later chapters.

The microwave spectrum of cyclopentanone has been investigated several times[9-12] and the principal moments of inertia, I_a, I_b and I_c have been determined. The dipole moment has been measured.[12] The rotational constants found by different workers are in good agreement. The results are collected in Table 1.1.

The inertial defect, $\Delta = I_C - I_A - I_B$ is a measure of the deviation from planarity of the molecule. According to Erlandsson, the value of $\Delta = 17.47$ amu - Å^2 for cyclopentanone is too large to be caused by the hydrogen atoms alone; they may be expected to contribute $\sim$ 12 amu - Å^2. Puckering of the carbon ring is therefore postulated. The conformation of the ring and the magnitude of puckering cannot be determined from these results alone. Erlandsson[11] was able to give some indication of the molecular geometry by assuming that the ring was planar and regularly pentagonal. His molecular parameters are shown in Figure 1.1 (a).

The ground state geometry of cyclopentanone calculated in the present study is shown in Figure 1.2. The calculations will be discussed in detail in Chapter 6.

The infrared and Raman spectra of cyclopentanone[e] have received considerable attention from previous workers.[13-25] Two studies of CPD4[16,17] have been made, but the spectra of CPD8 have not been studied previously. Despite the extensive work, there has been neither a complete assignment of the fundamental frequencies of vibration, nor normal coordinate analysis.

No determination of the structure of cyclopentanone by electron diffraction or by x-ray diffraction has been reported.

---

[e] Normal cyclopentanone will be referred to throughout the text of this thesis as CPH8. The deuterated derivatives, cyclopentanone -$\alpha,\alpha,\alpha',\alpha'$-$d_4$ and cyclopentanone - d_8 will be called CPD4 and CPD8, respectively.

TABLE 1.1

MICROWAVE DATA FOR CYCLOPENTANONE[†]

Reference	(9)	(10)	(11)	(12)
I_A	76.361	76.3354	76.369	-
I_B	150.837	150.7908	150.85	-
I_C	209.73	209.7114	209.75	-
A	0.22063	0.220715	0.22063	0.220814
B	0.11169	0.1117331	0.11169	0.111723
C	0.08033	0.0803406	0.08033	0.080312
κ	-0.5529	-0.5527298	-0.5529	-0.55325
Δ	17.47	17.4148	17.47	-
μ				3.30 ± .10

[†] I_A, I_B, I_C and Δ in units of amu - $\mathring{A}^2$; A, B, and C in units of cm^{-1}; κ is dimensionless; μ, the dipole moment, is in Debyes.

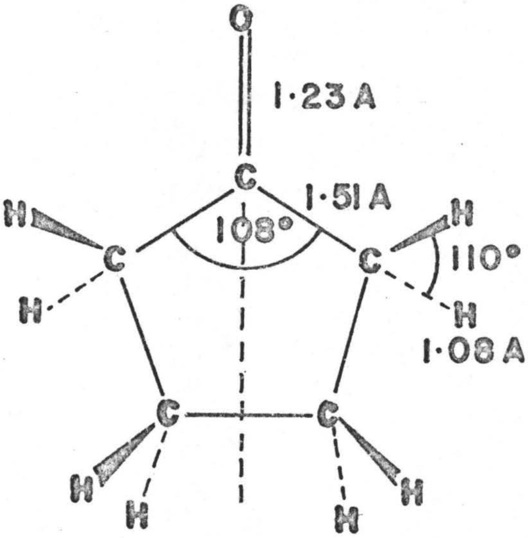

FIGURE 1·1(a) Erlandsson's(11) Parameters for Cyclopentanone.

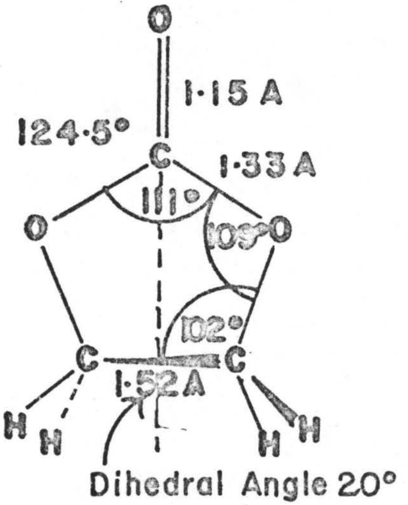

FIGURE 1·1(b) Structure of Ethylene Carbonate.(39)

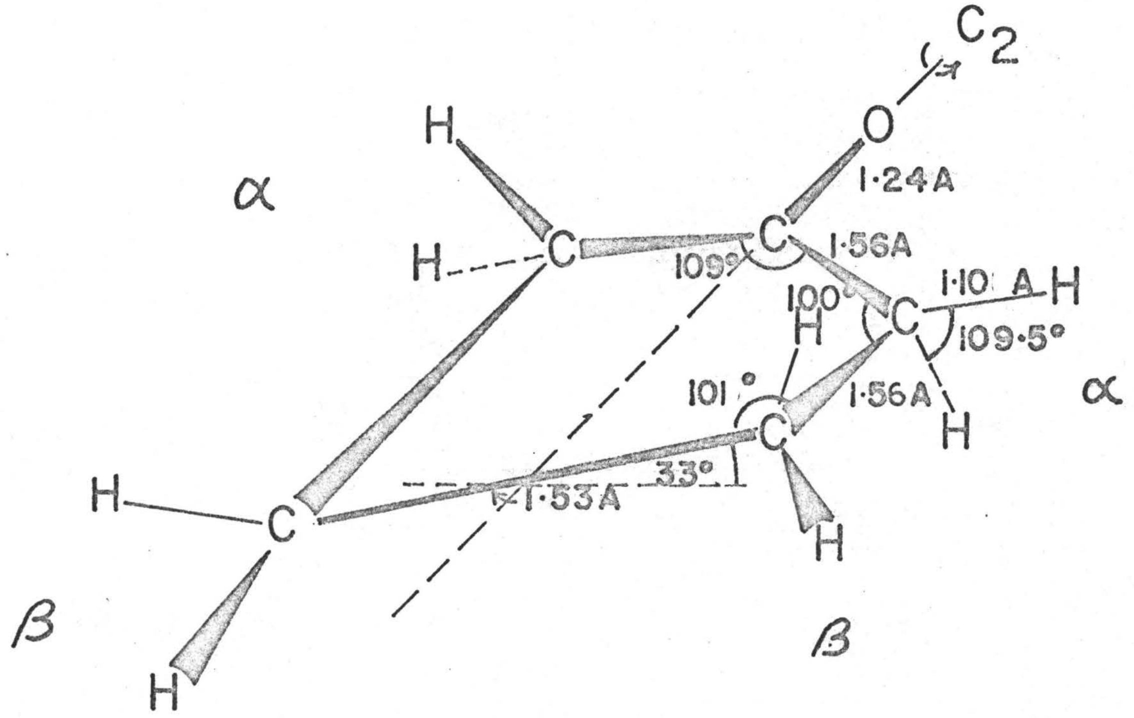

FIGURE 1·2 Ground State Geometry of Cyclopentanone. (This Work)

The photochemistry of cyclic ketones has been reviewed by Srinivasan.[26] The vapour phase photolysis of CPH8[27,28] and CPD8[28] has been investigated at 3130Å and 2537Å under various pressures and exposure times. Energy transfer processes have been studied in the benzene photosensitization of CPH8 and cyclopentanone - 2 - t.[29] The photolysis products are carbon monoxide, cyclobutane and 4-pentenal. The rearrangement of cyclopentanone into 4-pentenal occurs when a β-hydrogen atom moves to the carbon atom at the carbonyl group, and at the same time a carbon-carbon bond adjacent to the carbonyl group breaks.[26]

The nuclear magnetic resonance of CPH8 has been measured by several authors.[30-33] The results are inconclusive as to the conformation of the molecule.

Fluorescence and phosphorescence emission from cyclopentanone have been observed for liquid and solid solutions.[34] The fluorescence maximum was found at 4000 - 4100Å, the phosphorescence maximum at 4400 - 4500Å. For the gas phase only fluorescence was observed; the band was identical to that observed for the solution. (see Figure 6.1).

The ultra-violet absorption spectrum of cyclopentanone vapour in the region 2700 - 1670Å has been reported.[35,36] Two moderately intense absorption systems were found -- system A with λ_{max} at 1950Å and system B with λ_{max} at 1750Å. System A was assigned as a symmetry-allowed transition.[35]

The near ultraviolet absorption spectrum of cyclopentanone in hexane solutions has been investigated by Taboury and Gray.[13] The vapour phase absorption spectrum has been studied over the region 2900 - 3316Å by Lestrade and Thouvenin[37], who attempted an analysis of nineteen bands.

A more detailed study of the spectrum covering the region 2760 - 3470Å has been made by I. A. Rao, N. V. R. A. Rao and V. R. Rao.[38] Assignments differing from those of Rao, Rao and Rao are reported in this thesis for most of the bands measured by them.

1.4 Previous Studies of Related Molecules

Ethylene carbonate is isoelectronic with cyclopentanone. The electronic absorption spectrum of ethylene carbonate has not been reported, but the crystal structure has been determined[39] and a study of the infrared and Raman spectra has been made.[40] The crystal structure determined by x-ray diffraction is illustrated in Figure 1.1 (b). The line joining the two carbon atoms opposite the carbonyl group makes an angle of 20^o (the dihedral angle) with the plane of the rest of the ring.

Analyses have been made of the infrared and Raman spectra of cyclopentane.[15,41,42] Because of the work of Kilpatrick, Pitzer and Spitzer, the pseudorotation of the molecule is well known -- the ring is non-planar, and "the puckering of the ring is not of a definite type, but the angle of maximum puckering rotates around the ring". These authors have pointed out that the equilibrium configuration depends on which of two effects is predominant: in a regular pentagon, each interior angle has a value close to that of the tetrahedral angle (108^o vs $109^o28'$), and so the planar structure is favoured. On the other hand, there are repulsions between the hydrogen atoms of adjacent methylene groups; these repulsions produce torsions about the carbon-carbon bonds, and so the puckered configuration is favoured.

Pitzer and Donath[44] have calculated the magnitude of the puckering in the equilibrium conformation of cyclopentane (which belongs to the C_2 point group). The maximum out-of-plane displacement of a carbon atom is ∿ 0.2Å. They also have discussed the expected conformations of cyclopentane derivatives: cyclopentanone, tetrahydrofuran and pyrrolidine should have C_2 puckered configurations. It has been shown by calculation that the pseudorotation in cyclopentanone should be restricted by a barrier of 2.4 kcal.

The electron diffraction of cyclopentane has been studied.[45] The results indicate that the carbon ring is non-planar; determination of the magnitude of non-planarity awaits further refinements of the structure. A carbon-carbon bond length of 1.539Å ± 0.003 and a carbon-hydrogen bond length of 1.095Å ± 0.010 were reported.

Other five-membered ring compounds for which vibrational spectra have been reported are tetrahydrofuran, tetrahydrothiophene, pyrrolidine, N-methyl pyrrolidine[46], cyclopentene, furan and pyrrole.[15] Some of the vibrational frequencies of cyclopentanone will be correlated with frequencies of these molecules (see Chapter 5).

The ring bending vibrations of 1, 3, 2-dioxaborolane and vinylene carbonate[48,49] have been studied. The potential barriers of ring puckering in cyclopentene[50] and in furan derivatives[51] have been investigated.

The four-membered ring ketone, cyclobutanone, has been the subject of a vibrational analysis and normal coordinate treatment.[52] The vacuum ultraviolet spectrum has been reported[36] and the high resolution ultraviolet absorption spectrum is being analyzed.[53].

CHAPTER 2

THEORY OF VIBRATIONAL SPECTRA

2.1 Harmonic Vibrations

A convenient model for the purpose of analysing the vibrational motion of a polyatomic molecule is one in which N point masses, representing the nuclei, are coupled elastically. The positions of the N nuclei when displaced are specified by 3N coordinates, each measured from the equilibrium position of the relevant nucleus. A (non-linear) molecule as a whole has three translational and three rotational degrees of freedom. There are 3N-6 internal coordinates which define the motions of the nuclei relative to one another.

Only the important aspects of the theory of molecular vibrations will be summarized here; the details are found in references (5), (54), (55) and (56). The complex internal motions of a vibrating molecule can be analysed as a superposition of 3N-6 relatively simple motions known as the normal modes of vibration . Each non-degenerate[a] normal mode is associated with motion along a single normal coordinate. The normal coordinates are a set of 3N-6 parameters, $Q_1 \ldots Q_{3N-6}$, in terms of which both the kinetic and potential energies are the sum of squared terms only.

---

[a] The treatment for non-degenerate vibrations only is considered here. A molecule belonging to a point group with only one-dimensional irreducible representations cannot have degenerate vibrations.

The energy of each normal mode is quantized as in a one-dimensional harmonic oscillator, and the total vibrational energy, E_v, is the sum of 3N-6 independent contributions, each involving only one normal coordinate[b]:

$$E_v = h\nu_1 (v_1 + \tfrac{1}{2}) + h\nu_2 (v_2 + \tfrac{1}{2}) + \ldots + h\nu_{3N-6} (v_{3N-6} + \tfrac{1}{2}) \quad (2.1)$$

where ν_1, ν_2 ... ν_{3N-6} are the classical oscillator frequencies and v_1, v_2 ... v_{3N-6} are the vibrational quantum numbers, which can independently take on any positive integral values, including zero. In the harmonic model, the vibrational wave function is

$$\psi_v = \psi(Q_1)\ \psi(Q_2)\ \ldots\ \psi(Q_{3N-6}) \quad (2.2)$$

where each $\psi(Q_i)$ is a one-dimensional vibrational wave function of the coordinate Q_i.

2.2 Selection Rules

The intensities of infrared bands depend on the magnitude of the variation of the dipole moment with nuclear displacement during vibration. Similarly, the intensities of Raman bands depend on the magnitude of the variation of the polarizability with vibrational nuclear displacement. If vibrational and rotational motions can be separated, the probability of a transition between vibrational states ψ_v' and ψ_v'' is proportional to the square of the vibrational transition moment, R_v, which has three Cartesian components of the form,

---

[b] If 3N normal coordinates are used, six normal modes of zero frequency (corresponding to the translations and rotations) are obtained.

$$R_{vi} = \int \psi_v{}'^{*}\mu_i\ \psi_v{}''d\tau_v, \quad i = x,y,z \qquad (2.3)$$

The dipole moment component can be expanded in a power series as a function of the normal coordinates Q_j:

$$\mu_i = (\mu_i)_0 + \sum_j \left(\frac{\partial\mu_i}{\partial Q_j} \right)_0 Q_j + \ldots, \quad j = 1 \ldots 3N\text{-}6 \qquad (2.4)$$

The first term on the right in equation (2.4) is the permanent dipole moment at equilibrium. The second term represents the change in dipole moment with displacement during vibrations, and higher terms in the expansion are sufficiently small to be neglected. Substitution of equation (2.4) into equation (2.3) gives for the transition moment,

$$\int \psi_v{}'^{*}\mu_i\psi_v{}''d\tau_v = (\mu_i)_0 \int \psi_v{}'^{*}\psi_v{}''d\tau + \sum_j \left(\frac{\partial\mu_i}{\partial Q_j} \right)_0 \int \psi_v{}'^{*}Q_j\psi_v{}''\ d\tau \qquad (2.5)$$

The first term on the right side in equation (2.5) vanishes because $(\mu_i)_0$ is a constant and $\psi_v{}'$ and $\psi_v{}''$ are orthogonal.[c] Substitution of ψ_v from equation (2.2) into the second term gives for the integral

$$\int \psi_v{}'^{*}Q_j\psi_v{}''d\tau_v = \int \psi'^{*}(Q_1)\psi''(Q_1)dQ_1 \int \psi'^{*}(Q_2)\psi''(Q_2)dQ_2 \ldots$$

$$\int \psi'^{*}(Q_j)Q_j\psi''(Q_j)dQ_j \qquad (2.6)$$

which is zero unless $\psi'(Q) = \psi''(Q)$ for all Q except Q_j. If this condition is fulfilled, the jth term in the summation in (2.5) becomes

---

[c] $\psi_v{}'$ and $\psi_v{}''$ are two of the vibrational eigenfunctions and therefore belong to a complete orthonormal set.

$$\left(\frac{\partial \mu_i}{\partial Q_j} \right) \int \psi'^* (Q_j) Q_j \psi''(Q_j) dQ_j \tag{2.7}$$

The integral in (2.7) is non-zero if the harmonic oscillator selection rule is obeyed:

$$\Delta v_j = \pm 1 \tag{2.8}$$

In equation (2.8), Δv_j is the change in vibration quantum number of the jth normal vibration, all other Δv's being zero. Thus ψ_v' and ψ_v'' must differ by a single quantum excitation of one normal vibration.

For an observable infrared transition to occur, the quantity $\left(\frac{\partial \bar{\mu}_i}{\partial Q_j} \right)$ in equation (2.7) also must be non-zero; that is, there must be a change in the dipole moment during a vibrational motion. There are also restrictions imposed by symmetry on the values of the integral in (2.3). The harmonic oscillator approximation is only a limiting one, but the symmetry selection rules are rigorous for wave functions representing either harmonic or anharmonic vibrations. According to group theory,[5,54,55] R_i is non-zero only if the integral in equation (2.3) contains the totally symmetric species. The components of the dipole moment operator transform according to the same irreducible representations as the translation vectors T_x, T_y and T_z. Therefore the direct product representation of the two wave functions must transform, or have a component that transforms, like the representation of one of the translational displacements:

$$\Gamma\,(\psi_v') \otimes \Gamma\,(\psi_v'') \sim \Gamma(T_i),\ i = x,y,z,\ \ldots \tag{2.9}$$

Most observed transitions in absorption originate on the vibrationless ground level for which the wave function ψ_v'' is totally symmetric; therefore, if ψ_v' belongs to the same representation as one of the translation vectors, the direct product $\psi_v' \otimes \mu \otimes \psi_v''$ will contain the totally symmetric representation.

The selection rules for Raman scattering may be obtained by similar arguments. The intensity of scattered light depends on the induced dipole moment $\bar{P}$, given by

$$\bar{P} = \alpha\bar{E} \tag{2.10}$$

In equation (2.10), α is the polarizability tensor and $\bar{E}$ is the electric vector of the incident radiation. Terms of the form

$$\left(\frac{\partial\alpha_i}{\partial Q_j} \right)_0 \bar{E} \int \psi'^{*}(Q_j) Q_j \psi''(Q_j) dQ_j$$

are non-zero if the harmonic oscillator selection rule $\Delta v_j = \pm 1$ is obeyed, and if there is a change in the polarizability of the molecule during the vibration associated with Q_j. The symmetry selection rule holds for actual vibrational wave functions, whether harmonic or anharmonic: a transition between two vibrational levels will be Raman active if the direct product of the vibrational wave functions, $\psi_v' \otimes \psi_v''$ belongs to the same irreducible representation as one or more of the six components α_{xx}, α_{xy} ..., of the polarizability tensor of the molecule. Most of the observed bands in the Raman spectrum result from fundamental transitions

($v_j'' = 0 \rightarrow v_j' = 1$). ψ_v'' is totally symmetric, and therefore ψ_v' must belong to the same irreducible representation as one or more of the components of α.

2.3 Band Contours and Depolarization Ratios

The selection rules for the rotational structure of a vibrational band depend on the orientation within the molecule of the vibrational transition moment. In the spectra of large polyatomic molecules individual rotational lines are not usually resolved, but the intensity distribution of unresolved groups of lines forms a "band contour".[5] Band types A, B and C indicate that the transition moments are directed along the a, b and c principal axes of the molecules, respectively. Band contours usually will be distinguishable only for the vapour phase infrared spectra.

The depolarization ratio[d] of a Raman line is defined as

$$\rho = I_{\perp} / I_{||} \tag{2.11}$$

where $I_{\perp}$ is the intensity of scattered light polarized in the xy plane and $I_{||}$ is the intensity of scattered light polarized parallel to the yz plane. Here the x-axis is taken in the direction of propagation of the incident light which is linearly polarized in the xz plane and observation is made along the y axis. It has been shown that for linearly polarized incident light, as from a laser source, the maximum value of the ratio ρ is $\rho_{\ell} = \frac{3}{4}$. A Raman line with a depolarization ratio of $\frac{3}{4}$ is said to be

---

[d] see reference (55), pp. 247, 270.

depolarized. If $\rho_\ell < \frac{3}{4}$ the line is polarized. Only totally symmetric vibrations yield polarized lines, having ρ_ℓ between 0 and $\frac{3}{4}$ (p); non-totally symmetric vibrations yield lines having $\rho_\ell = \frac{3}{4}$ (dp). For measurement of the depolarization ratio, an analyser may be placed in two orientations (0^o and 90^o) between the sample and spectrometer.

2.4 Consequences of Anharmonicity

In equation (2.4), terms of order higher than linear contribute to the intensity of bands with $\Delta v > 1$; that is, there is electrical anharmonicity. Secondly, the convergence of vibrational levels is evidence of mechanical anharmonicity; that is, the harmonic approximation is only valid for very small displacements.

2.4.1 Overtones

In an actual molecule the vibrations are anharmonic. Although the fundamental frequencies are the most intense, weak bands may be observed which violate the selection rule (2.8). If one vibration alone is doubly excited, this transition is called the first overtone of the fundamental; if triply excited, the second overtone. If two or more vibrations are simultaneously excited, by one or more quanta of each, the resulting band is called a combination band. The bands produced by overtones and combination vibrations are usually an order of magnitude less intense than the bands produced by fundamentals.

2.4.2 Fermi Resonance (of Vibrational Energy Levels)

Fermi resonance is the interaction of two vibrational levels which have the same symmetry species and have in the zeroth order harmonic approximation, nearly the same energy. The levels may be fundamentals, overtones or combinations. In the expansion of the potential function in terms of normal coordinates, the anharmonic terms may be treated as perturbing terms. Perturbation theory shows that the magnitude of the interaction depends inversely on the magnitude of the difference between the zero-order energies of the interacting states. Spectroscopic transitions involving these states may produce bands which are displaced from their expected wavenumber and have anomalous intensities.

2.4.3 Dissociation

A parabolic potential curve (harmonic oscillator approximation) allows for no dissociation of a molecule into fragments. An actual molecule has in each stable electronic state a dissociation energy which corresponds to the separation of the molecule into fragments with zero kinetic energy. Therefore the actual potential curve for a vibration must approach a constant value at large displacements; this constant value gives the dissociation energy. Figure 2.1 illustrates these ideas schematically. The deviation of the actual curve from the parabolic curve (dashed line) is a measure of the anharmonicity of the vibration.

The term values of the anharmonic vibrational levels are given empirically by

$$G(v) = \omega_e (v + \tfrac{1}{2}) - \omega_e x_e (v + \tfrac{1}{2})^2 + \omega_e y_e (v + \tfrac{1}{2})^3 + \ldots \qquad (2.14)$$

In most molecular states, the anharmonicity constant $\omega_e x_e$ is positive and $\omega_e x_e >> \omega_e y_e$. The energy levels are not equidistant; they converge as v increases. The constant x_e usually has a value 0.01 to 0.05. The

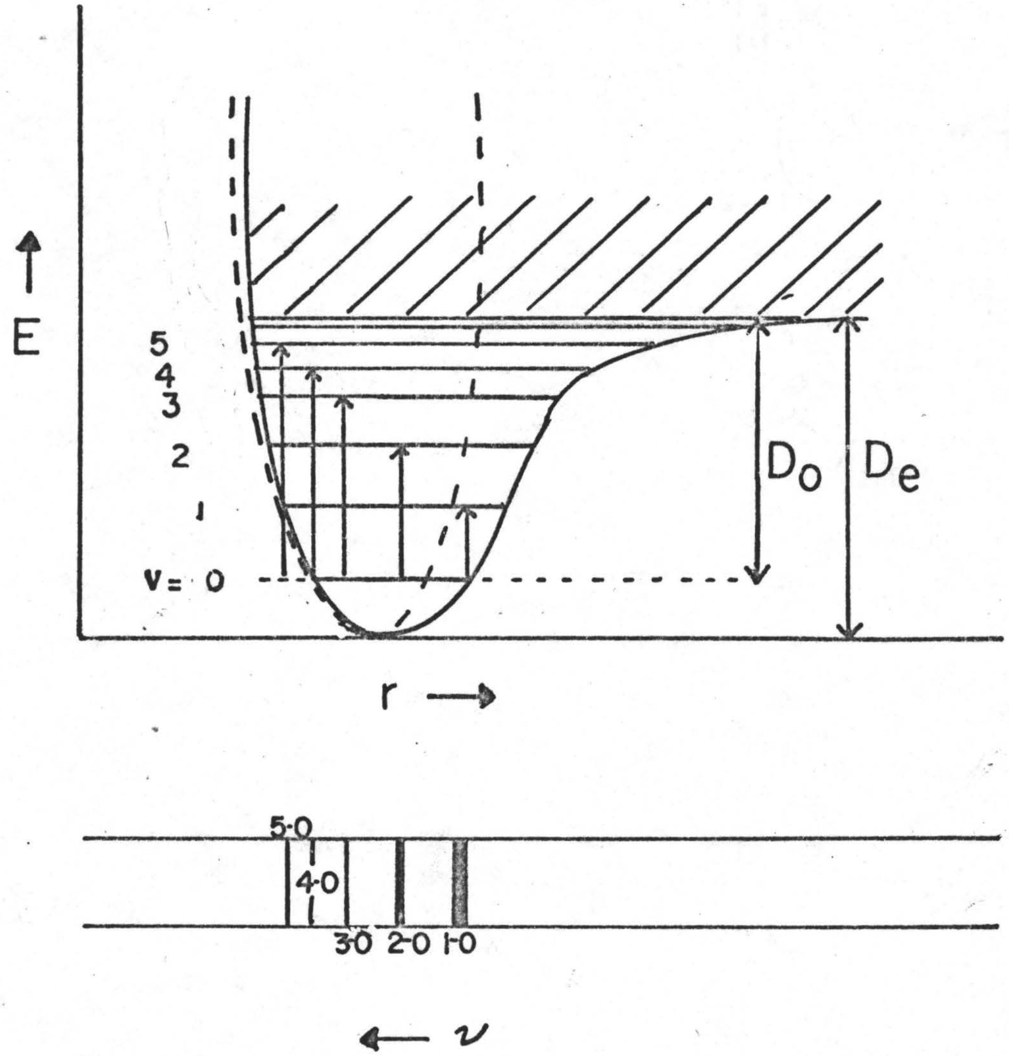

Figure 2·1 Energy Levels and Infrared Transitions of the Anharmonic Oscillator selection rule for the anharmonic oscillator is Δv = any integer; that is, overtones are now permitted. The intensity of a transition in absorption also depends on the population of the lower combining levels. At normal temperatures most molecules are in the vibrationless ground state. Thus the observed infrared spectrum in absorption consists of a progression of bands produced by transitions from the v"=0 to v'=1,2,3 .. levels. The 1-0 fundamental, for which Δv = + 1, is the most intense band; successive overtone bands, 2-0, 3-0, 4-0 ..., become progressively weaker. With higher v, the series of bands converges and terminates in a continuum produced by transitions to states above the dissociation limit (see Figure 2.1). This continuum is not expected to be observed because of its very low intensity.

The observed wavenumbers of the fundamental and overtones are fitted empirically to the power series (2.4). The zero point energy (relative to the minimum of the potential well) is obtained by setting v=0:

$$G(0) = \frac{1}{2}\omega_e - \frac{1}{4}\omega_e x_e + \frac{1}{8}\omega_e y_e + \ldots \tag{2.15}$$

The separation between successive terms is

$$\Delta G(v + \frac{1}{2}) = \omega_e - \omega_e x_e\,(2v + 2) + \omega_e y_e\,(3v^2 + 6v + \frac{13}{4}) + \ldots \tag{2.16}$$

At high enough v, say v_n, $\Delta G(v + \frac{1}{2})$ becomes zero. The dissociation energy, D_0, (measured from v=0) is given by

$$D_0 = \sum_{v=0}^{v_n} \Delta G(v + \frac{1}{2}) \tag{2.17}$$

The summation may be conveniently made graphically by the method of

Birge and Sponer.[57] $\Delta G(v + \frac{1}{2})$ is plotted as a function of $v + \frac{1}{2}$; the area under the curve is approximately D_0.

Because values for only a few of the lower vibrational energy levels are usually observed, an extrapolation must be made to the point $\Delta G(v + \frac{1}{2}) = 0$. Omission of cubic and higher terms from equation (2.14) leads to a linear Birge-Sponer extrapolation. Dissociation energies obtained thus are generally too high by ∿ 25%.

Often a normal mode can be ascribed approximately to a bond stretching vibration or to a deformation vibration of a particular group of atoms in a molecule. For example, one normal mode may be essentially localized in the C-H bond or bonds in a molecule (see Section 5.1). The C-H stretching vibration may be considered approximately as the vibration of a simple diatomic molecule. Bernstein[58] has shown by second order perturbation theory that the X-H stretching mode in a polyatomic molecule is coupled to the rest of the vibrational modes by terms of the order of only 0.01 - 0.002 of the main terms.

2.5 Symmetry

Cyclopentanone has 14 atoms and therefore (3N-6) = 36 normal modes of vibration. There are four possible equilibrium configurations for the ground electronic state. The molecule may belong to one of the four point groups, C_{2v}, C_1, C_2 or C_s. The possible symmetries are illustrated in Figure 2.2. The character tables for these point groups are listed in Table 2.1. The last two columns on the right give respectively the symmetry species of (1) the translations and rotations, and (2) the components of the polarizability tensor. The tables show that in the

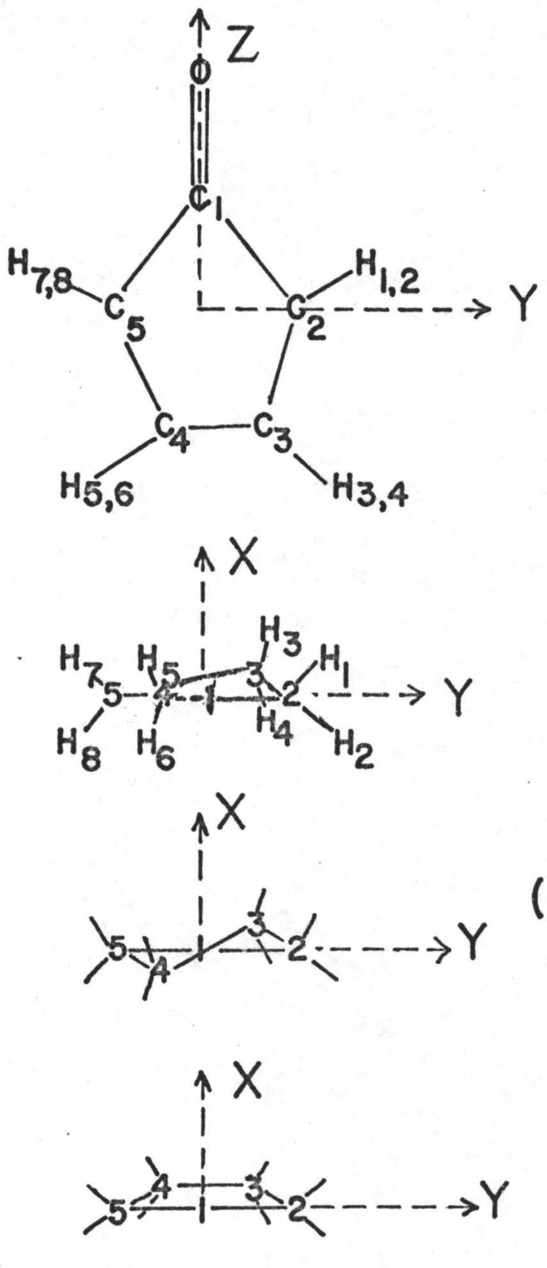

(a) C_{2v} if ring planar. C_2 along Z
$\sigma_v(xz)$
$\sigma'_v(yz)$

(b) C_1
No elements of symmetry except E.

(c) C_2
C_2 along Zaxis

(d) C_s
σ_h in xz plane

FIGURE 2.2 Possible Symmetries of Cyclopentanone. Projections on (a) yz plane (b), (c) & (d) xy plane.

C_1, C_2 and C_s point groups all vibrations are formally allowed in both the infrared and Raman spectra. In the C_{2v} point group vibrations of species A_2 are infrared forbidden but Raman allowed; the other vibrations are allowed in both.

The group operations, R_i, applied to the set of 3N displacement coordinates written in the form of a column vector generate a set of transformation matrices, [R], of character $\chi(\Gamma_{3N})$. The matrices [R] form a group representation which is in general reducible. $\chi(\Gamma_{3N})$ may be decomposed by the formula

$$C_\alpha = \frac{1}{g} \sum_R \chi(\alpha)\ \chi(\Gamma_{3N}) \tag{2.18}$$

where C_α is the number of times the αth irreducible representation of character $\chi(\alpha)$ appears, and g is the order of the group. By this means $\chi(\Gamma_{3N})$ can be expressed as the direct sum of characters of irreducible representations. These give the number and symmetry species of the normal modes of vibration provided that the sum of characters for the three translational and three rotational motions, $\chi(\Gamma_{T,R})$, of the molecule are first subtracted.

In the C_1 point group the result is obviously 36 normal vibrations of species A. In the C_2 point group, the purely vibrational modes have the character system $\chi(\Gamma^{vib}_{3N-6}) = (36, 0)$, which may be decomposed into the direct sum of irreducible components with the aid of equation (2.18) to give:

$$C_A = \frac{1}{2}[36 + 0] = 18$$

$$C_B = \frac{1}{2}[36 + 0] = 18$$

Therefore in C_2:

$$\Gamma_{vib} = 18\ \Gamma_A \oplus 18\ \Gamma_B \qquad (2.19)$$

Similarly, in the C_s point group the decomposition gives

$$C_s: \quad \Gamma_{vib} = 19\ \Gamma_{A'} \oplus 17\ \Gamma_{A''} \qquad (2.20)$$

and in C_{2v}

$$C_{2v}: \quad \Gamma_{vib} = 11\ \Gamma_{A_1} \oplus 7\ \Gamma_{A_2} \oplus 8\ \Gamma_{B_1} \oplus 10\ \Gamma_{B_2} \qquad (2.21)$$

The infrared and Raman activity of the vibrations of cyclopentanone under the point groups C_2, C_s and C_{2v} is indicated in Table 2.2, together with the expected band contour and polarization for each species.

2.6 Non-Rigid Molecules

According to Longuet-Higgins,[59] a non-rigid molecule is one "which can change easily from one conformation to another". That is, the molecule has only a small potential barrier impeding a change between different equilibrium configurations. Recently there have appeared a number of discussions on the applications of group theory to non-rigid molecules.[59-65] In this section we consider some of these group theoretical ideas and show how they may be applied to cyclopentanone.

The usual type of geometrical symmetry operation may always be described by some permutation of identical nuclei in the molecule. If the geometrical operation is a chiral[e] one, the permutation is accompanied

---

[e] A chiral operation changes the "handedness" of the axis system.

TABLE 2.1

CHARACTER TABLES

C_1	E
A	1

C_2	E	C_2		
A	1	1	z, R_z	$\alpha_{xx},\alpha_{yy},\alpha_{zz},\alpha_{xy}$
B	1	-1	x,y,R_x,R_y	α_{yz},α_{xz}

C_s	E	σ_h		
A'	1	1	x,y,R_z	$\alpha_{xx},\alpha_{yy},\alpha_{zz},\alpha_{xy}$
A"	1	-1	z,R_x,R_y	α_{yz},α_{xz}

C_{2v}	E	C_2	$\sigma_v(xz)$	$\sigma_v'(yz)$		
A_1	1	1	1	1	z	$\alpha_{xx},\alpha_{yy},\alpha_{zz}$
A_2	1	1	-1	-1	R_z	α_{xy}
B_1	1	-1	1	-1	x,Ry	α_{xz}
B_2	1	-1	-1	1	y,Rx	α_{yz}

TABLE 2.2

NUMBER AND SYMMETRY OF VIBRATIONS FOR CYCLOPENTANONE

Point Group	Symmetry Species	No. of Vibr.	No. of Infrared Active Vibrations	Band Type	No. of Raman Active Vibrations	Polarization
C_2	A	18	18	A	18	p
	B	18	18	B + C hybrid	18	dp
C_s	A'	19	19	A + C hybrid	19	p
	A"	17	17	B	17	dp
C_{2v}	A_1	11	11	A	11	p
	A_2	7	0	-	7	dp
	B_1	8	8	C	8	dp
	B_2	10	10	B	10	dp

by an inversion at the origin of the coordinates of all particles in the molecule. (The inversion operation is denoted by *). The converse, however, does not hold. There may be permutations and permutation-inversions which do not have geometrical equivalents.

Longuet-Higgins[59] (LH) has found that the molecular symmetry group for a non-rigid molecule is the set of (1) all feasible permutations of the positions and spins of identical nuclei and (2) all feasible permutation-inversions which simultaneously invert the coordinates of all particles in the centre of mass. The complete permutation-inversion group also contains elements that correspond to motions opposed by high energy barriers. By removing such elements, one obtains the practical subgroup of feasible operations. The property of feasibility cannot be defined absolutely. Feasible operations correspond to changes in the nuclear configuration which can occur if there is not an insurmountable energy barrier to these changes.

For example, the rotational levels of methane occur theoretically as inversion doublets.[55] This phenomenon arises because, if the hydrogen atoms are labelled, two equivalent equilibrium configurations can be drawn, which are related to each other as are right and left hands. Because these doublets are so closely spaced, they cannot be resolved by any normal spectroscopic technique. The barrier to inversion is so high that the molecule remains for all practical purposes in just one form. Only observables associated with this one configuration can be measured. It is therefore sufficient to have a classification scheme that distinguishes between different doublets and not between the individual components of a doublet. To obtain such a scheme, one discards from the complete permutation-inversion group as non-feasible those operations which convert a right-handed carbon atom axis system into a left-handed one. One is left with a group of 24 elements with 5 symmetry species, corresponding to the point group T_d. This is the point group of the equilibrium configuration, and it is a sub-group of the full permutation-inversion group.

The phenomenon just described is a very general one. Many molecules can be thought of as existing in one of several frameworks between which interconversion is not feasible. If some interconversion takes place, then some of the degeneracy associated with the existence of several configurations is removed. In the language of Watson,[60] the tunneling between symmetrically equivalent regions of vibrational phase space is called the tunneling between localized domains. The extended domain for the tunneling problem is called a delocalized domain. The group of a delocalized domain includes all the elements of the groups of the localized domains contained in the delocalized domain, together with the elements which convert these localized domains into each other. To use a familiar example, treatment of the inversion of ammonia is said to involve two localized C_{3v} domains within a delocalized D_{3h} domain. The group of the delocalized domain is always larger, and it therefore gives rise to additional symmetry distinctions.

For a molecule with a delocalized domain which encompasses a set of localized domains, there are certain vibrational coordinates of large amplitude that take the nuclei from one localized domain to another. In the ammonia molecule, the motion of the nitrogen atom perpendicular to the plane of the three hydrogen atoms is such a coordinate. Tunneling through the plane is a feasible motion. The examples of CH_4 and NH_3 illustrate the concepts of nonfeasibility and feasibility. It can be seen that there is no absolute criterion of feasibility; feasibility depends on the probability of interconversion of configurations, and on the resolution of the spectroscopic technique employed.

According to Altmann[63] it is unsatisfactory to require that all symmetry operations be feasible. A symmetry operation is essentially a change of axes and not a physical operation. "It exists not in nature but on the theoretician's writing paper." He treats the symmetry of non-rigid molecules as follows: The desired group for the non-rigid molecule, called the Schrödinger supergroup, possesses two subgroups. One of them is the group of all the symmetry operations defined for the rigid molecule in the familiar way. The other is a group of operations of a new type called _isodynamic operations_. Two configurations of a molecule that cannot be converted one into another by a Schrödinger group operation but have identical energy eigenvalues, are called _isodynamic configurations_[f]. The operations that interconvert these isodynamic configurations are the _isodynamic operations_. They are not symmetry operations. Rather they are translations or rotations of an atom or group of atoms with respect to the rest of the molecule.

Altmann denotes an isodynamic operation by a conventional symmetry operation symbol with the addition of a superscript I. Thus $\sigma_v{}'^{I}$ designates not a reflection but a displacement of an atom or a group of

---

[f] cf. Watson's "localized domains".

atoms perpendicularly to the yz plane into what would be its corresponding position on the other side of that plane. The set of all the isodynamic operations of a given configuration forms a group called the isodynamic group, I. The Schrödinger groups, G, of two isodynamic configurations are identical. The group product of I and G is a group. It is called the Schrödinger supergroup, S, given by

$$S = I \wedge G \tag{2.21}$$

where the caret denotes the semidirect product, and the invariant subgroup must always appear on the left. In ammonia, if the hydrogen atoms are labelled 1, 2, 3 and the nitrogen atom is allowed to tunnel to its symmetrical position with respect to the H_3 plane, the Schrödinger group G is C_{3v}, the isodynamic group, I, is $C_s{}^I$ (the isodynamic operation is $\sigma_h{}^I$) and

$$\begin{aligned} S &= C_s{}^I \wedge C_{3v} \\ &= C_s{}^I \otimes C_{3v} \\ &\sim D_3h \end{aligned}$$

where $\sim$ means "is isomorphous to". The semidirect product can be replaced by the direct product, since C_s and C_{3v} commute in detail.

In cyclopentanone, the ground state equilibrium configuration probably belongs to either the C_2 or C_s point group. Although the microwave work is indeterminate as to the exact conformation of the puckered ring, the C_2 or "skew" configuration in which the molecule is non-planar twisted has been proposed as the most reasonable one.[11,44] "Skew" structures have been determined for ethylene carbonate and cyclopentane (see

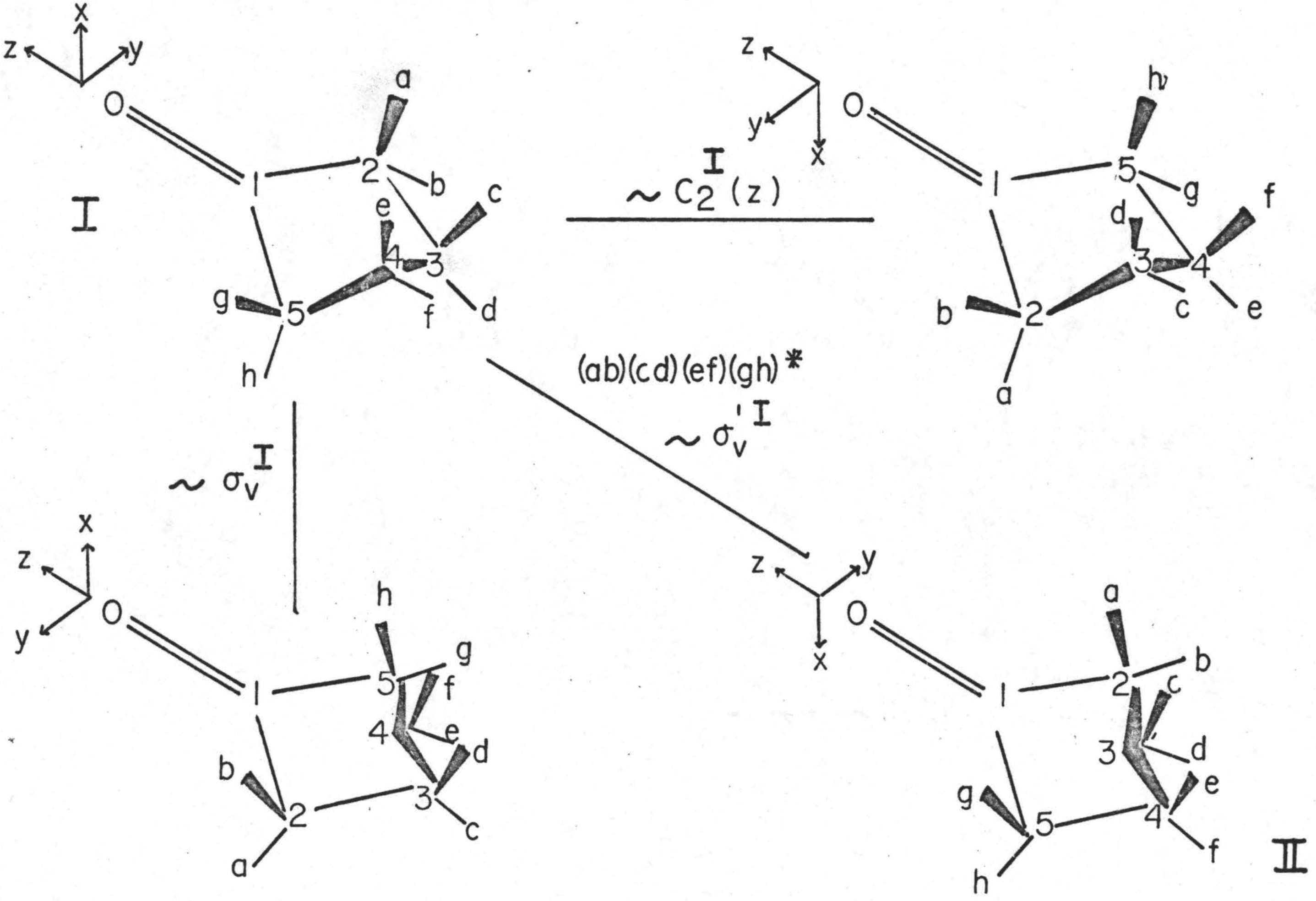

Figure 2·3 Operations of the Non-rigid Molecule.

section 1.4).

There are two possible geometrically equivalent conformations for cyclopentanone under the C_2 point group. These are labelled I and II in Figure 2.3. Configurations I and II each possess the symmetry elements of C_2 but there is no element in C_2 which converts I to II. In the LH permutation-inversion notation, the operations E and C_2 may be written E and (25)(34)(ah)(bg)(cf)(de). If the barrier to inversion through a large amplitude ring puckering vibration is not too high, the transformation I ↔ II is feasible. An operation corresponding to this transformation is seen to be (ab)(cd)(ef)(gh)*. In order that the elements form a group,[g] a fourth operation, (25)(34)(ah)(bg)(cf)(de)*, is required.

If the carbon ring in cyclopentanone were planar, the molecule would belong to the C_{2v} point group; it can be seen that the above permutation-inversion operations may be applied to the planar molecule and that they may be correlated with the operations of C_{2v} as follows:

$$E \leftrightarrow E$$

$$(25)(34)(ah)(bg)(cf)(de) \leftrightarrow C_2$$

$$(25)(34)(ah)(bg)(cf)(de)^* \leftrightarrow \sigma_v(xz)$$

$$(ab)(cd)(ef)(gh)^* \leftrightarrow \sigma_v'(yz)$$

Thus the set of LH permutation-inversion operations form a group which is isomorphous to C_{2v}.

Alternatively, the Altmann approach may be used. The large amplitude ring puckering motions of the carbon atoms C_3 and C_4 constitute

---

[g] The product of each pair of elements is also a member of the group.

the isodynamic operation, $\sigma_v'(yz)^I$. The isodynamic group containing the elements $E + \sigma_v'(yz)^I$ is $C_s'^I$ (where the prime indicates that the symmetry plane coincides with the yz plane). The Schrödinger group is C_2. The Schrödinger supergroup is

$$\begin{aligned} S &= I \wedge G \\ &= C_s'^I \wedge C_2 \\ &= C_s'^I \otimes C_2 \\ &\sim C_{2v} \end{aligned}$$

Thus the two approaches are seen to give the same result for cyclopentanone:[h] the non-rigid molecule may be classified under the point group C_{2v}. Whether this classification is useful or not depends on the feasibility of the inversion, or in other words, on the height of the potential barrier restricting the ring from planarity. Figure 2.4 illustrates the spacing of vibrational energy levels if there is a double minimum in the potential with respect to the ring puckering mode. For a barrier lower than the zero point energy, the vibrational levels are scarcely perturbed from their values if the barrier were not present. (2.3a). For a medium energy barrier (of the order of one or two vibrational quanta), the components of the inversion doublets are well separated (2.3b). For a high barrier (of the order of many vibrational quanta) the levels below the top of the barrier are coalesced into very closely spaced inversion doublets; the doublet splittings near the potential minima may be

---

[h] According to Altmann, the LH treatment does not always give the same result as his.

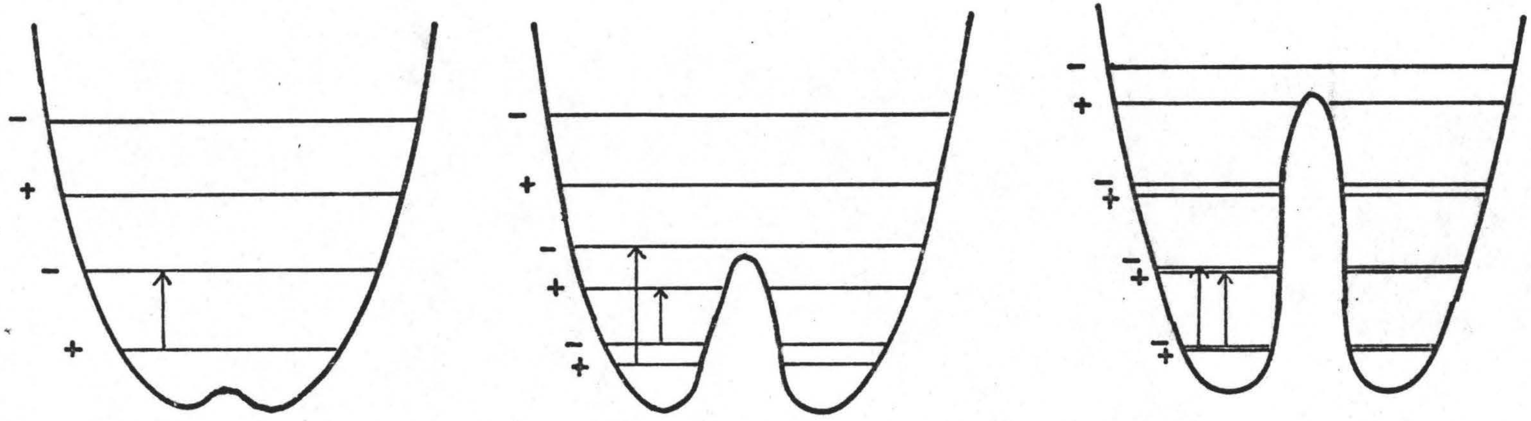

Figure 2·4 Effect of Barrier Height on Level Spacing.

too small to be observed.

Studies of ring puckering potentials in four- and five-membered rings[47,49-51,66-69] have shown that in general the potential barriers are low, of the order of 200-400 cm^{-1}, often below the zero point energy of the ring puckering vibration. The available data are summarized in Table 2.3. The tendency of adjacent methylene groups to adopt staggered positions of the hydrogen atoms predominates (see section 1.4) in the puckered molecules (numbers 3,4,5,6). The five-membered ring molecules with no adjacent methylene groups are planar (numbers 7,12). For most of the four-membered rings, the planar structure is stabilized; the forces which tend to keep the bond angles as close to the tetrahedral value as possible predominate (numbers 1,2,11). (If the ring is puckered, the angles become even smaller). For trimethylene oxide and cyclobutanone, the ring strain is sufficiently large to keep the molecules planar. Trimethylene sulfide is puckered because the C-S-C bond angle is more easily altered than the C-O-C bond angle, and the C-S bonds are longer than the C-O bonds. Similar arguments apply to silacyclobutane and there is an additional repulsive force between the SiH_2 group and adjacent-CH_2-groups.[68] The barrier height evidently is qualitatively proportional to the number of adjacent -XH_2 groups.

Since low barriers are common for the puckered ring molecules, it is reasonable to assume that interconversion of isodynamic configurations is feasible in these molecules, and that it will be so in cyclopentanone.

TABLE 2.3

DATA FOR PUCKERING OF RING MOLECULES

Number	Molecule	Barrier Height cm^{-1}	Dihedral Angle, °	Reference
1	cyclobutanone	5	0	68
2	trimethylene oxide	15.3	0	68
3	trimethylene sulfide	274	28	67,68
4	silacyclobutane	440	35.9	68
5	cyclobutane	448	33	68
6	cyclopentene	232	23.3	50
7	2,5 dihydrofuran	0	0	66
8	2,3 dihydrofuran	86.8	?	51
9	2,3 dihydrothiophene	206.1	?	51
10	1,3,2 dioxaborolane	∿15	0	47
11	β-propiolactone	∿ 0	∿ 0	69
12	vinylene carbonate	∿ 0	∿ 0	49

CHAPTER 3

THE THEORY OF ELECTRONIC SPECTRA

3.1 The n→π* Transition

Electronic transitions in many unsaturated organic molecules may be regarded as localized in certain chemical groups or bonds. If a series of related molecules contain such a group -- called a chromophore -- they will often have absorption spectra similar in appearance and intensity in a characteristic spectral region. In a simple approximation, the electronic transition in absorption may be considered as resulting from the promotion of an electron between molecular orbitals associated with the chromophore. Kasha[70] introduced a notation for such transitions in which σ or π electrons are bonding according to local symmetry, σ* and π* electrons are antibonding, and n electrons are nonbonding or "lone-pair".

Very weak absorption in the near ultraviolet region is characteristic of the (non-bonding to anti-bonding) n→π* transitions in carbonyl compounds. The intensity of a transition is dependent on the transition moment, R, which may be written

$$R = \int \psi^{*}_{\pi^*}(i)\mu\psi_n(i)d\tau \qquad (3.1)$$

The intensity of a transition[a] at wavenumber ν is usually described in

---

[a] The details are given in reference (71).

terms of the oscillator strength, f, which is related to the transition moment by

$$f = 1.085 \times 10^{-5} \nu R^2 \qquad (3.2)$$

Integration of the molar extinction coefficient, ε, gives the experimental value of the oscillator strength:

$$f = 4.317 \times 10^{-9} \int \varepsilon d\nu \qquad (3.3)$$

For symmetrical band profiles, the integral may be approximated by

$$\int \varepsilon_\nu \, d\nu = \gamma \, \varepsilon_{max} \, \Delta\nu_{\frac{1}{2}} \qquad (3.4)$$

where ε_{max} is the maximum extinction coefficient, $\Delta\nu_{\frac{1}{2}}$ is the width of the absorption band at half-height in cm^{-1}, and $\gamma = 1.06$ for an assumed Gaussian band shape. Thus the oscillator strength is given by

$$f = 4.317 \times 10^{-9} \, \gamma \, \varepsilon_{max} \, \Delta\nu_{\frac{1}{2}} \qquad (3.5)$$

An allowed electronic transition has f in the range 0.1 - 1. The $\underline{n}\rightarrow\pi^*$ transition in carbonyl compounds usually has $f \sim 10^{-4}$. The corresponding ε_{max} value is usually about 10 to 100.

3.2 Excited State Configurations

By analogy with the behaviour of formaldehyde and other related molecules on $\underline{n}\rightarrow\pi^*$ promotion, it is anticipated that in the corresponding excited state configuration of cyclopentanone the oxygen atom is bent out of the C_1-C_2-C_5 plane. If this is so, and assuming that the ring is non-planar, three different equilibrium geometries may be drawn for the molecule. These are the skew, boat and chair forms, as shown respectively in Figures 3.1 (a),(b) and (c).

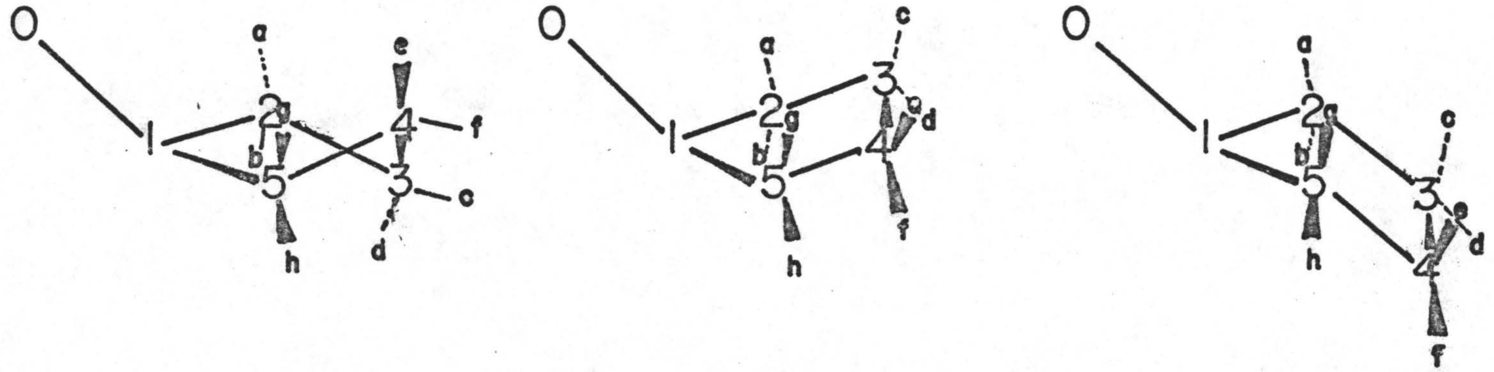

(a)

Skew

(b)

Boat

(c)

Chair

FIGURE 3·1 Possible Excited State Configurations of Cyclopentanone

The rigid boat and chair conformations belong to the point group C_s, the skew to C_1. Because of the non-zero possibility of inversion by a large amplitude vibration -- either the oxygen-wagging vibration or the ring puckering vibration, or both -- isodynamic configurations exist for each conformation. Figure 3.2 illustrates (in a side view of the carbon-oxygen skeleton) the two isodynamic configurations for each of the boat and chair forms. For the skew conformation, four isodynamic configurations may be drawn. These are shown in Figure 3.3.

While all these configurations may exist, there is no isodynamic operation (in the sense defined by Altmann[b]) which takes boat to chair, boat to skew or chair to skew. In fact the symmetry group for interconversion of non-geometrically equivalent configurations has not been treated theoretically. This is a serious handicap since the phenomenon of tunneling between configurations that are not geometrically equivalent occurs in many non-rigid molecules.[62] The boat-chair-skew interconversion involves a change in energy. Configurations for which the Hamiltonian is different cannot be isodynamic. Altmann[72] refers to molecules having such configurations as "extremely non-rigid". It is obviously feasible for the molecular configuration to change between any of the three forms. In principle, spectroscopic transitions can occur to excited states in which the excited state molecular configuration has any one of the three forms (provided symmetry selection rules are obeyed). The problem is

---

[b] We have been in correspondence with Professor S. L. Altmann, who has published most original papers on this topic.

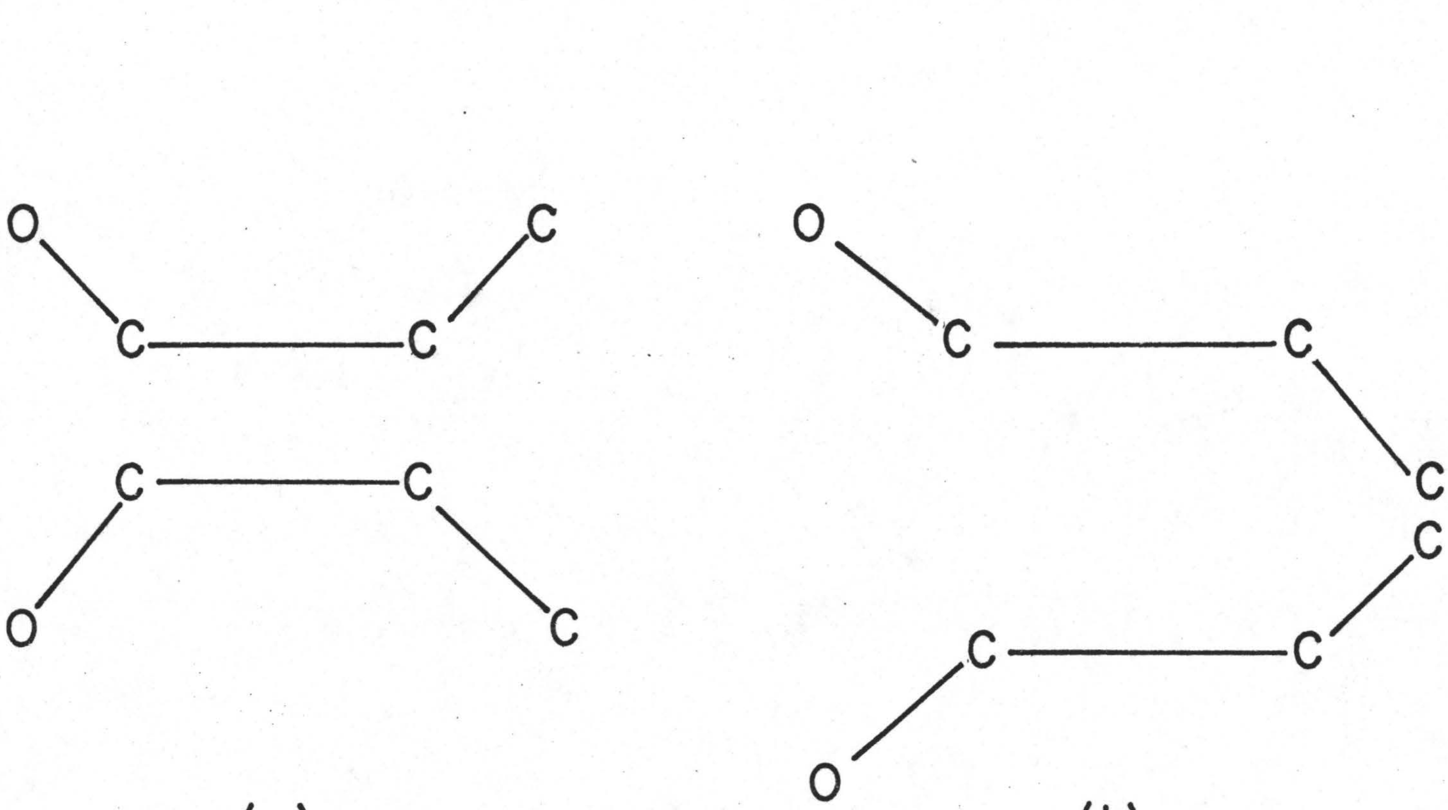

(a)
Boat

(b)
Chair

FIGURE 3·2 Boat and Chair Isodynamic Configurations

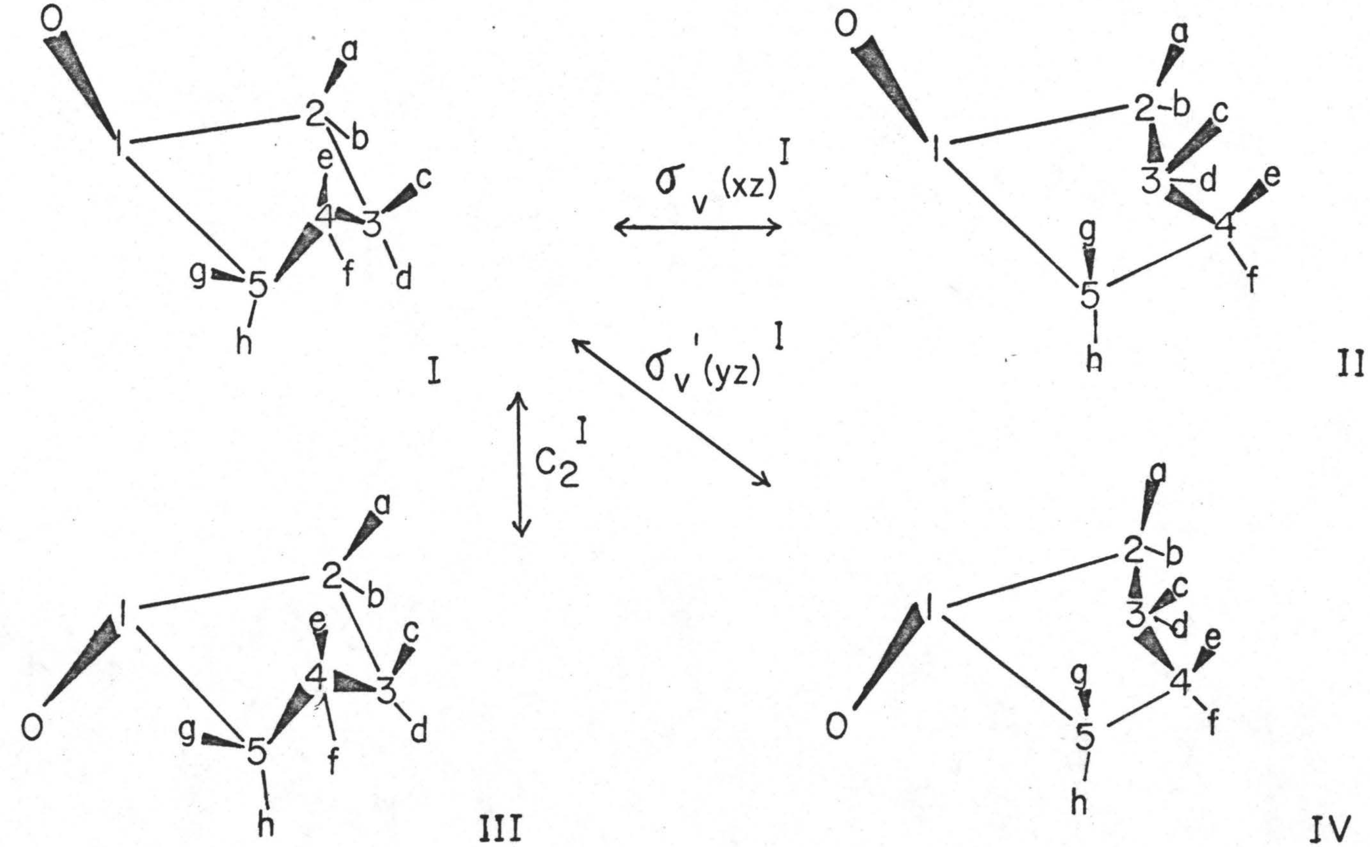

FIGURE 3·3 Skew Isodynamic Configurations that the Hamiltonians for the three forms are different. Altmann has written to us:

> "The configurations for which, as you say, the Hamiltonians are different, cannot be isodynamic. Therefore, a group cannot be defined in the same manner as done either by Longuet-Higgins or myself. However, I am sure that spectroscopic transitions between all the configurations that you mention might be interesting, since presumably the difference in energy would be very small. I think that molecules of this type require a different type of treatment ... I have already referred to molecules of this type as 'extremely non-rigid' and I am sure that they deserve quite a bit of thinking."[c]

While it is beyond the scope of this work to solve the theoretical problem, it is suggested here that a solution may be found in the application of the theory of double groups. The Schrödinger supergroup for one configuration is augmented by a <u>new type</u> of isodynamic operation denoting interconversion of non-geometrically equivalent configurations, and a double non-rigid symmetry group is formed.

Because of the theoretical difficulties in the treatment of the electronically excited state configuration, we limit our discussion to the assumption of a skew configuration. In any case, it seems reasonable to assume that the nature of the ring puckering in the excited state will be similar to that in the ground state. The rigid skew configuration has no elements of symmetry (except E), but it has four isodynamic forms. Besides the identity, E, three different isodynamic operations may be

---

[c] S. L. Altmann, private communication.

defined. The operation which takes form I to form II (or III to IV) (see Figure 3.3) will be denoted $\sigma_v(xz)^I$; the one that takes I to III (or II to IV) will be denoted C_2^I, and the one that takes I to IV (or II to III) will be called $\sigma_v(yz)^I$. Therefore, the Altmann treatment of the excited states gives the Schrödinger group $G=C_1$, the isodynamic group $I = E + C_2^I + \sigma_v^I + \sigma_v'^I \sim C_{2v}$, and the Schrödinger supergroup is

$$\begin{aligned} S &= C_1 \wedge C_{2v}^I \\ &\sim C_{2v} \end{aligned}$$

Thus the molecule cyclopentanone may be classified under a group isomorphous to C_{2v} in the excited state as well as in the ground state. This situation arises, in spite of the lowering of the symmetry of the molecule in its excited state equilibrium configuration, because of the feasibility of interconversion of isodynamic configurations -- two in the ground state and four in the excited state. The operation C_2^I may be described as essentially a large amplitude oxygen wagging motion, the operation σ_v^I as a large amplitude ring puckering motion, and the operation $\sigma_v'^I$ as the inversion of the molecule by means of simultaneous large amplitude oxygen-wagging and ring puckering motions. In the limit of high energy barriers restricting interconversion, the levels in the excited state will be four-fold degenerate. If the barrier to inversion through oxygen-wagging alone is low enough that this operation is feasible, while the barrier to ring puckering is high, the levels will be two-fold degenerate. If both energy barriers are sufficiently low that interconversion of all four equivalent configurations is feasible, then all the degeneracy will be removed.

3.3 The Molecular Orbitals

In a simple, localized MO model, the near ultraviolet absorption spectrum of cyclopentanone may be considered as arising from the $\underline{n}\rightarrow\pi^*$ promotion of an electron localized in the carbonyl group. The construction of localized LCAO/MO's for the carbonyl group is shown schematically in Figure 3.4. The AO's are on the left and the MO's on the right in order of increasing energy[d]. The symmetries of the MO's under the point group C_{2v} are indicated on the right.

The lowest energy σ-orbital and its antibonding counterpart, σ^*, result from in-phase and out-of-phase combinations, respectively, of AO's directed along the C=O bond. Similarly the π and π^* orbitals are formed by combination of the $2p_x$ AO's on the carbon and oxygen atoms, and are directed above and below the yz plane. The non-bonding $\underline{n}$ orbital is derived from the $2p_y$ oxygen AO which lies in the yz plane, perpendicular to the C=O axis. The $\underline{n}\rightarrow\pi^*$ promotion is illustrated in Figure 3.5. The electronic configuration of the ground state is $(\sigma a_1)^2(\pi b_1)^2(\underline{n}b_2)^2$ which gives the state $^1A_1$. The electronic transition of lowest energy results from an $\underline{n}\rightarrow\pi^*$ promotion and the excited electronic configuration $(\sigma a_1)^2$ $(\pi b_1)^2(nb_2)(\pi^* b_1)$ gives the states $^1A_2$ and $^3A_2$.

The electronic transition $A_2 \leftarrow A_1$ is forbidden by the electric dipole selection rules since $A_1 \otimes A_2 \sim A_2$ and none of the dipole moment components transform as A_2. (see Table 3.1) In any given electronic state, however, the molecule may be excited to any of the possible vibrational levels. Each of these levels may be regarded as a vibrational-

---

[d] The ordering of the orbitals follows that given for formaldehyde.[73]

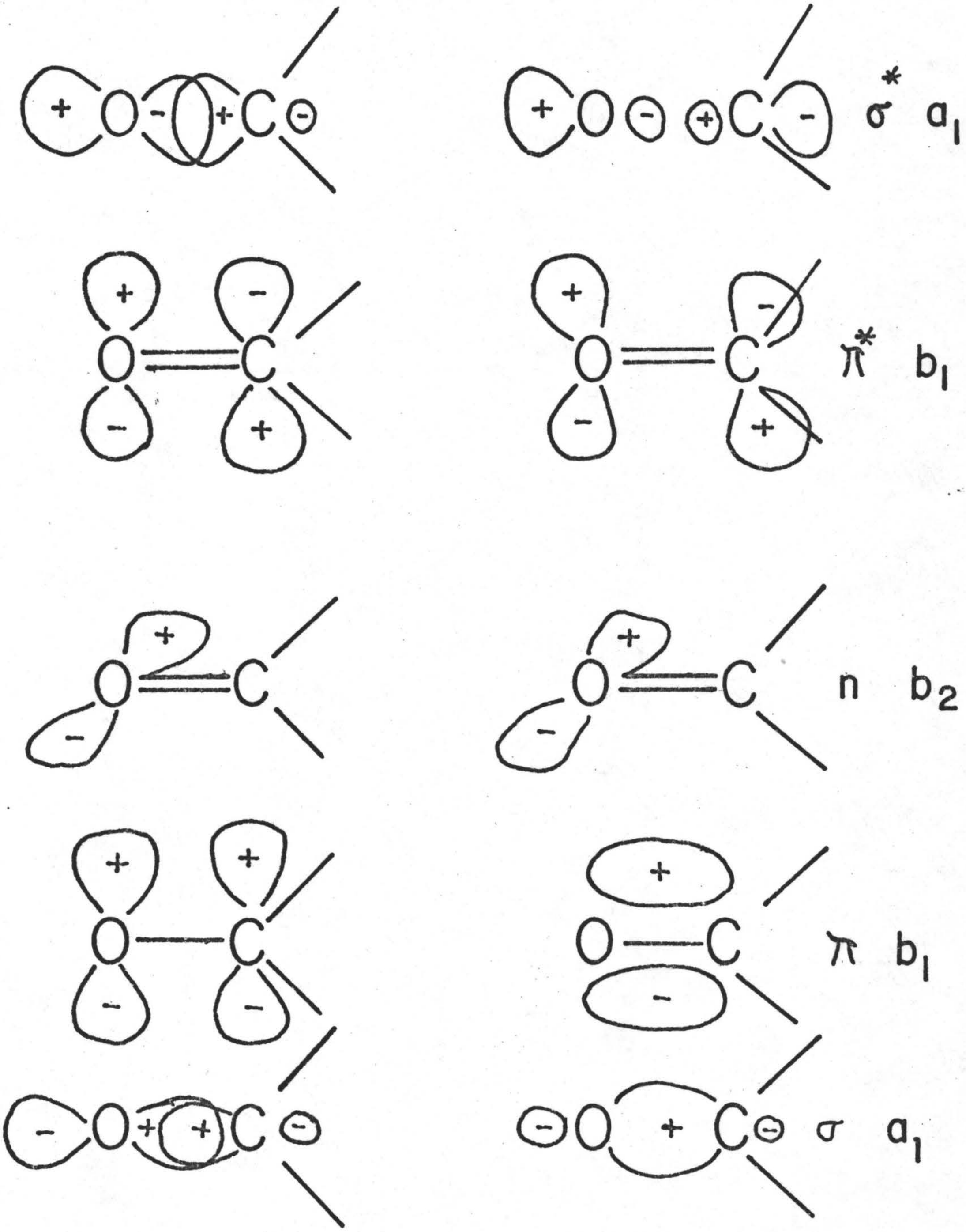

FIGURE 3·4 Electron Density Maxima for Carbonyl Molecular Orbitals

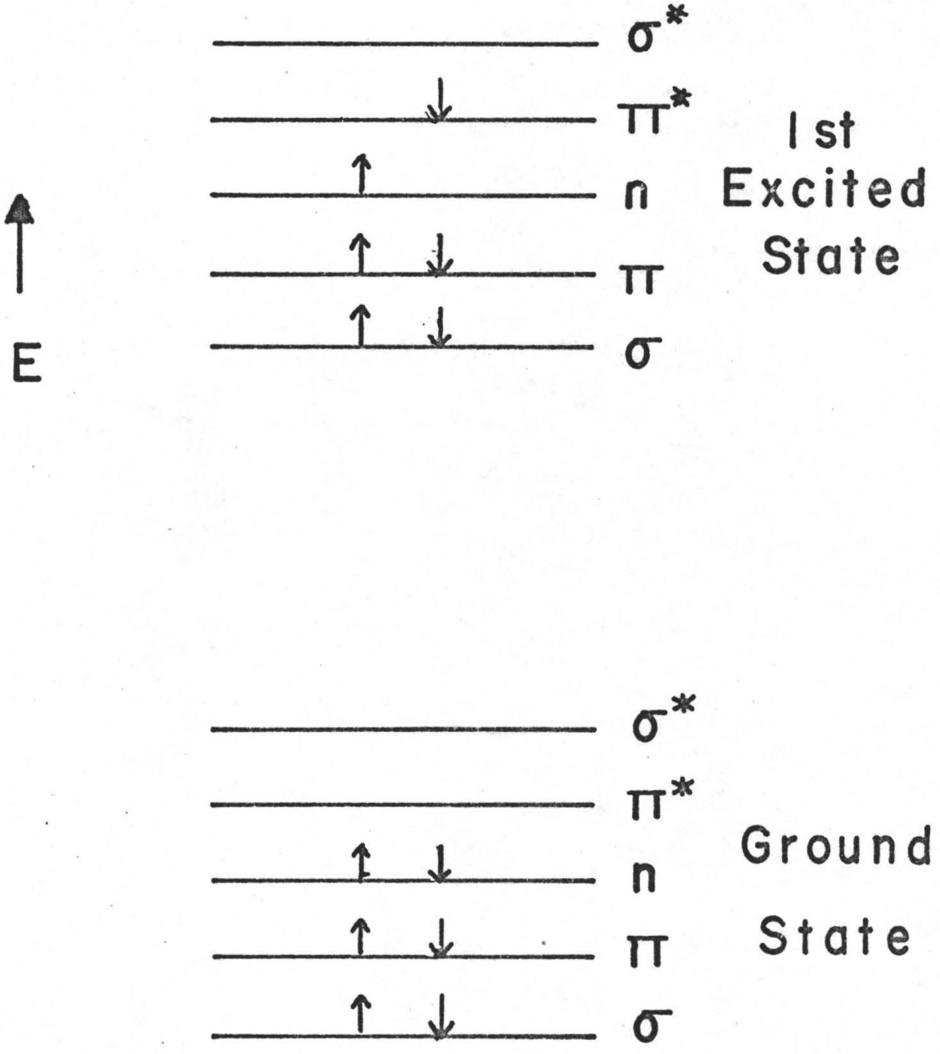

Figure 3·5 n→π* Promotion in the Carbonyl Chromophore

TABLE 3.1

TRANSITION MOMENTS* OF ELECTRONIC OR VIBRONIC TRANSITIONS FOR CYCLOPENTANONE UNDER THE C_{2v} POINT GROUP

C_{2v}	A_1	A_2	B_1	B_2
A_1	M_z	f	M_x	M_y
A_2		M_z	M_y	M_x
B_1			M_z	f
B_2				M_z

---

[*] f, forbidden

electronic state, or vibronic state.

3.4 Vibronic Selection Rules

The vibronic wavefunction, ψ_{ev}, may be written $\psi_e\psi_v$ and the transition moment has the form

$$R_{ev} = \int \psi_e'^{*}\psi_v'^{*}\, M\, \psi_e''\psi_v''\, d\tau_{ev} \qquad (3.6)$$

A transition will occur if the direct product of the vibronic species of the two states involved contains at least one component of the electric dipole moment. Thus while an $A_2 \leftarrow A_1$ electronic transition is forbidden, transitions to levels where various vibrations in these electronic states are excited may be allowed. Vibronic states which can combine with each other are given in Table 3.1.

The intensity of the electronically forbidden transition $A_2 \leftarrow A_1$ depends on the proximity of a third electronic state to which a transition is allowed from the A_1 ground state. The $B_2 \leftarrow A_1$ and $B_1 \leftarrow A_1$ transitions are two possibilities; it will become evident later that the $B_2 \leftarrow A_1$ transition is the more probable one. The $A_2 \leftarrow A_1$ transition could "borrow intensity"[e] because of the mixing of vibronic eigenfunctions of the electronic states A_2 and B_2. On the assumption that the perturbing electronic state has B_2 symmetry, only those vibrational levels of the A_2 electronic state which have the right symmetry to produce a vibronic level of symmetry B_2 will be perturbed and will therefore combine with the ground state A_1. Thus only normal vibrations of species B_1 ($A_2 \otimes B_1 \sim B_2$) are expected to be active in the electronic spectrum. Vibronically allowed (but electronically

---

[e] See reference (7), p. 139.

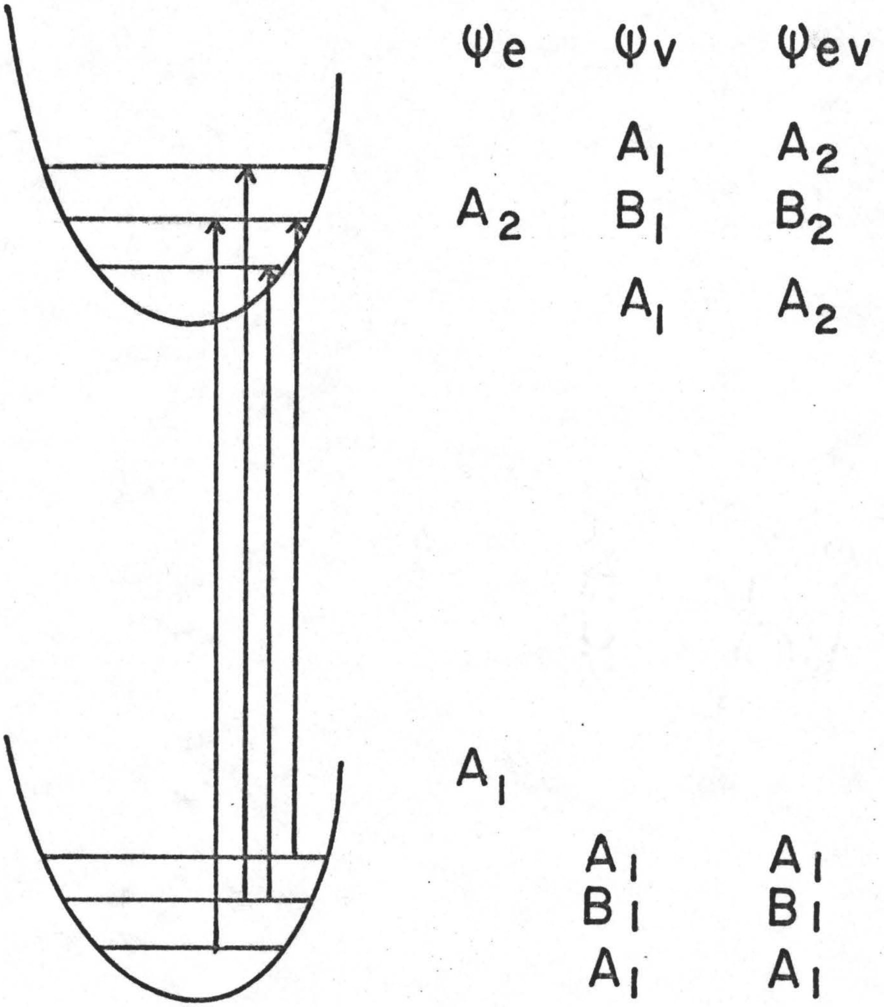

Figure 3·6 Allowed Vibronic Transitions

forbidden) transitions involving the excitation of quanta of a B_1 vibration are illustrated in Figure 3.6.

Vibronic states A_1 and B_1, resulting from the excitation of vibrations of species A_2 and B_2, respectively, in the A_2 electronic state can combine with the A_1 ground state (see Table 3.1) but the resulting bands will be very weak because there can be no "intensity borrowing" from the B_2 electronic state.

In principle, two electronic states of any species can perturb each other if vibrations of the right symmetry are excited, but, according to Herzberg[f], this perturbation will be very weak unless the species of the two electronic states differ only by the species of one of the normal vibrations. That is, the product of the species of a normal vibration and the species of one of the electronic states must equal the species of the other electronic state. For this reason certain combinations of vibrations,[g] while symmetry allowed, are expected to be extremely weak in the spectrum.

3.5 Population of Vibrational Levels in the Ground Electronic State

The relative number of molecules in each vibrational level is approximately proportional to the Boltzmann factor, $e^{-E_v/kT}$, where E_v is the energy of the vibrational level relative to the energy of the lowest (v=0) vibrational level. T is the absolute temperature and k is the

---

[f] See reference (7), p. 67.

[g] For example, if normal vibrations of species A_2 and B_2 are excited in combination, the resulting product species is B_1. Totally symmetric vibrations A_1 in combination with B_1 vibrations give a product species B_1 also.

Boltzmann constant; at 25°C, kT has the value ∼ 200 cm^{-1}. The vibronic ground state is the most densely populated level, and in the absorption spectrum, bands originating from this level are expected to be the most intense. The relative populations of higher vibrational levels vary with temperature and the intensity of the bands originating from these levels will increase with increase in temperature. These bands are called "hot bands". This change in intensity is greatest for bands originating from vibrational levels which have large energy separations from the zero-point level.

3.6 The Franck-Condon Principle

According to Franck's classical description,[h] the geometry of a molecule and the relative momenta of the nuclei remain sensibly unchanged at the moment of an electronic transition. Therefore the geometry corresponding to one of the turning points of a vibration in the excited state is almost identical with the equilibrium geometry in the ground state. Figure 3.7 illustrates[i] that the vertical transition $0 \rightarrow n$ will be the most probable, and therefore the most intense, transition.

---

[h] The principle is discussed in detail in references (5) and (6).

[i] In Figure 3.7, the potential energy V is plotted as a function of a single normal coordinate Q to give, in effect, a section through the polydimensional surface for V.

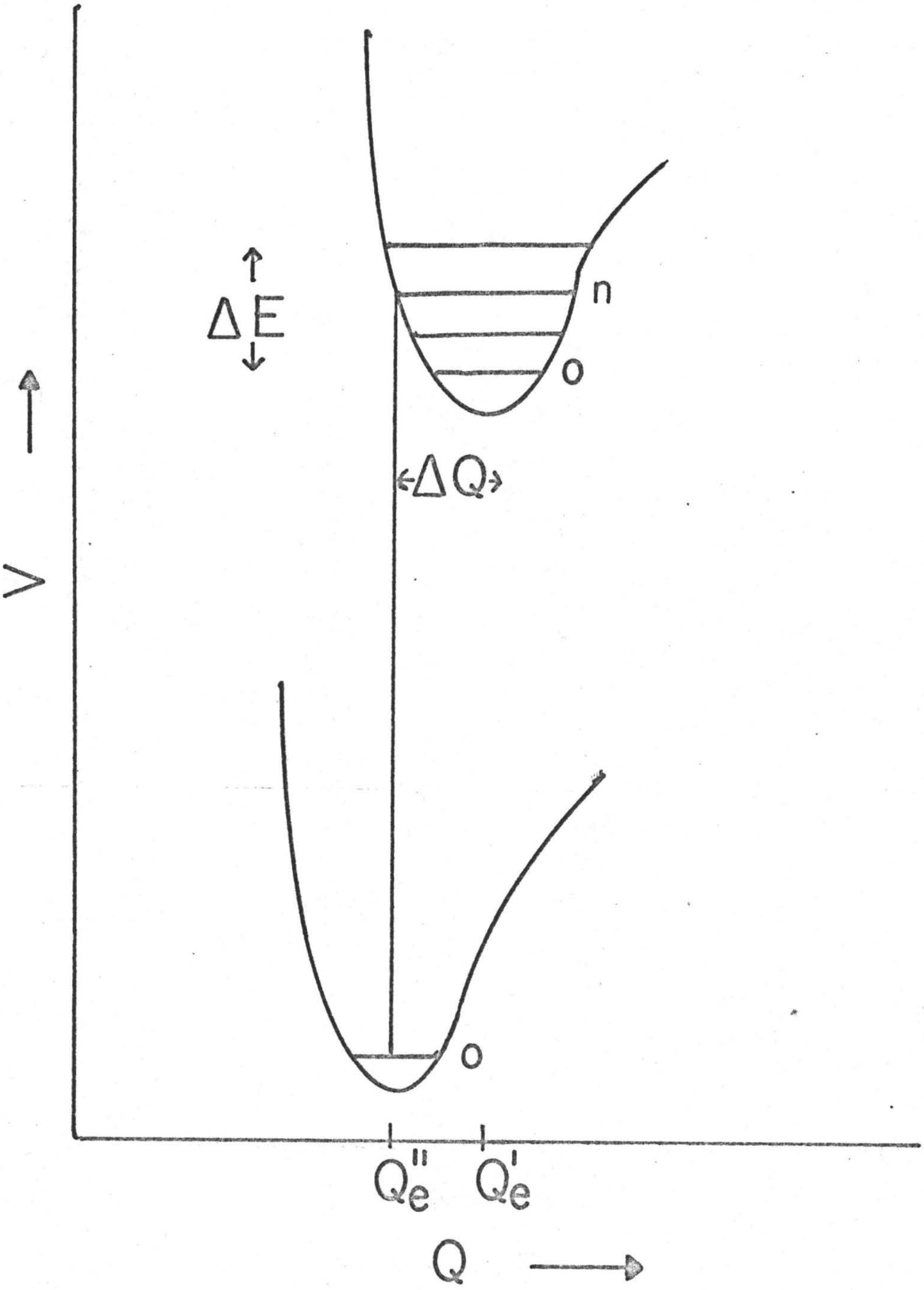

Figure 3.7 The Franck-Condon Effect

According to Condon's[74] quantum-mechanical interpretation[j] of the principle, the relative intensities of various bands are proportional to the Franck-Condon factor, defined by

$$q_{v'v''} = [\ \int \psi^*_{v''} \psi_{v'} d\tau]^2 \tag{3.7}$$

If the electronic transition is accompanied by a large change in the length of one bond or a large change in one bond angle, bands arising from the vibrations whose normal coordinates most closely correspond to the change in geometry will be prominent in the spectrum. The "hot bands" of such vibrations will be more intense than one would expect from the Boltzmann factor alone. For example, in the electronic spectrum of H_2CO, the progression in the out-of-plane bending vibration is prominent.[75] The prediction that the equilibrium geometry in the excited state would be pyramidal instead of planar as in the ground state has been confirmed by rotational analysis of the electronic band spectrum. In the electronic spectra of larger polyatomic molecules, where the rotational structure is too closely spaced to permit rotational analysis, estimates of changes in geometry may be made from the observed intensity distribution of

---

[j] It is assumed that $\int \psi_e'^* M \psi_e'' d\tau$ remains constant and equation (3.6) can be factored into $R_{ev} = \int \psi_e'^* M \psi_e'' d\tau_e \int \psi_v'^* \psi_v'' d\tau_v$. For a forbidden electronic transition, by definition the first factor is zero; however, if there is vibronic interaction, because of the variation of ψ_e with Q, the first factor is non-zero for nuclear configurations which are not totally symmetric. See for example, reference (7), p. 174. If the variation of ψ_e with Q is slow, the first factor may be treated essentially as a constant, so that

$$R_{ev} = \overline{R}_e \int \psi_v'^* \psi_v''\ d\tau_v$$

vibrational bands.

3.7 The Estimation of Geometry Changes

For a nearly harmonic potential function, it can be seen from Figure 3.7 that the expression

$$\Delta E = \frac{1}{2} k'(\Delta Q)^2 \tag{3.8}$$

roughly represents the separation, ΔE, of the 0,0 band from the most intense member (the 0→n band) of a progression. k' is the force constant for the normal vibration in the excited state and ΔQ is the change in the corresponding normal coordinate. Equation (3.8) can be used to obtain a rough estimate of the changes in geometry of the equilibrium configuration in the upper state relative to the lower state.

Various equations have been proposed[72,73,74] to express empirical relationships between the force constants of bonds, or the frequencies of vibration, and interatomic distances. Badger[76] proposed (for diatomic molecules in particular) the equation

$$k_0(r_e-d_{ij})^3 = 1.86 \times 10^5 \tag{3.9}$$

where k_0 is a force constant in dynes/cm, r_e is the interatomic distance in Å, and d_{ij} is a constant (equal to 0.68 for the vibration of a diatomic molecule having both nuclei in the first row of the periodic table).

Douglas-Clark's[77] rule has the form[k]

$$\omega_e r^3 = \text{constant} \tag{3.10}$$

Layton et al.[78] have plotted the carbon-oxygen bond stretching vibrational frequency against bond length for various molecules containing a carbon-oxygen group. If such a frequency is known, the corresponding bond length can be estimated from their graph.

3.8 The Rotational Fine Structure of Electronic Band Spectra

The moments of inertia of a molecule about the three mutually perpendicular principal axes of inertia, a, b and c, are designated by I_a, I_b and I_c in order of increasing magnitude. Molecules may be classified in five categories depending on the relative values of the moments of inertia:

$I_a=I_b=I_c$	spherical top
$I_a < I_b=I_c$	prolate symmetric top
$I_a=0,\ I_b=I_c$	linear(special prolate case)
$I_a=I_b < I_c$	oblate symmetric top
$I_a<I_b<I_c$	asymmetric top

---

[k] Strictly, the expression (3.10) does not apply to different electronic states of the same molecule; instead the relationship $r_e^2\omega_e$ = constant holds fairly well. Either expression should be applied only to diatomic molecules; the agreement between observed r_e and ω_e values and the values obtained from these expressions is ±5%. The error is expected to be larger for polyatomic molecules. See reference (6), p. 456 ff.

Rotational constants A, B and C are defined by

$$A = \frac{h}{8\pi^2 cI_a}, \quad B = \frac{h}{8\pi^2 cI_b}, \quad C = \frac{h}{8\pi^2 cI_c} \qquad (3.11)$$

where $\frac{h}{8\pi^2 c} = 16.852$ and I is in amu-Å^2. The asymmetry parameter κ is defined by

$$\kappa = (2B-A-C)/(A-C) \qquad (3.12)$$

For an oblate symmetric top κ is +1, (A=B) and for a prolate symmetric κ is -1 (B=C). κ=0 corresponds to the highest degree of asymmetry where $B = \frac{1}{2}(A+C)$.

The rotational term values (in cm^{-1}) for a prolate symmetric top in a vibronic state v are given by

$$F_v(J,K) = B_v\, J(J+1) + (A_v-B_v)K^2 \qquad (3.13)$$

where J is the total angular momentum quantum number and K is the quantum number for the component of the total angular momentum along the figure axis (a axis here). K has the values 0, 1, 2 ... $|J|$; all levels with K values greater than zero are doubly degenerate.

The rotational term values for a vibronic state, v, of a molecule which is an asymmetric top are given by

$$F_v(J,\tau) = \tfrac{1}{2}(A_v+C_v)\, J(J+1) + \tfrac{1}{2}(A_v-C_v)E_v(\kappa) \qquad (3.14)$$

where τ is a running number which labels different levels and $E(\kappa)$ is a function which depends on κ, J and τ.

The rotational term values for a vibronic state, v, of a molecule which is nearly a prolate symmetric top are given approximately by

$$F_v(J,K) = \overline{B}_v\, J(J+1) + (A_v-\overline{B}_v)K^2 \tag{3.15}$$

where

$$\overline{B}_v = \frac{1}{2}(B_v+C_v)$$

In asymmetric top molecules,[1] K is not a valid quantum number, although for small asymmetry it is still defined. The double degeneracy of the $K \neq 0$ levels is removed in a top that is slightly asymmetric. The deviations from the symmetric top approximation decrease as K increases.

---

[1] See reference (5), pp. 304-308.

CHAPTER 4

EXPERIMENTAL WORK

4.1 Origin, Properties and Purity of Cyclopentanone

Cyclopentanone (CPH8) (Eastman) was purified by distillation under vacuum. CPD4 (5 g.) and CPD8 (2 g.) were supplied by Merck, Sharp and Dohme, Montreal. All samples were vacuum distilled immediately before observation of their spectra. The samples were stored under vacuum at -78°C in glass bulbs surrounded with aluminium foil to minimize photodecomposition.

Pure cyclopentanone is a clear, colourless liquid which boils at 130.6°C and has a vapour pressure of ∿ 10 mm. at 25°C. Vapour pressure measurements have been reported[79]; from the published data, a plot of vapour pressure as a function of temperature was made (see Figure 4.1).

Cyclopentanone is easy to handle, although it dissolves stop-cock grease. Teflon stop-cocks were used on most of the apparatus; Kel-F grease was used to lubricate the large glass stop-cocks on the multiple reflection cells.

The purity of the cyclopentanone (CPH8) is estimated to be quite high. The nmr spectrum agreed with the published spectrum[31] and showed no impurities. The infrared and Raman spectra of CPH8 and CPD4 showed essentially the same bands as those reported by previous workers[15,16,17,19]. Each of the high resolution ultraviolet spectra for the three isotopic species was free from bands of the other two species. In studies on enol titration, cyclopentanone was found to have an abnormally low enol

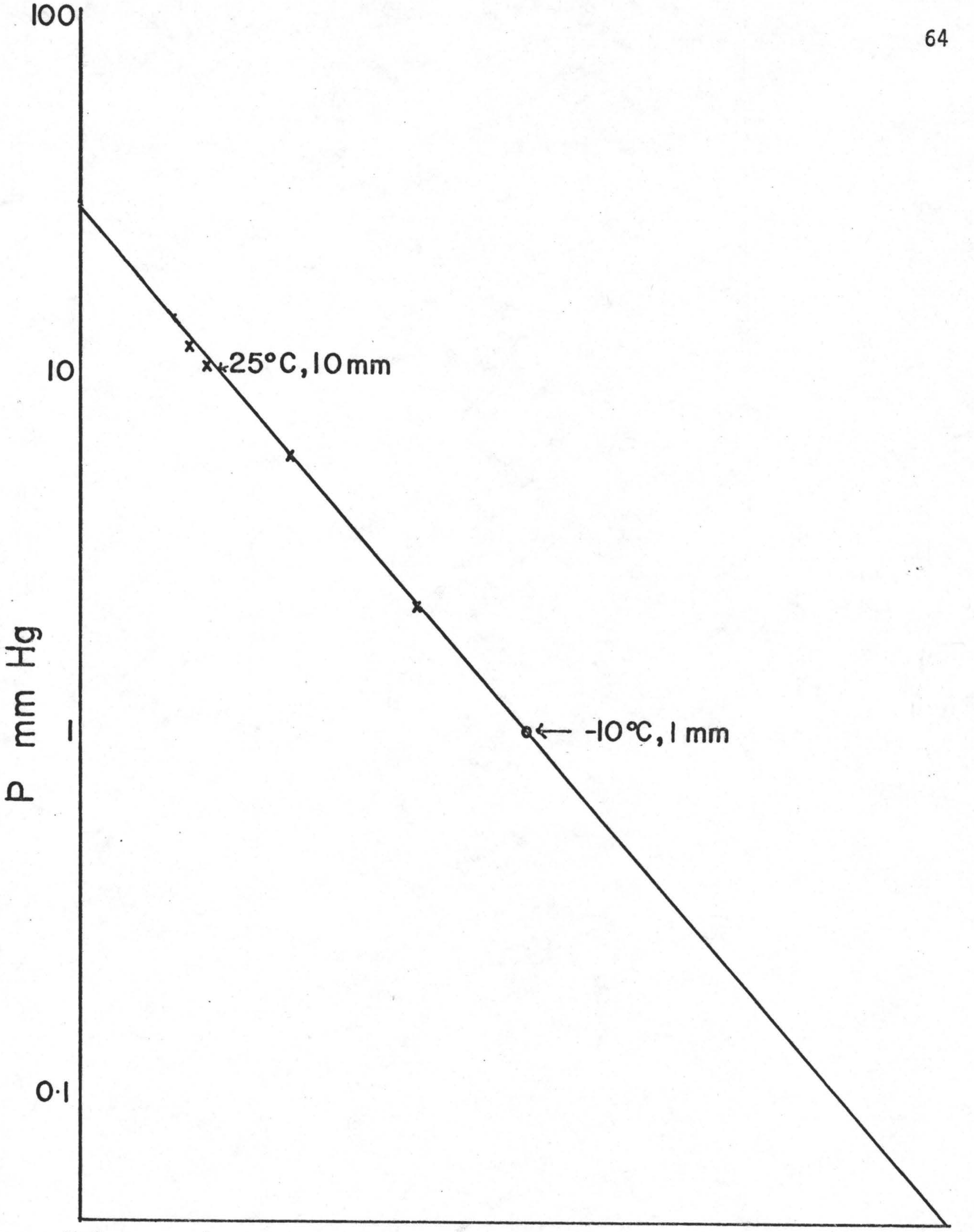

FIGURE 4·1· Vapour Pressure of Cyclopentanone.

content -- only 0.09% compared with 0.55% for cyclobutanone and 1.18% for cyclohexanone[80]. Little interference in the infrared spectra arising from the enolized form is expected. There were no bands observed in the C = C (1610 - 1660 cm^{-1}) or O-H (3300 cm^{-1}) regions of the infrared spectrum, either in this work or in previous studies. Photodecomposition of cyclopentanone by ultraviolet light is known to produce 4-pentenal; however, the quantum yield of 4-pentenal at 5 mm pressure of cyclopentanone (irradiated with light at 3000Å) is only 0.075.[29]

The infrared spectrum of CPD8 showed only a faint band at the same frequency as that of the C-H stretching band in CPH8. Towards the end of this work, the C-H band in CPD8 showed an increased intensity; apparently, the isotopic purity of the CPD8 has deteriorated.[†]

4.2 The Infrared Spectra

The infrared spectra of CPH8, CPD4, and CPD8 were recorded on a Perkin-Elmer model 521 grating spectrophotometer over the region 4000 - 250 cm^{-1}. The spectrum of polystyrene film was superimposed on each sample spectrum for calibration of wavenumber. The uncertainty in the measurement of the cyclopentanone vibrational frequencies is estimated to be ± 0.5 cm^{-1}.

For the region 4000 - 400 cm^{-1} vapour phase spectra at room temperature were obtained with the samples contained in a 10 cm cell equipped with KBr windows. The liquid phase spectra over the same region were obtained with the samples in a 0.1 mm path liquid cell fitted with KBr windows. For the region 600 - 250 cm^{-1} the samples were contained either in a 10 cm vapour cell with polyethylene windows or in a thin polyethylene

---

[†] This deterioration was verified by Dr. D. B. MacLean, who kindly did a mass spectral analysis.

liquid cell. The liquid cell was constructed from two rectangular pieces of rigid polyethylene, the edges of which were heat sealed on all four sides to make a closed cell. The liquid sample[a] was then injected into the cell by means of a hypodermic syringe, and the resulting tiny hole was heat sealed to prevent evaporation.

The Perkin-Elmer 301 grating spectrophotometer was used to search for infrared bands at frequencies below 600 cm^{-1}. The polyethylene liquid cell was used over the region 600 - 30 cm^{-1} (CPH8 only).

It was noticed that the liquid sample acquired a faint yellow colour after an infrared run. Decomposition had apparently occurred. While the photodecomposition by ultraviolet light is well known, no photodecomposition by infrared light has been reported. Therefore, it was decided to irradiate a pure sample of cyclopentanone with infrared light and to look for resulting impurities. A 10 cm quartz cell was filled with freshly distilled (colourless) cyclopentanone and mounted at one of the focal points of an ellipsoidal reflector; a 1 kw. infrared lamp was placed at the other focal point. An orange filter cutting out all wavelengths below 5700Å was placed around the cell. The cell was cooled by air from a fan throughout the exposure of 20 hours. In order to check for impurities, nmr spectra were run before and after irradiation; for the nmr work, a sample concentration of 10% cyclopentanone in spectrograde CCl_4 was used. The spectra after irradiation showed weak bands which

---

[a] The polyethylene liquid cell was used for CPH8 only; there was not sufficient CPD4 or CPD8 available.

were not present in the spectra of pure cyclopentanone, but it was not possible to identify the impurities.

Overtones of the infra-red frequencies of CPH8 were searched for in the near infrared region of 11,000 - 4000 cm^{-1} with the Cary model 14 recording spectrophotometer. Liquid samples were contained in quartz cells with path lengths ranging from 0.1 mm to 10 cm.

During the course of this work, a multiple reflection cell became available for use with the Perkin-Elmer 301 instrument. The region from 600 to 20 cm^{-1} was examined for low frequency fundamentals of CPH8, CPD4 and CPD8 at path lengths of 1 m and 5 m at $\sim$ 10 mm vapour pressure. No new bands were observed in this region although the band at 467 cm^{-1} in CPH8 (438 cm^{-1} in CPD4, 433 cm^{-1} in CPD8) was observed with greater intensity and resolution than was obtained on the Perkin-Elmer 521. The B-type contour of the band was clearly resolved (see Figure 5.8). The observed frequencies and the band assignments for the infrared spectra will be presented in Chapter 5.

4.3 The Raman Spectra

Liquid samples of CPH8, CPD4 and CPD8 were injected into Pyrex melting point tubes by means of a fine hypodermic needle. Raman spectra were excited by the 6328Å line of a helium-neon laser and were recorded on a Czerny-Turner-type Spex laser Raman recording spectrograph, which contained a double monochromator. The instrument settings were: input response, 3 seconds; speed, 170; all slits, 0.2 mm. The input amplification setting was 10^{-9} for most of the spectrum; at this setting the very strong symmetrical breathing mode band at 888 cm^{-1} in CPH8 was off scale, but it could be brought on scale on the 10^{-8} range. Very weak bands near the exciting line were brought out on the 10^{-10} range. At least three spectra were run for each sample. First a spectrum with polarized incident (laser) light and no analyser was recorded. Then the analyser was inserted between the sample and the entrance slits and spectra were run under identical instrumentation conditions (a) with the analyser at 0° and (b) with the analyser at 90°. From these last two spectra depolarization ratios, ρ, could be measured. The instrument contained a depolarizer between the analyzer and the entrance slit, so that errors due to polarization of light by the grating in the monochromator were avoided. The CCl_4 line at 459 cm^{-1} was recorded under conditions identical to (a) and used as a standard of intensity. This peak was obtained on the 10^{-8} range and was more intense than the peak at 888 cm^{-1}. The wavelengths of the peaks were read in Å from a scale which was marked every 5Å. (Calibration with a hollow cathode iron lamp has shown this scale is not significantly in error). For the cyclopentanone bands the average of three readings which gave agreement to within 1Å was taken. The vacuum corrections were calculated for some peaks but were found to be within the experimental error: they could be approximated by subtracting 0.5 cm^{-1} at 1700 cm^{-1} and 0.3 cm^{-1} at 500 cm^{-1}. A curve for making the vacuum corrections was drawn. The uncertainty in the frequency measurements is estimated to be about ± 2 cm^{-1}. The spectra of CPH8 and CPD4 agreed very well with the published spectra[17].

4.4 The Ultraviolet Spectra

4.4.1 Low Resolution

For preliminary work the vapour phase absorption spectrum of cyclopentanone (CPH8 only) was observed over the region 7000Å to 2000Å on a Cary model 14 recording spectrophotometer. A 10 cm quartz cell, wound with nichrome wire, which could be heated electrically up to ∿ 150°C was used. A 50 cm quartz cell containing CPH8 vapour was used for observation of the spectrum on a Hilger quartz model E492 Littrow prism spectrograph.

Most of the spectra were obtained on a Bausch and Lomb 1.5 m grating spectrograph, model 11. The region 3700 - 7000Å in the first order or the region 1850 - 3700Å in the second order could be photographed in a single exposure. The instrument has reciprocal dispersions at the film of 14.8 Å/mm and 7.4Å/mm for these two orders, and theoretical resolving powers of 35,000 and 70,000 respectively. A slit width of 10 μm was used. A 50 cm cell containing the vapour was used when recording the diffuse, high energy bands at wavelengths down to 2500Å. Much longer path lengths were required to observe the weaker long wavelength bands. A 1.8 m. multiple reflection cell of the White type[81] was used to obtain path lengths from 3.6 to 72 m. The light source was a 250 watt 115 V. D.C. high pressure Osram Xe arc lamp which was run at 15 amps. The banded absorption spectrum of cyclopentanone appears in the region 2500 - 3500Å and so pictures were taken in the second order of the Bausch and Lomb spectrograph. The separation of the first and second order spectra was accomplished by the use of different combinations of optical filters and spectral emulsions. In a search for other systems to longer wavelengths, the first order spectrum was photographed at pressure paths of up to 6m - atm. Cyclopentanone slowly attacked the mirrors of the multiple reflection cell and so they had to be cleaned and realuminized every few days.

The temperature dependence of the ultraviolet absorption spectrum was studied over the range 25°C to 170°C. The Bausch and Lomb spectrograph was used in conjunction with the 1.8 m. multiple reflection absorption cell. The cell was wound with nichrome wire and asbestos paper so that it could be heated electrically up to ∿ 200°C. Two separate cylindrical heaters, fitted over the end pieces of the cell, were maintained at ∿ 10C° higher than the main body of the cell to prevent condensation of the compound on the mirrors and windows. The temperature was recorded by a chromel-alumel thermocouple and by a thermometer placed inside the cell. Only a few pictures were obtained because several practical difficulties were encountered. Spectra could not be taken at - 78°C because the vapour pressure of cyclopentanone is so low that no absorption is observed, even at path lengths of 80 m. As the temperature is increased the discrete spectrum is gradually obscured by an intense continuum shifting towards lower frequencies. Also, at high temperatures the compound decomposes and the mirrors are quickly attacked.

Attempts to photograph the emission spectrum of cyclopentanone vapour on the Bausch and Lomb spectrograph were unsuccessful. A flow apparatus consisting of auxiliary traps and a 25 cm quartz cell for emission was used. The apparatus was supported at several points on a rigid, portable rack constructed of aluminium rods. The vapour was pumped through the cell, with the entrance side-arm being nearest the slit of the spectrograph and the exit side-arm at the opposite end of the cell. The vapour pressure was regulated by means of a Teflon capillary stopcock. The discharge was excited by means of a Tesla coil at the exit sidearm. With the vapour pressure as high as would sustain the discharge, a very deep blue discharge, constricted into a thin line down the center of the cell, was observed. Under these conditions, the emission spectrum of propynal was obtained by Moule[82] with a relatively small proportion of impurity bands. Photographs of the emission from cyclopentanone were taken with exposure times varying from 1/2 hr. to several hours but only impurity bands were observed. The attempt was finally abandoned.

4.4.2 High Resolution Spectra

The high resolution absorption spectra of CPH8, CPD4 and CPD8 were photographed in the first order of a 20-foot Ebert grating spectrograph[83]. A few of the sharper bands were photographed in the second order. The reciprocal dispersion at the plate at 3300Å is 0.72 Å/mm in the first order and 0.27 Å/mm in the second order. The theoretical resolving powers are 150,000 and 300,000 in the first and second orders, respectively, and the practical values have been found to be close to these values. The optimum slit settings range from 25 to 35 μm over the region 3000 - 3500 Å.

1.8 m. and 6m reflection cells were used to obtain long absorption paths. The procedure for alignment of the multiple reflection cells described by Herzberg and Bernstein was used[84]. With a 450 watt 115V. D.C. Xe arc run at 23 amp., 40 traversals of the 1.8m cell and 80 traversals of the 6m cell could be obtained. Spectra were photographed over the region 3100Å to 3500Å with pressure paths of 0.1 to 1 m - atm. in the 1.8 m cell and over the region 3300Å to 3500Å with pressure paths of up to 6 m - atm. in the 6 m cell.

4.4.3 Photography and Measurements

The spectra obtained on the grating spectrographs were recorded on Kodak Spectrum Analysis No. 1 and Ilford FP3 35 mm films. For the Hilger spectrograph, Kodak Spectrum Analysis No. 1 plates (thin glass, 2" x 10") were used. The plates and films were developed for four minutes in Kodak D-19 developer, rinsed, fixed for ten minutes in Kodak acid fixer, washed for at least thirty minutes in running water, and suspended with clamps to dry in the air. The temperature of the solutions and rinse water was kept at 68°F. Enlargements were printed on Kodak Kodabromide E4 single weight photographic paper. The prints were developed in a dilute D-19 solution for varying times (usually about two minutes), fixed for ten minutes, washed, and dried.

For calibration of the spectra, an iron emission spectrum was recorded adjacent to each absorption spectrum. The iron spectra were excited either by a Pfund arc run at 4 amps. or by a neon-filled hollow cathode iron lamp run at 20 milliamps; the exposure times were about 2 seconds and 5 minutes, respectively. Accurate values for the iron and neon wavelengths were obtained from the M.I.T. tables[85]. Conversion to vacuum wavelengths was made using Edlén's tables[86]. Accurate values of the vacuum wavenumbers of the iron lines were also available in a set of N.R.C. tables[87]. Sharp band heads together with selected iron lines were measured from first order Ebert films on a travelling microscope with a precision of ~ 0.001 mm. The error is estimated to be within about ± 0.2 cm^{-1}. The wavenumbers of band heads are listed in Table 6.5. The band heads need not necessarily coincide with the band origins, and so the errors in the latter may be greater than 0.2 cm^{-1}. Wavenumbers of bands which were weak or diffuse were measured from enlarged photographic prints. The agreement between different measurements was within 0.2 cm^{-1}. (see Table 6.5). The wavenumbers of diffuse bands at high frequencies (photographed under low resolution) were measured from traces made with a Joyce-Loebl Mk III C double beam recording microdensitometer. The diffuseness caused large uncertainties in measurement of the band centers. The errors are estimated to increase from 5 - 10 cm^{-1} at 3000Å to about 40 cm^{-1} at 2500Å. See Table 6.4.

CHAPTER 5

THE INFRARED AND RAMAN SPECTRA

5.1 Introduction

The objective of this part of the research is both to help place the assignment of the fundamental modes of vibration on a firmer basis, and, in connection with the work on the ultraviolet spectrum, to determine the frequencies of the oxygen wagging and ring puckering modes.[a]

A complete assignment of the thirty-six normal modes of vibration is a complex task that invariably must lead to some uncertainties. Reasonable assignments, however, can be made for most of the frequencies observed. Although the vibrational spectra of CPH8 have been discussed many times,[13-25] and those of CPD4 twice,[16,17] none of the previous workers has made a comparative study of three isotopic species of cyclopentanone. The spectra of CPD8 have not been previously reported at all. The results of this section confirm and complement the results of previous workers on CPH8 and CPD4. In addition, measurements of the spectra have been extended into both the near and far infrared regions.

As discussed in Chapter 2, the application of new group theoretical ideas makes it possible to treat cyclopentanone as a non-rigid molecule

---

[a] Vibrational modes of b_1 symmetry species are expected to be active in the ultraviolet spectrum. (see section 3.4).

belonging to a point group isomorphous with C_{2v}.[b] In the discussion of the spectra, the representations of the C_{2v} point group can still be used to classify the states of the molecule. It is convenient to designate the symmetry species of the irreducible representations by the symbols of the C_{2v} point group.

Cyclopentanone has 36 normal modes of vibration and under the C_{2v} point group these comprise 11 of a_1 symmetry, 7 of a_2 symmetry, 8 of b_1 symmetry and 10 of b_2 symmetry. The conventional method of labelling vibrations will be used. Thus ν_1-ν_{11} are totally symmetric modes of species a_1; ν_{12}-ν_{18} are modes of species a_2; ν_{19}-ν_{26} are modes of b_1 symmetry; and ν_{27}-ν_{36} are modes of b_2 symmetry.

It is found empirically that the motions of certain groups of atoms present in different molecules consistently give rise to "characteristic frequencies"; that is, absorption bands in the same spectral regions. Characteristic group modes arise from the vibrations of groups in the molecule, and their frequencies are only slightly affected by the molecular framework to which the group is bonded. In a complex molecule, some of the observed frequencies may be assigned to the fundamental transitions of characteristic groups in the molecule by means of correlations with frequencies of simpler molecules which have been analyzed mathematically. Frequencies for the non-characteristic fundamentals (mainly those associated with the molecular framework) are then selected from the remaining

---

[b] Reitz[15] assumed the rigid molecule cyclopentanone was C_{2v} planar; Rey-Lafon and Forel[19] assumed it was C_s.

unassigned bands in the spectrum, as dictated by experience.[88,89] The vibrations of cyclopentanone may be sorted into the following three groups:

(1) the vibrations of the -CH$_2$- groups,
(2) the vibrations of the ring, and
(3) the vibrations of the -C=O group.

5.2 The Group Vibrations

5.2.1 The Vibrations of the -CH$_2$ Groups

The vibrations of a single -CH$_2$- group[90] are illustrated in Figure 5.1(a). In cyclopentanone, the simultaneous motions of the four -CH$_2$- groups give rise to four symmetric stretching modes, four asymmetric stretching modes, four deformation modes, four wagging modes, four twisting modes, and four rocking modes. Figures 5.1(b) and (c) show schematically the possible phase combinations and symmetry species for all these modes.

Because the CH bond stretching motions are localized within the -CH$_2$- groups, the frequencies arising from the eight C-H stretching vibrations will be concentrated in two main groups, one group comprising the frequencies of the symmetrical modes, and the other, the asymmetric. Each group will have four components because of the four possible phase combinations; these components are spectroscopically unresolved in most molecules having four or more -CH$_2$ groups, but they were resolved in the vapour phase spectra of cyclopentanone, recorded on the Perkin Elmer 521 (see Figure 5.4). ?.

In the deformation modes, the motions are also well localized within the -CH$_2$- groups, and so the resulting four fundamental frequencies will fall in a narrow spectral region. (Two or more may not even be separately resolved).

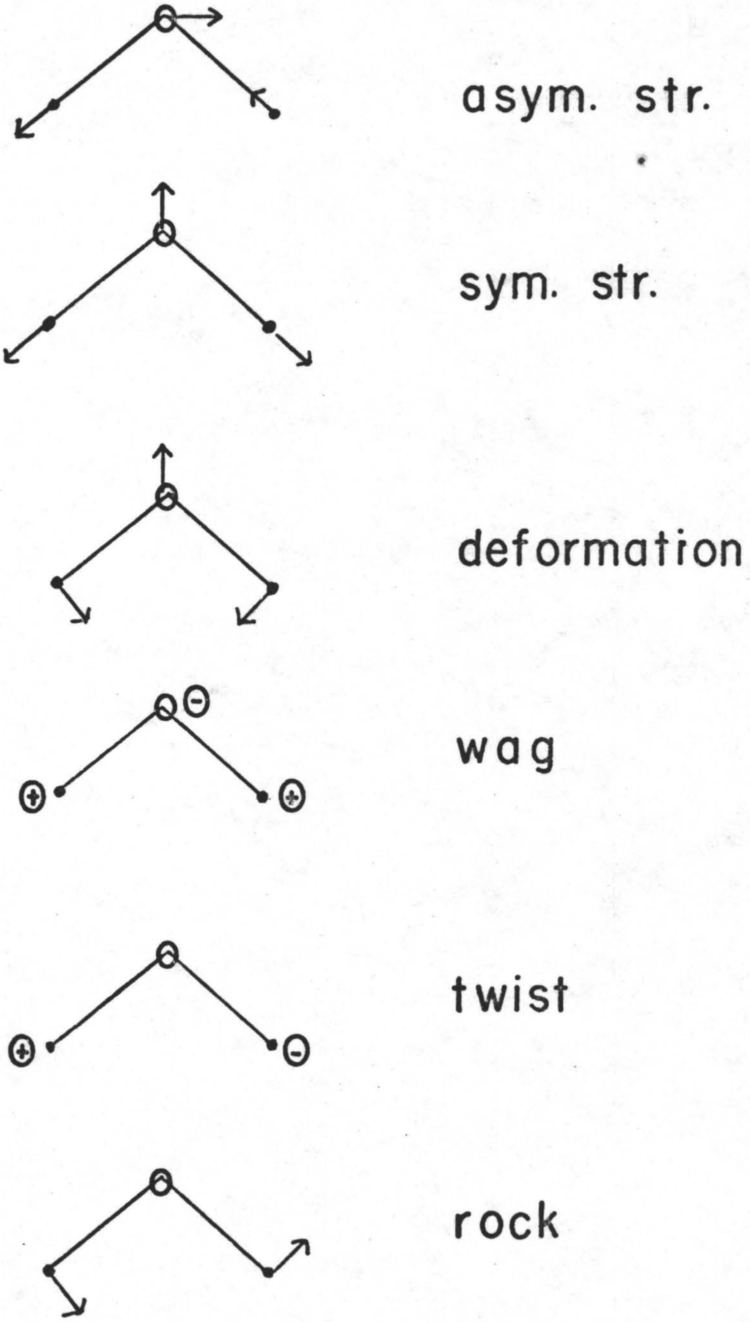

Figure 5-1 $-CH_2-$ Group Vibrations.

(a) A Single CH_2 Group.

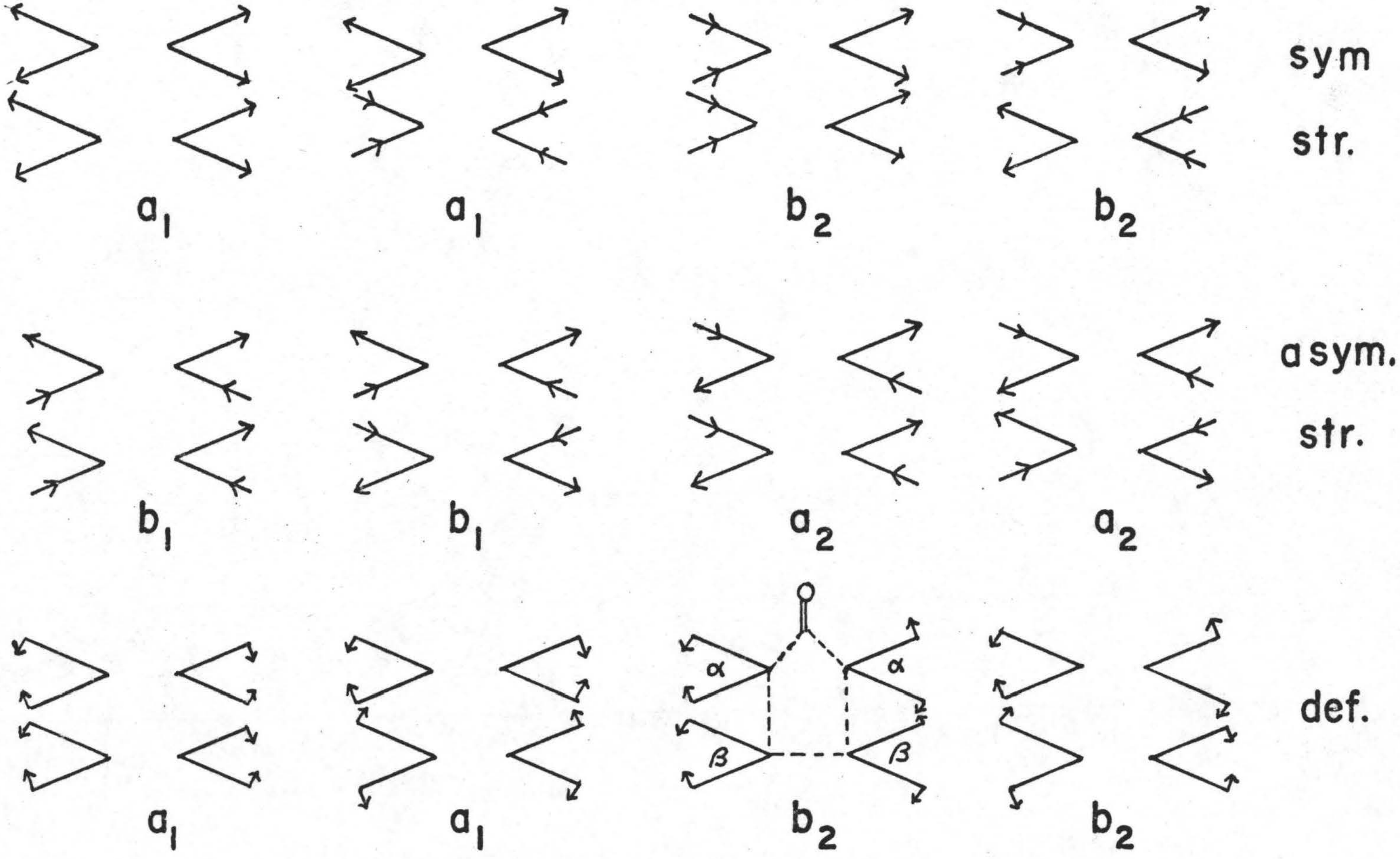

Figure 5·1 (b) -CH_2- Group Vibrations in Cyclopentanone.

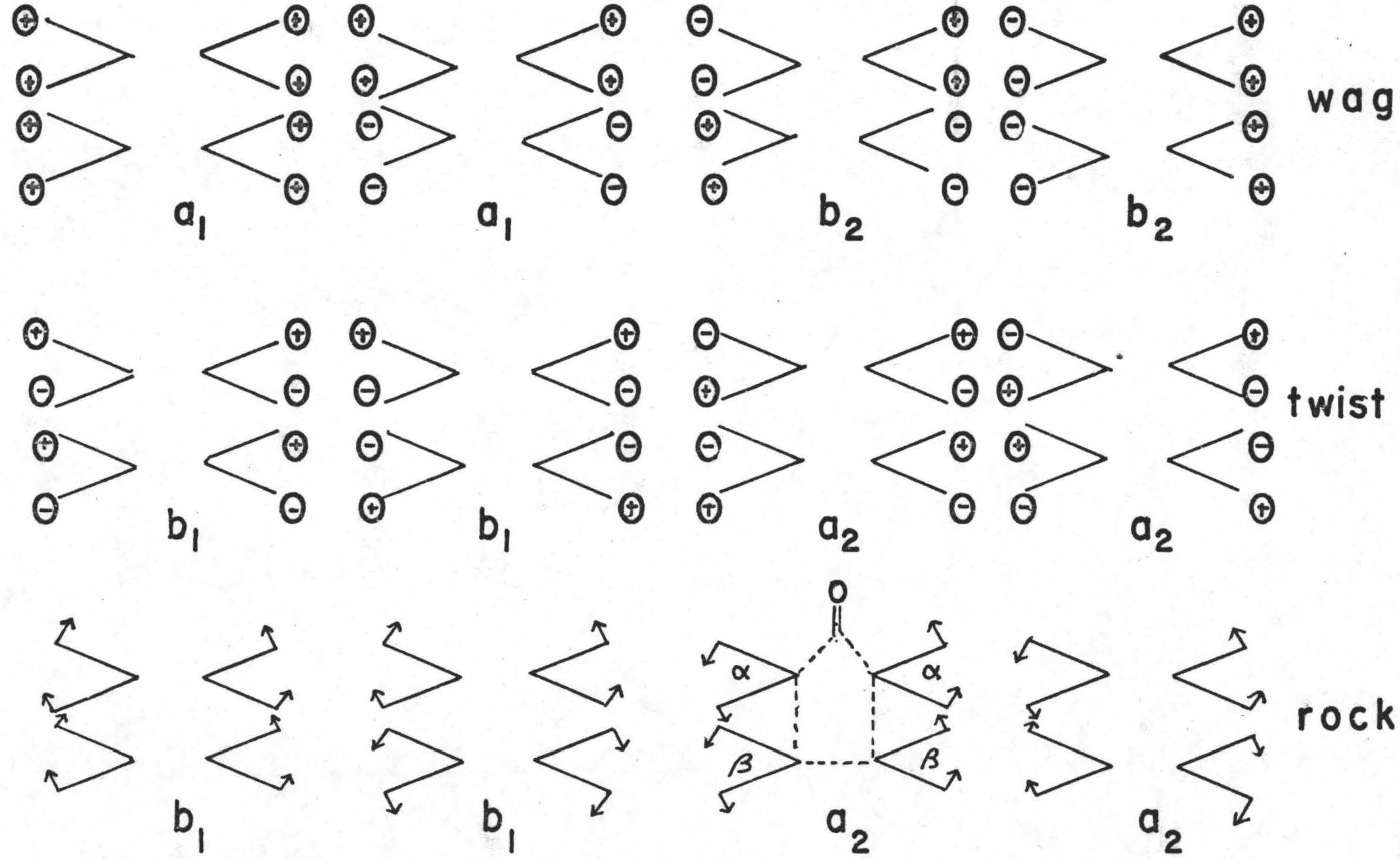

Figure 5·1 (c) $-CH_2-$ Group Vibrations in Cyclopentanone.

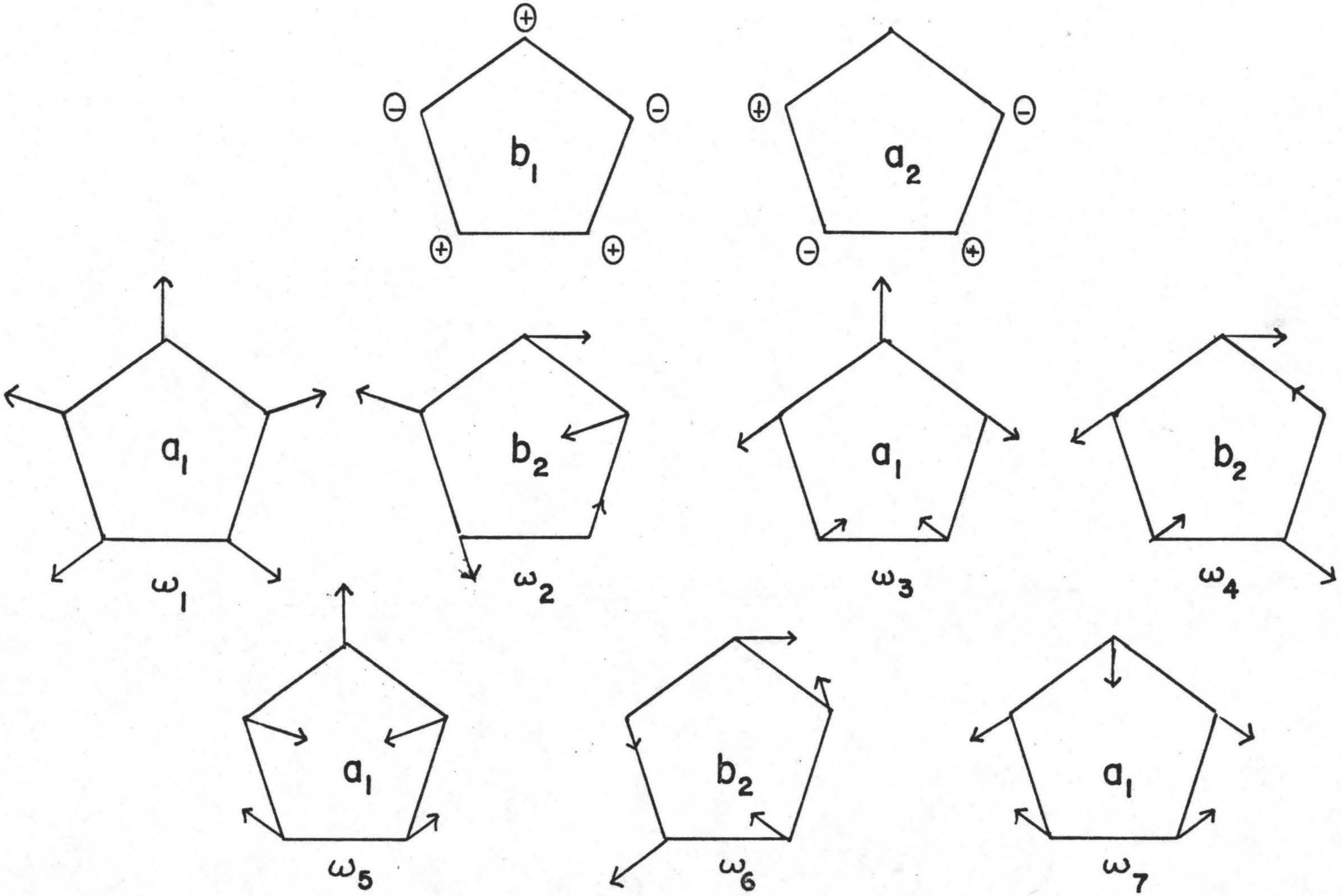

Figure 5·2 The Vibrations of the Five Membered Ring Skeleton.

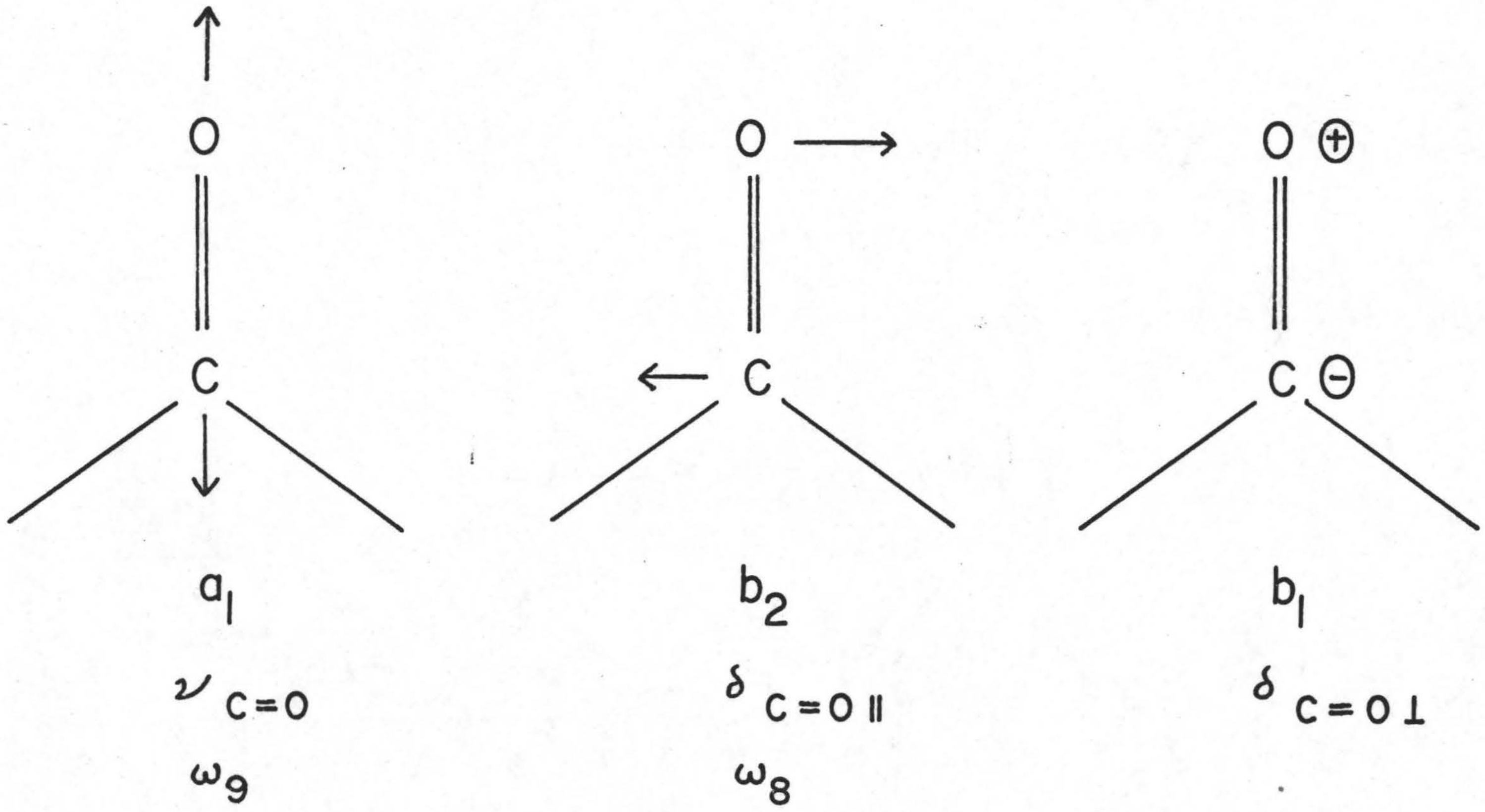

Figure 5·3 The Vibrations of the -CO Group

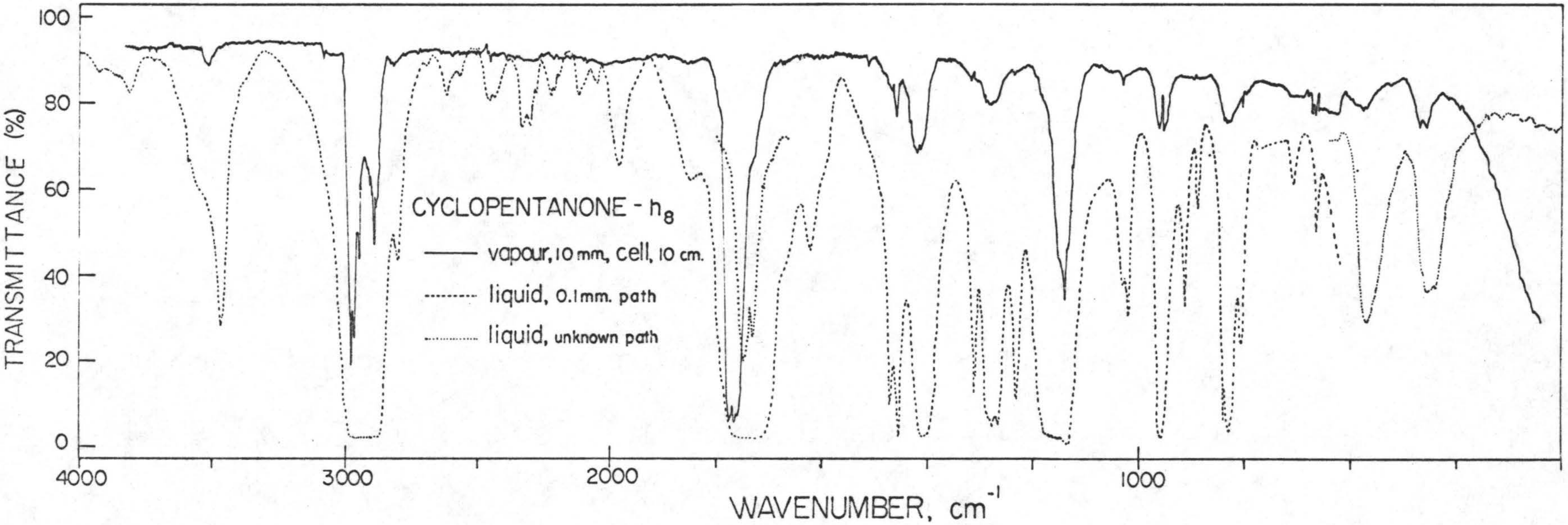

Figure 5·4 The Infrared Spectrum of CPH8

In the wagging, twisting and rocking modes, however, the atoms adjacent to each $-CH_2-$ group will be mechanically involved in the vibrations. As a result, there will be coupling between adjacent $-CH_2-$ groups and the frequencies of the four wagging modes, for example, will not be confined to a narrow spectral region. The same applies to the twisting and rocking modes, and the frequencies of all these modes are difficult to correlate. A further aid to the assignment of the $-CH_2-$ group modes is their frequency change on deuteration. These changes are expected to be much greater for such modes than for motions of the carbon ring or carbonyl group.

5.2.2 The Vibrations of the Ring Framework

There are nine vibrational modes associated with the five-membered ring;[15,89,90] that is, with the carbon atom skeleton of the molecule. These are shown schematically in Figure 5.2. If the ring were planar, in seven vibrations the motions would be parallel to the plane of the ring ($\|$ ring) and in two vibrational modes the motions would be perpendicular to the plane of the ring ($\perp$ ring). Since the C_{2v} point group is being used, the ring vibrations can be analysed as though the molecule remained in the (delocalised) domain of this point group. Reitz[15] classified the skeletal vibrations under the C_{2v} group on the assumption that the ring was planar. The labels ω_1 to ω_7 are those used by Reitz.

5.2.3 The Vibrations of the -C=O Group

There are three vibrations associated with the -C=O group. These are the totally symmetric C=O stretching vibration , $\nu_{C=O}(a_1)$, the in-plane C=O deformation, $\delta_{C=O}\|(b_2)$, and the out-of-plane C=O deformation

TABLE 5.1

THE VIBRATIONS OF CYCLOPENTANONE

Symmetry	Number	Description*	Activity
A_1	ν_1	β sym C-H str.	infrared active,
	ν_2	α sym C-H str.	A-type;
	ν_3	$\nu_{C=O}$	
	ν_4	β δCH_2	Raman active,
	ν_5	α δCH_2	polarized.
	ν_6	α w	
	ν_7	β w	
	ν_8	$\parallel$ ring	
	ν_9	$\parallel$ ring	
	ν_{10}	$\parallel$ ring	
	ν_{11}	$\parallel$ ring	
A_2	ν_{12}	β asym C-H str.	infrared inactive;
	ν_{13}	α asym C-H str.	
	ν_{14}	β CH_2 t	Raman active,
	ν_{15}	α CH_2 t	depolarized.
	ν_{16}	α CH_2 rock	
	ν_{17}	β CH_2 r	
	ν_{18}	$\perp$ ring	

---

* sym	symmetric
str	stretch
ν	stretch
β	opposite carbonyl group
α	adjacent to carbonyl group
w	wag
asym	asymmetric
t	twist
r	rock
δ	deformation

continued on
next page

TABLE 5.1 (continued)

Symmetry	Number	Description	Activity
B_1	ν_{19}	β asym C-H str.	infrared active,
	ν_{20}	α asym C-H str.	C-type;
	ν_{21}	β CH_2 t	Raman active,
	ν_{22}	α CH_2 t	depolarized.
	ν_{23}	β CH_2 r	
	ν_{24}	α CH_2 r	
	ν_{25}	$\delta_{C=O}\perp$	
	ν_{26}	$\perp$ ring	
B_2	ν_{27}	β sym C-H str.	infrared active,
	ν_{28}	α sym C-H str.	B-type;
	ν_{29}	β δCH_2	Raman active,
	ν_{30}	α δCH_2	depolarized.
	ν_{31}	β CH_2w	
	ν_{32}	α CH_2w	
	ν_{33}	$\|\|$ ring	
	ν_{34}	$\|\|$ ring	
	ν_{35}	$\|\|$ ring	
	ν_{36}	$\delta_{C=O}\|\|$	

or "oxygen wagging" mode $\delta_{C=O\perp}(b_1)$. These vibrations are illustrated in Figure 5.3.

In table 5.1 the 36 vibrational modes are listed according to their symmetry species and the probable magnitudes of their frequencies. The ordering of the frequencies is based on the values expected for the characteristic group frequencies from correlation charts[90] and on the reported assignments for various ring molecules having vibrational modes which may be empirically related to those of cyclopentanone.[40,41,42,] Traces of the infrared spectra (recorded on the Perkin Elmer 521 instrument) are shown in Figures 5.4, 5.5 and 5.6. Traces of the Raman spectra are shown in Figure 5.7: the dotted line is the spectrum representing $I_{\perp}$. The frequencies are listed in Tables 5.2-5.5 together with those of previous workers for comparison. Table 5.6 lists the assignments.

5.3 Discussion

(a) The $-CH_2$ group

In most hydrocarbons the CH_2 asymmetric stretching band appears at $\sim$ 2930 cm^{-1}, the symmetric stretching band near 2850 cm^{-1}, and the deformation near 1465 cm^{-1}.[91,92] The presence of a carbonyl group has been found to decrease the intensity of the stretching vibrations of an adjacent (alpha) $-CH_2$ group.[93]

In cyclic compounds the frequency of the $-CH_2-$ symmetric stretching vibration increases as the ring becomes more strained. In a six-membered ring this frequency is at $\sim$ 2930 cm^{-1}, whereas in a three-membered ring it is at $\sim$ 3080 cm^{-1}.[94]

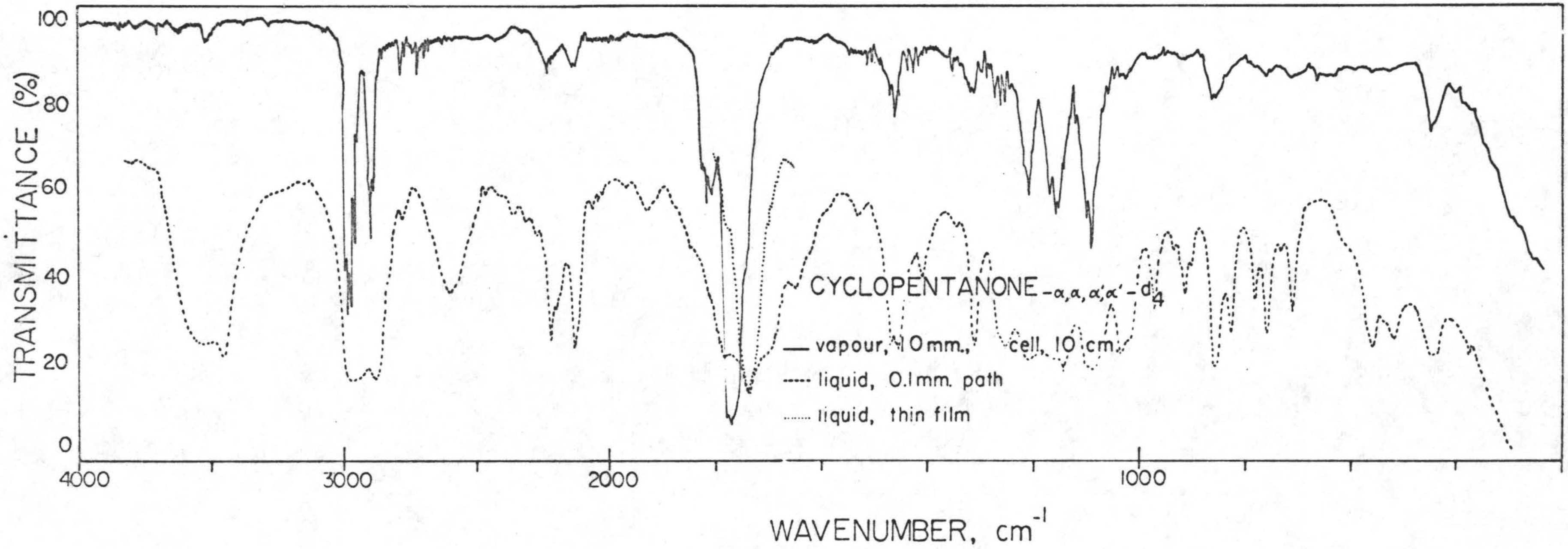

Figure 5·5 The Infrared Spectrum of CPD4

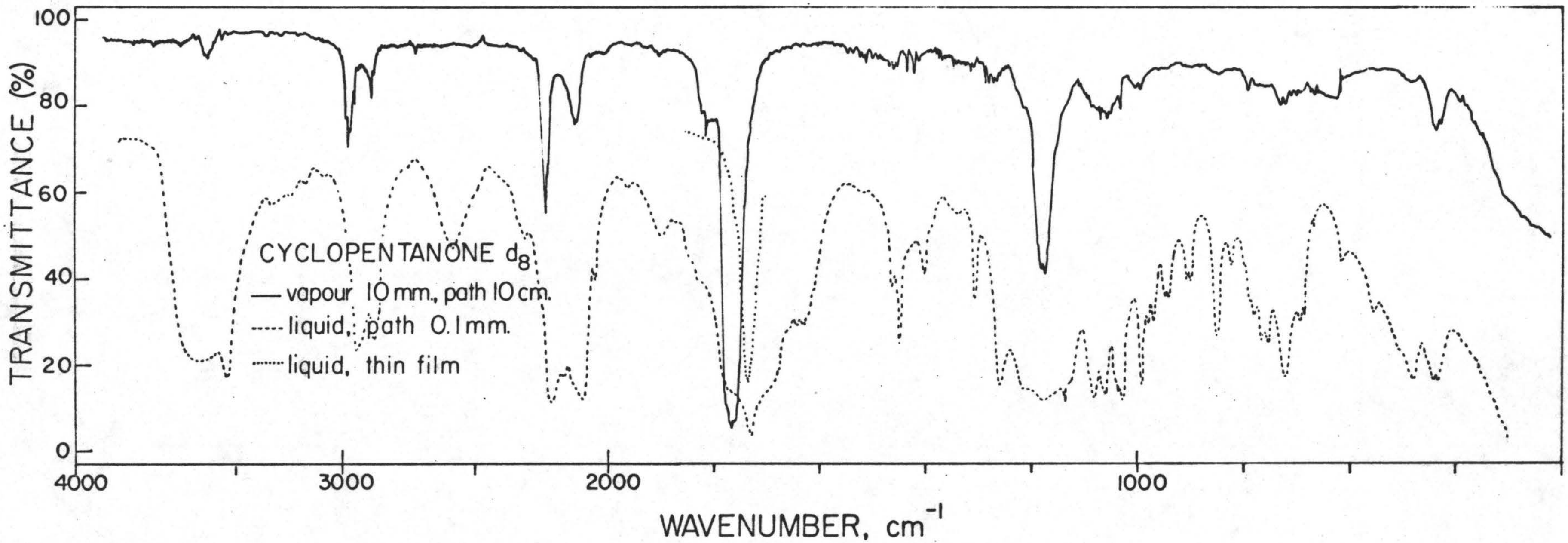

FIGURE 5.6 THE INFRARED SPECTRUM OF CPD8

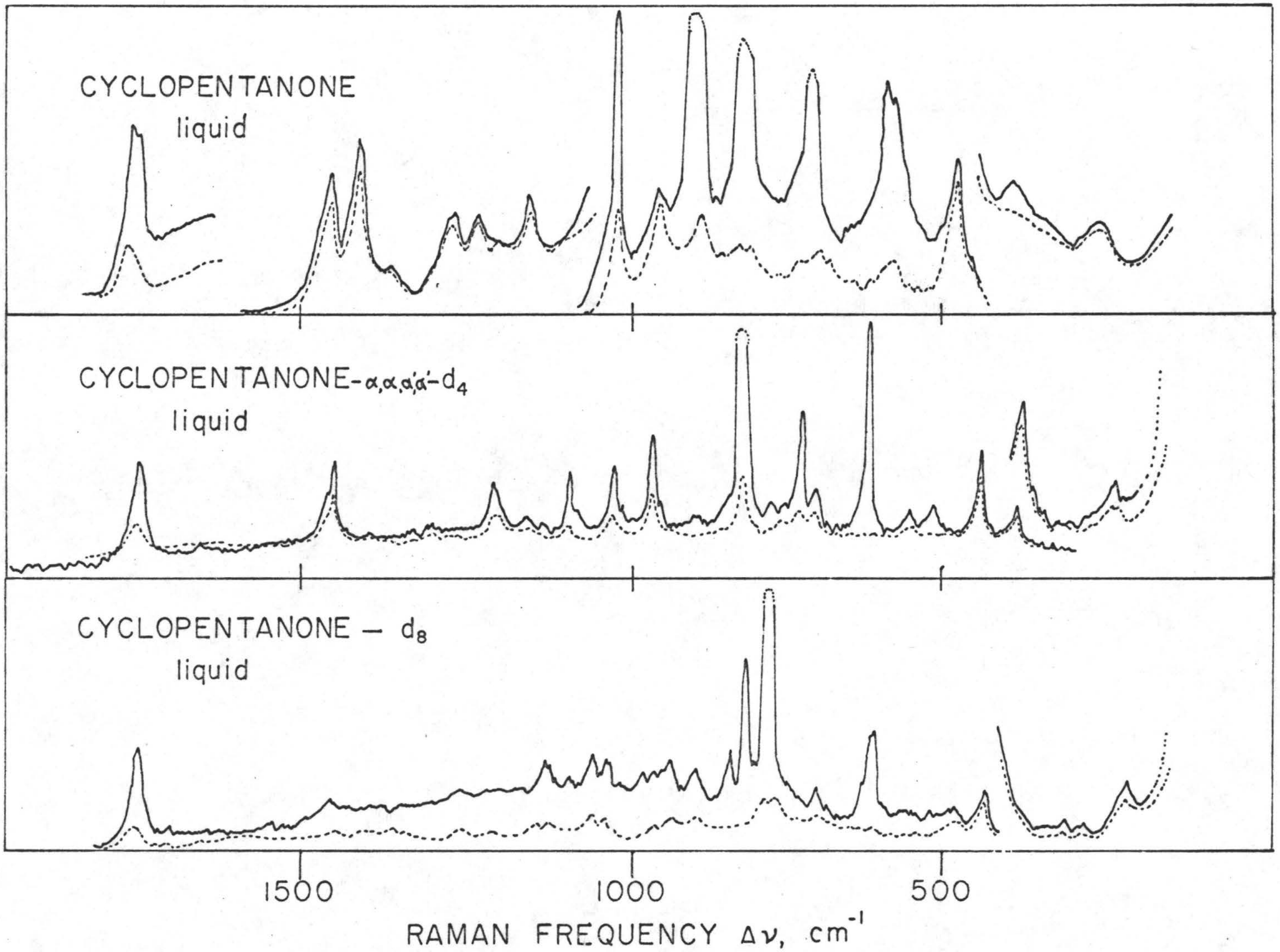

Figure 5·7 The Raman Spectra

Notes on Tables: 5.2 - 5.5

Symbols used:

I	intensity
ρ	depolarization ratio
p	polarized
dp	depolarized
ν	stretching mode
δ	deformation mode
w	wagging
ω_i	Reitz designations; cf. Figure 5.
?	uncertain
d	diffuse or broad
v	very
wk	weak
m	medium
s	strong
sh	shoulder
B	B-type (perpendicular) band contour
c	components
R_i	skeletal modes

TABLE 5.2

FREQUENCIES OF THE RAMAN SPECTRA OF CPH8

Reitz[15] cm^{-1}	I	ρ		Piaux[99] cm^{-1}	I	Suetaka[14] cm^{-1}	I	Jones et al[17] cm^{-1}	This Work cm^{-1}	I	ρ
236	(2)	dp	-	-		236	(1)d	-	241	0.4	0.7
302	(1)	-	?	-		-		-	375	0.4d	0.2
442	(2)	0.93	-	-		444	(2)	450	446	sh	dp
467	(4)	1.02	ω_8	473	(m)	468	(4)	472	469	1.0	1.0
554	(1)	?	?	-		564	(1)d	-	559	0.9	p
578	(3)	0.47	-	580	(d)	581	(3)	583	576	1.1	0.2
706	( )	0.13	ω_7	711	(m)	706	(4)	711	705	2.3	<0.1
807	(5)	0.21	-	811	(m)	806	(5)	809	806	2.5	<0.1
									832	vw	p
888	(9)	0.09	ω_1	893	(s)	888	(10)	889	888	10.0	<0.1
									948	sh	-
956	(3)	dp	ω_6	960	(m)	956	(3)	959	957	0.5	1.0
1022	(6)	0.74	ω_3	1024	(ms)	1016	(6)	1023	1021	1.5	0.6
1149	(4)	0.81	ω_5	1153	(m)	1152	(3)d	1152	1151	0.6	0.8
1195	(1)	0.82	ω_2	-		1196	(1)	1197	1200	0.4	1.0

continued ...

TABLE 5.2 (continued)

Reitz cm^{-1}	I	ρ		Piaux cm^{-1}	I	Suetaka cm^{-1}	I	Jones et al cm^{-1}	This Work cm^{-1}	I	ρ
1228	(3)	1.00	-	1232	(d)	1224	(2)	1230	1232	0.6	1.0
1267	(3)d	1.00	ω_4	1272	(d)width 20cm^{-1}	1266	(2)	1270	1272	0.5	0.75
-		-	-	-		1303	(1)d	1310	1314	vw	dp?
1407	(6)	0.89	}δCH_2	1408	(ms)	1408	(7)	1408	1409	1.1	0.8
1453	(5)	0.92		1454	(ms)d	1452	(6)	1454} 1468}	1451} 1470}	1.1 sh0.6	0.8 dp
1733	(6)d	0.50	ω_9	1726	(ms)	1723	(6)d	1727	1728	1.0	0.4
-		-	-	1746	(ms)	1744	(6)d	1740	1744	1.1	0.4
2878	(12)	} 0.26	νCH_2	2882	(s)	2876	(10)	-	-		
2898	(10)d			2905	(s)	2903	(10)d	-	-		
2967	(15)d	0.34		2972	(vs)width 200 cm^{-1}	2970	(12)d	-	-		

TABLE 5.3

INFRARED FREQUENCIES OF CPH8

Reference	Rey-Lafon et Forel[19]			This Work		
Liquid	Vapour	Liquid		Vapour	% Abs.	Liquid
481 (a)		285 vwk	R_8			
485	461 mB	450 sh	γC=O			
495	474	472 s	R_7A''	467	11,B	445,470
601 (a)	574	560 sh	R_6A' or δC=O	575	6	570,580
619		581 s		670	? vwk	665 wk
	720 wk	710 wk	r CH_2			707 wk
	807 wk	809 wk	R_5A'	804	5 sharp	805 wk
825 (b)	830 m	833 m	R_4A'	830	10 d	830 s
		888 wk	R_3A'			888 wk
925 (b)		912 wk	r CH_2			913 m
	953 965 mB	957 s	R_2A''	957	15 B	957 s
		1021 wk				1020 m
	1031 wk			1031	5	1030 m
	1145 s	1151 s	R_1A''	1142	56 (c)	1160 vs
		1179 sh				
	1235 m	1231 m		1232	4?	1230
	1271 m	1267 m				1264 s
	1279	1277 m	w CH_2	1280	10 (4c)	1276
	1281	1284 sh				1284 sh

continued ...

(a) Katon & Bentley[18] (phase not mentioned, assume liquid)

(b) Jones et al.[17]

Table 5.3 (continued)

Reference	Rey-Lafon et Forel			This Work		
Liquid	Vapour	Liquid		Vapour	% Abs.	Liquid
	1307 1319 }wk	1311 m	w CH_2	1318	5?	1312 m
1406 (b)	1419 s	1406 s	$\delta CH_3\alpha$	1415	22	1408 s
1455 (b)	1460 m	1453 m	δCH_2	1458	14	1454 1466 }m
		1468 m				
						1620 wk
1742 (b)	1758 1767 }vs 1775	1730 vs 1746 vs		1765 1775 }	85 84	1740 vs $\nu_{C=0}$ Fermi Res.
						1900 wk 2 x 957
						1960 mwk
						2040 vwk
						2110 wk
						2200 2215 }wk
						2270 wk
						2300 2325 }mwk 2 x 1160
						2430 2450 }wk
						2560 vwk 1160+1408
						2610 wk 1160+1460

continued ....

Table 5.3 (continued)

Reference	Rey-Lafon et Forel		This Work		
Liquid	Vapour	Liquid	Vapour	% Abs.	Liquid
			2820	4	2800 wk 2 x 1408
			2882	35	2930 vs ν_{C-H}
			2893	43	
			2910	29	
			2950	47	
			2970	65	
			2978	70	
			3510	5	3457 ms 2 x $\nu_{C=0}$
					3808 vwk
					3920 vwk

TABLE 5.4

VIBRATIONAL FREQUENCIES OF CPD4

Jones et al.[17]	This Work						
Raman	Raman				IR Vapour		
CPD4 cm^{-1}	CPD4 cm^{-1}		I	ρ	cm^{-1}	% Abs. I	
	220		0.05	0.75			
391	375		0.2	0.75			
444	437		0.7	0.75	438	15	
	515		0.25	0.4	535	3	
566	554		0.2	0.5	560	3	
638	624		1.8	<0.05			
713	707		0.4	0.7	710	4	
735	731		1.0	0.25			
761	758		0.25	0.7	762	4	
781	781		0.3	<0.05			
827	821		10.0	0.055	858	10	B
901	904		0.15	<0.05			
914	-						
920	-						
974	955	sh	0.2	0.4			
	970		0.8	0.54			
1019	1016	sh	0.2	0.4			
1034	1029		0.6	0.4	1030	5	d

continued .....

Table 5.4 (continued)

Jones et al.	This Work								
Raman CPD4 cm^{-1}	Raman CPD4 cm^{-1}		I	ρ	IR Vapour cm^{-1}	% Abs. I			
	1058		<0.1	p	1030	5	d		
1102	1079	sh	0.2	p					
	1101		0.5	0.3	1095	45	B		
1152	1140		0.1	p	1140			2140	7
					1155	35		2235	8
1182	1165		0.15	0.8	1168			2730	7
1219	1204	sh	0.3	0.8	1209	30		2790	7
	1215		0.45	0.5				2888	40
1273					1255			2895	
					1261	10 sharp		2995	50
					1275			2945	
1310	1305		0.3	0.8	1310	10		2955	60
					(1360)	vw		2970	
1455	1451		0.7	0.7				2975	
	1461		0.4	0.7	1461	17		2975	
	1646 ?	vw						2985	
1734	1732		0.8	0.3	1769	90		3510	6
					1809	35			
					1818	38			

continued in
next column

TABLE 5.5

VIBRATIONAL FREQUENCIES OF CPD8 (THIS WORK)

Raman			Infrared, Vapour		
cm^{-1}	I	ρ		I % Abs.	Desc.
197	0.1	0.7			
(340)	?	?			
378	1.2	0.7			
444	2.2	0.8	433	15	B
486	1.1		488	vwk 4	d
623	2.8	0.1			
713	1.1	0.4	730	10	dB
783	10.0	<0.1			
			795	vwk 5	
828	1.1	<0.1			
852	0.5	0.1			
904 913	1.0	0.75			
948	0.7	0.7			
972	0.2	0.75			
988	0.2	<0.1	1000	5	
1044	1.0	0.72	1031	5	sharp
1070	1.8	0.72	1065	10	d
1105	1.5	0.7 ?			
1144	1.3	0.3			
			1181	50	
1261	0.2	0.8			

continued .....

Table 5.5 (continued)

	Raman		Infrared, Vapour		
cm^{-1}	I	ρ		I % Abs.	Desc.
1270	0.2	0.8	1275	5	
1430	0.2	<0.1		- CH impurity	
1459	0.2	0.5			
1734	1.0	0.25	1767	90	
			1818	20	sharp
			2120	20	3 c
			2235	40	2 c
			2712	3	
			2892	13	4 c
			2950	15	
			2970	22	
			2978	25	
			2985	18	
			3507	5	

TABLE 5.6

ASSIGNMENTS OF THE VIBRATIONAL FREQUENCIES OF CPH8, CPD4 AND CPD8*

Mode	CPH8	CPD4	CPD8	Activity
a_1 ν_1	2890	2890	2140	IR
ν_2	2890	2140	2140	IR
ν_3	1770 Fermi Resonance Doublet	1769	1767	IR, R
ν_4	1458	1458	1078	"
ν_5	1409	1058	1045	"
ν_6	1280	948	948	"
ν_7	1280	948	948	"
ν_8	1157	1029	988	R (p)
ν_9	1021	955	904	R (p)
ν_{10}	888	821	783	R (p)
ν_{11}	559	515	486	R (p)
a_2 ν_{12}	2970	2235	2235	IR
ν_{13}	2970	2235	2235	IR
ν_{14}	1031	832	828	IR
ν_{15}	1031	832	623	IR
ν_{16}	801, 705	781, 624	713, 623	R (dp)?
ν_{17}	801, 705	781, 624	713, 623	R (dp)?
ν_{18}	241	220	197	R (dp)

* units of cm^{-1}

continued .....

Table 5.6 (continued)

Mode	CPH8	CPD4	CPD8	Activity
b_1 ν_{19}	2970	2970	2235	IR
ν_{20}	2970	2235	2235	IR
ν_{21}	1031	832	828	IR
ν_{22}	1031	832	828	IR
ν_{23}	801, 705	781, 624	623	IR
ν_{24}	801, 705	781, 624	623	IR
ν_{25}	442	376	378	R (dp)
ν_{26}	-	-	-	
b_2 ν_{27}	2890	2890	2140	IR
ν_{28}	2890	2140	2140	IR
ν_{29}	1458	1458	1078	R (dp)
ν_{30}	1409	1058	1045	R dp
ν_{31}	1280	948	948	R dp
ν_{32}	1280	948	948	R dp
ν_{33}	1272	1165	1144	
ν_{34}	1200	1101	1070	
ν_{35}	957	858	730	IR (B)
ν_{36}	467	438	433	IR(B), R(dp)

The assignment of the infrared band at 2970 cm^{-1} to the C-H asymmetric stretching vibration and of the band at 2890 cm^{-1} to the symmetric stretching vibration is in agreement with these general observations and with the assignments of previous authors.[16] In the spectra of CPD4, the bands at 2235 cm^{-1} and 2140 cm^{-1} assigned to the $-CD_2-$ (α groups) stretching vibrations are much less intense than the bands at 2890 cm^{-1} and 2970 cm^{-1} assigned to the $-CH_2-$ (β groups) stretching vibrations. In the spectra of CPD8 the bands at 2235 cm^{-1} and 2140 cm^{-1} are more intense than the bands at the same frequencies in CPD4.

Noether[95] has found empirically that the ratio $\nu_k/\nu_k{}^i$ is the same for corresponding vibrational frequencies of different but similar molecules. For example, from the reported spectra of cyclobutanone and cyclobutanone-$\alpha,\alpha,\alpha',\alpha'$-$d_4$,[52]

$$\nu_{C-H}/\nu_{C-D} = \frac{2930}{2197} = 1.33$$

The ratio for the corresponding frequencies in CPH8 and CPD4 is 1.35.

A doublet at 1458 cm^{-1} in the CPH8 spectrum has the same intensity and frequency as in the CPD4 spectrum and is assigned to the β-CH_2 deformation mode. There is no band at 1458 cm^{-1} in CPD8. The band at 1070 cm^{-1} in CPD8 is assigned to the same mode. The ratio $\nu_{\delta CH_2}/\nu_{\delta CD_2} = 1.36$ for this vibration.

The more intense band at 1409 cm^{-1} in CPH8 is assigned to the α-CH_2 deformation mode. This assignment is in agreement with the observations of Francis that a C=O group lowers the deformation frequency of an α-CH_2 group and increases the intensity of the band.[93] As expected, there is no band at 1409 cm^{-1} in either CPD4 or CPD8. The bands at 1058 cm^{-1} (CPD4) and 1045 cm^{-1} (CPD8) are assigned to the α-CD_2 deformation modes in CPD4 and CPD8, respectively (ratios, 1.34, 1.35). There is some indication that the ratio $\nu_{(CH_2)}/\nu_{CD_2}$ is constant for all the characteristic vibrations of the -CH_2- and -CD_2- groups in cyclopentanone. A band at 1360 cm^{-1} was observed by Streitwieser et al.[16] for CPD4 and assigned to the α-CD_2 deformation mode. In the present study, however, the band observed at 1360 cm^{-1} is far too weak to be assigned reasonably to a fundamental; moreover, the ratio, $\frac{1409}{1360} = 1.04$, is too low for this mode.

The wagging, twisting and rocking vibrations are difficult to assign. In general, -CH_2- wagging modes produce a series of sharp bands in the region 1347-1182 cm^{-1}.[90] Twisting modes are weak and usually occur at slightly lower frequencies than wagging modes. The in-phase rocking mode of four or more adjacent -CH_2- groups produces a band at ∿ 720 cm^{-1}.[96,97] The broad band in the CPH8 spectrum at 1280 cm^{-1} is assigned tentatively to some or all of the unresolved -CH_2- wagging mode fundamental bands, the weak band at 1031 cm^{-1} to twisting modes and the bands at 801 and 705 cm^{-1} to rocking modes. Wagging, twisting and rocking modes are assigned respectively to bands at 948, 832 and (781 and 624) cm^{-1} (CPD4) and 948, 828 and (713 and 623) cm^{-1} (CPD8). The frequencies of corresponding modes in related molecules are shown in Table 5.7. Because of ambiguities, these assignments for cyclopentanone must be considered to be tentative.

(b) Two of the ring modes can be assigned with certainty; the others, tentatively. The very intense (Raman active, polarized) band at 888 cm^{-1} (CPH8), 821 cm^{-1} (CPD4) and 783 cm^{-1} (CPD8) is undoubtedly produced by the totally symmetric "breathing" mode. Reitz[15] assigned the band at 888 cm^{-1} in CPH8 to this mode (his ω_1) The ratios $\frac{\nu(CPH8)}{\nu(CPD4)} = \frac{888}{821} = 1.08$

TABLE 5.7

-CH_2- FREQUENCIES*

Molecule	Wag	Twist	Rock	Reference
ethylene carbonate	1380,1418	1264,1225	770,1008	(40)
cyclobutanone	1402,1332, 1242	1200,1073	1013,735? 902	(52)
cyclobutanone-$\alpha,\alpha,\alpha',\alpha'$-$d_4$	1252,1408 1054?	1186,901	901?,673 680	(52)
cyclopentane	1304,1285, 1270,1088 1060	1200,1187 1183,1169 1122	1055,1034 833,850 779	(42)
tetrahydrofuran	1238,1338? 1290?,1367?	1104(1238) (1174)	964(1028)	(46)
cyclopentanone	1280	1031	705	(this work)
cyclopentanone-$\alpha,\alpha,\alpha',\alpha'$-$d_4$	948	832	624	(this work)
cyclopentanone-d_8	948	828	623	(this work)

---

* units of cm^{-1}.

TABLE 5.8

RING PUCKERING FREQUENCIES

Molecule	Ring Puckering Frequency cm^{-1}	Reference
tetrahydrofuran	215, 276	(46)
cyclopentane	207, 283	(42)
n-methyl pyrrolidine	228, 268	(46)
vinylene carbonate	258	(48)
tetrahydrothiophene	296	(46)
pyrrolidine	219, 303 (262)	(48)
cyclopentanone-h_8	238	(this work)
cyclopentanone $\alpha,\alpha,\alpha',\alpha'$-$d_4$	220	(this work)
cyclopentanone-d_8	197	(this work)

and $\frac{\nu\text{CPH8}}{\nu\text{CPD8}} = \frac{888}{783} = 1.03$ for this mode are smaller than the ratios for $-CH_2-$ group frequencies. The (Raman, depolarized) bands at 238 cm^{-1} (CPH8), 220 cm^{-1} (CPD4), and 197 cm^{-1} (CPD8) are assigned to a ring puckering mode, either $\nu_{18}(a_2)$ or $\nu_{26}(b_1)$. Known ring puckering frequencies of other molecules are listed in Table 5.8. The second low frequency ring puckering mode was not observed, either as the fundamental or in combination bands. Table 5.9 lists some of the other results of previous studies of five-membered ring molecules. Certain of these frequencies (apart from the $-CH_2-$ group frequencies) remain essentially constant in the different molecules. Tschamler and Voetter[46] have made the assignment of the skeletal modes as shown in Table 5.10.

The ring modes for cyclopentanone (CPH8, CPD4 and CPD8) are shown in Table 5.11.

ν_{35} has the same frequency as was designated ω_6 by Reitz.[15] There is a large amplitude motion of the β-carbons in this mode. Thus the large ratio 1.31 for $\frac{\nu 35(\text{CPH8})}{\nu_{35}(\text{CPD8})}$ may be explained. Reitz' ω_7 was assigned to the band[c] at 706 cm^{-1} (pol.). This frequency is here assigned to the $-CH_2-$ rocking vibration. Reitz did not assign the band at 578 cm^{-1}. In the present work the band at 559 cm^{-1} (pol.) is assigned to the skeletal mode $\nu_{11}(a_1)$. The polarization is correct and the isotope frequencies yield a ratio in agreement with the ratios for the other skeletal modes (∿ 1.1).

---

[c] Reitz examined only the Raman spectrum of cyclopentanone(CPH8).

TABLE 5.9

FREQUENCIES OF FIVE-MEMBERED RING MOLECULES

Compound	cm^{-1}										Reference
cyclopentanone	580			893	960			1272		1153	(99)
α-methyl-cyclopentanone	556			888	983			1278		1156	
β-methylcyclopentanone	539			812	990			1271		1156	
cyclopentane				886	967	1028		1216	1283		
cyclopentene		696		896	963	1020		1201	1292		(15)
cyclopentanone	578	706	807	888	956	1022		1228	1267		
tetrahydrofuran	596	651			964	1028		1230	1280	1174	(46)
tetrahydrothiophene	520	690	(820)	883	958	1037		1217	1281	1140	
pyrrolidine	593		(827)	898	975	1025		1218	1286	1155	
N-methyl pyrrolidine	573	(707)	(801)	899		1036		1205	1285		
2,5-diazacylopentanone	586		768	933	988	1037	1103	(1200)	1290		
α-pyrrolidone	538,627	684	805	887	915		1068		(1270)	1169	(98)
ethylenecarbonate	525,532,688	716	773	894	971		1071	(1226)		1140	
butyrolactone	494,535,635	675	800	929,890	(990)	1037		(1192)	(1284)	1166	
oxazolidone	513		770	918	(967)	1021	1077		1250	(1230)	

TABLE 5.10

SKELETAL MODES OF FIVE-MEMBERED RINGS[46]

	THF	Tetrahydro thiophene	Pyrrolidine	N-methyl Pyrrolidine	Cyclo-Pentane
Out of Plane	215	296	219	228	207
	276		303 (262)	268	283
Puckering	596	472	349	347	546
		520	593	573	
Totally Symmetric Breathing Mode	913	690	898	899	886
				1036	
		958	1218	1153	1207
Stretching	1174	1037		1205	

TABLE 5.11

SKELETAL MODES OF CYCLOPENTANONE (THIS WORK)

Mode		CPH8	CPD4	Ratio	CPD8	Ratio	Polarization
a_1	ν_8 ω_5†	1157*	1058	1.1	988	1.21	pol
	ν_9 ω_3	1021	955	1.07	904	1.13	pol
	ν_{10} ω_1	888	821	1.09	783	1.14	pol
	ν_{11}	559	515	1.08	486	1.15	pol
a_2	ν_{18}	238	220	1.08	197	1.21	dp
b_1	ν_{26}	-	-		-		
b_2	ν_{33} ω_4	1272 (B)	1165	1.09	1144(dp?)	1.12	dp
	ν_{34} ω_2	1200 (B)	1101(dp?)	1.09	1070	1.12	dp
	ν_{35} ω_6	956 (B)	858(B)+	1.11	730(B)+	1.31	dp

---

* units of cm^{-1}

† Reitz' notation

\+ not observed in Raman

Six skeletal modes in cyclobutanone and cyclobutanone-$\alpha,\alpha,\alpha',\alpha'$- d_4 have been assigned by Frei and Günthard.[52] From their reported frequencies the isotope ratios $\frac{\nu(d_4)}{\nu(h_6)}$ were calculated and found to be $\sim$ 1.1 for all except their ν_{18} which gave $\frac{1124}{852} = 1.32$. Their ν_{18} bands also had B type contours like the ν_{35} bands 957, 858 and 730 in CPH8, CPD4 and CPD8. It may be that this particular ring motion in both cyclobutanone and cyclopentanone possibly involves large displacements of the hydrogen (or deuteriem) atoms since the isotopic frequency ratio is close to that observed for vibrations of the $-CH_2-$ and $-CD_2-$ groups.

(c) The assignments of the vibrations of the -C=0 group are straightforward and are listed in Table 5.12. The frequency of the C=0 stretching vibration in ketones commonly falls in the region 1700-1900 cm^{-1}. It has been observed in cyclic ketones that a decrease of the C-C-C angle at the carbonyl group produces an increase of the C=0 stretching frequency.[25] This fundamental occurs at 1742 cm^{-1} in both acetone and cyclohexanone. In cyclopentanone this fundamental falls at 1770 cm^{-1} and in cyclobutanone, 1816 cm^{-1}. The C-C-C angles at the C=0 group in acetone and cyclohexanone are $\sim 117^o$ and in cyclobutanone, 90^o.[52] This angle in cyclopentanone is therefore expected to have a value between 117^o and 90^o, but closer to 117^o (see Figure 1.2; the calculated geometry shows this angle to be $\sim 109^o$). In cyclic ketones having 7 to 10 carbon atoms a lowering of C=0 bond stretching frequency by $\sim$ 13 cm^{-1} relative to that of cyclohexanone has been observed. This observation has been explained as the result of a slight opening of the -C-C-C angle at the -C=0 group.

TABLE 5.12

VIBRATIONS OF THE C=O GROUP

			CPH8	CPD4	CPD8	R.	IR
ν_3	a_1	$\nu_{C=0}$	$\left.\begin{matrix}1775\\1765\end{matrix}\right\}$	1769	1767	p	vapour
ν_{25}	b_1	$\delta_{C=0\perp}$	442	376	378	dp	
ν_{36}	b_2	$\delta_{C=0\|\|}$	467	438	433	dp	B

In liquid cyclopentanone the C=O stretching frequency is lower by $\sim$ 20 cm^{-1} than in cyclopentanone vapour. A similar effect has been observed in other carbonyl compounds. This effect in cyclopentanone is evident from the previously reported frequencies[19] although it has not been remarked on.

The spectrum of CPH8 is unique among the three isotopic species in showing two bands in the range 1760-1780 cm^{-1} in the infrared and in the range 1720-1745 cm^{-1} in the Raman. CPD4 and CPD8 both have single bands at 1769 and 1767 cm^{-1} respectively, although in CPD4 the band has a shoulder at 1810 cm^{-1}. The nature of the splitting of the -C=O stretching vibrational frequency in CPH8 has caused some controversy in the literature.[14,17,20-25] Some authors have attributed the splitting to dimeric structures.[13,20] Suetaka[14] assumed it was caused by hydrogen bonding between the oxygen atoms of one cyclopentanone molecule and the α-hydrogen atoms of another. Castinel et al.[22] postulated an equilibrium between two conformational isomers of cyclopentanone. Jones et al.[17] have established, however, that the splitting is caused by a Fermi resonance. The resonance involves the first overtone of ν_{10} at 888 cm^{-1} (which appears as a very strong Raman band). The pure harmonic overtone is at 1776 cm^{-1} and, if a small anharmonicity is assumed, this overtone coincides with the unperturbed frequency of the fundamental of -C=0 stretching vibration, ν_3. ν_{10} occurs at 821 cm^{-1} in CPD4 and at 783 cm^{-1} in CPD8 (both in Raman); the harmonic overtones are at 1654 cm^{-1} and 1566 cm^{-1}, respectively; these overtone frequencies are sufficiently removed from the fundamental frequencies of ν_3 that the perturbation is lost. The shoulder at 1810-1820 cm^{-1} in CPD4 may be a combination band. The assignment of weak

Zork

combination bands is necessarily speculative, since there are several pairs of bands whose frequencies add up to a given value -- for example,

$$624 + 1150 = 1774 \quad \text{and}$$
$$970 + 821 = 1791 \quad \text{--}$$

both combinations are near 1820.

Confirmation that the splitting of $\nu_{C=0}$ does indeed depend on the presence of a band at 850-890 cm^{-1} comes from a study of a series of cyclopentanones by Yates and Williams:[100] In the spectrum of 3,4-diphenyl-2-cyclopenten-1-one there is a doublet C=0 band and a band at 860 cm^{-1}. The spectrum of 3,4-diphenyl-2-cyclopenten-1-one-2,4,5,5-d_4 has a single C=0 band and lacks the 860 cm^{-1} band. 2,5-dimethyl-3,4-diphenyl-2-cyclopenten-1-one has a single C=0 band, as does cis-3,4-diphenylcyclopentanone; neither has the 860 cm^{-1} band.

Similarly, the doublet C=0 band in 1 - pyrenaldehyde has been attributed to a Fermi resonance involving the first harmonic of a C-H deformation at 855 cm^{-1}.[101a] Also in solid and liquid ethylene carbonate the doubling of the C=0 band has been explained as a resonance involving the first overtone of the skeletal breathing mode at 890 cm^{-1}. In the vapour phase the $\nu_{C=0}$ band is shifted to higher frequency and the perturbation is destroyed.[40]

The in-plane and out-of-plane C=0 deformation frequencies (ν_{36} and ν_{25}) agree well with values which have been established in analogous molecules, as shown in Table 5.13. The $\delta_{C=0||}$ vibrations in cyclopentanone produced infrared bands with good resolved B contours. See Figure 5.8.

TABLE 5.13

C=O DEFORMATION FREQUENCIES

Molecule	$\delta_{C=O\perp}$ cm^{-1}	$\delta_{C=O\parallel}$ cm^{-1}	Reference
vinylene carbonate	532	565	(48)
β-propiolactone	490	513	(69)
cyclobutanone	395	454	(52)
acetone	393	490	(18)

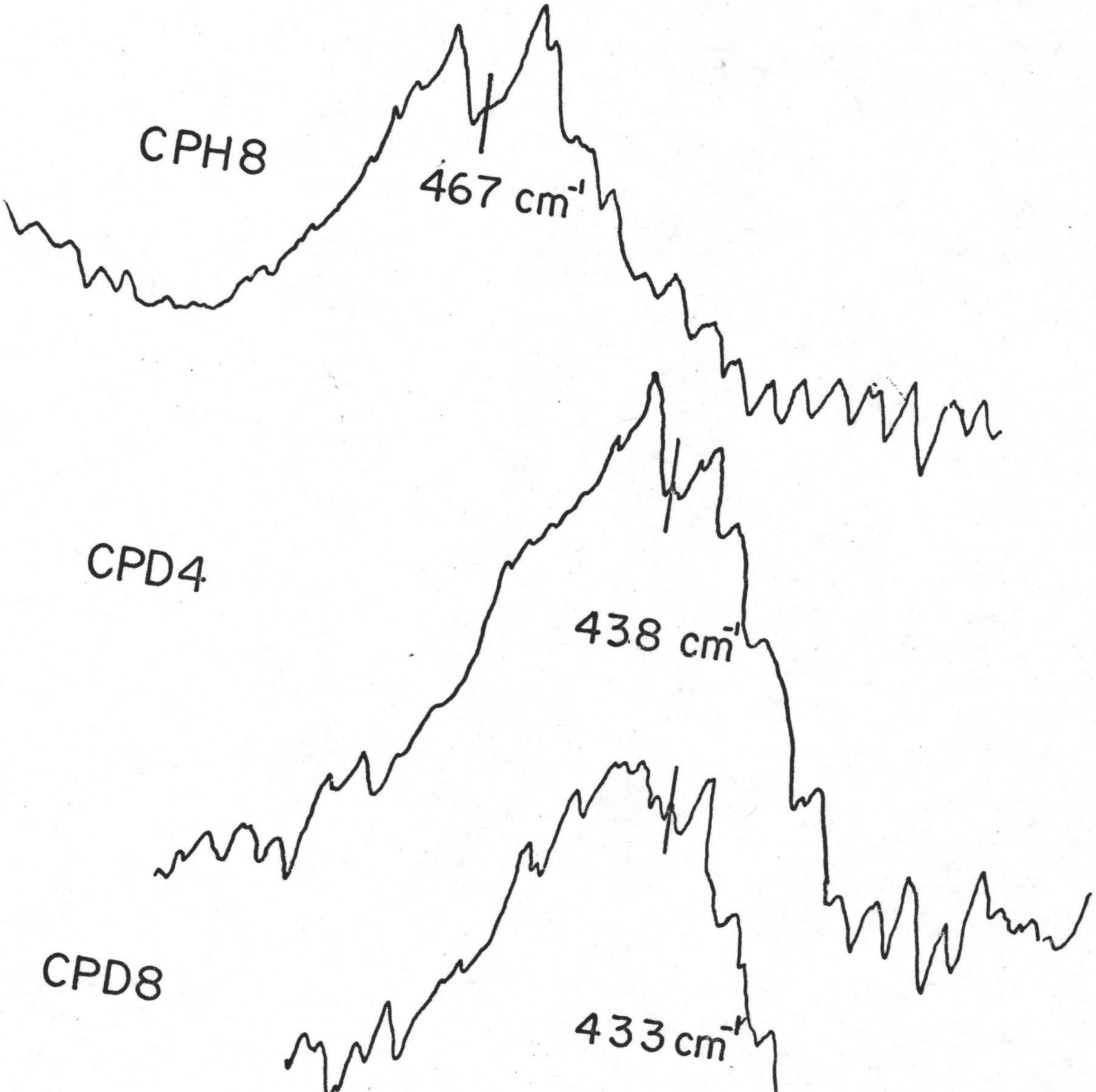

Figure 5·8 ν_{36}: A B-type Band.

5.4 The Near Infrared Spectrum of CPH8

The near infrared frequencies are listed in Table 5.14. The bands 5784 cm^{-1}, 8489 cm^{-1} and 11,062 cm^{-1} are assigned as the first, second and third overtones, respectively, of the C-H stretching frequency at 2978 cm^{-1}. With the use of equations (2.14) and (2.15), the anharmonicity constants for this vibration were found to be $\omega_e x_e$ = 47.8 cm^{-1} (x_e = 0.0167) and $\omega_e y_e$ = -6.5 cm^{-1} (y_e = 0.0023); the frequency ω_e is 2855 cm^{-1}. The Birge-Sponer extrapolation is shown in Figure 5.9. The dissociation energy for the C-H bond calculated from the graph is D_0 = 94 kcal mole^{-1}. This value of D_0 compares well with the values x_e = 0.02, D_0 = 98 (experimental 96 ± 1) kcal mole^{-1} found for chloroform.[101b]

The first two overtones of ν_3, the C=O bond stretching mode, were also observed; they fall at 3460 cm^{-1} and 5165 cm^{-1}. From these values, the anharmonicity factor, $\omega_e x_e$, is 14 cm^{-1}. An approximate calculation by means of the linear Birge-Sponer relationship gives the value D_0 = ∿ 158 kcal mole^{-1} for the C=O bond; an average value for ketones is 152 kcal mole^{-1}.[102]

The second overtone of the C-H deformation mode (1465 cm^{-1}) was observed at ∿ 4100 cm^{-1}. A few other weak bands observed are not assigned because of uncertainty in their description. The anharmonicity associated with the C-H vibration is far greater than that associated with the C=O vibration. Overtone bands of the C-H vibrations are more intense than the overtone bands of other vibrations and they are readily identified in the spectrum. It is known that the photodecomposition of CPH8 by ultraviolet light proceeds by the simultaneous breaking of a C-H and a C-C bond.[26]

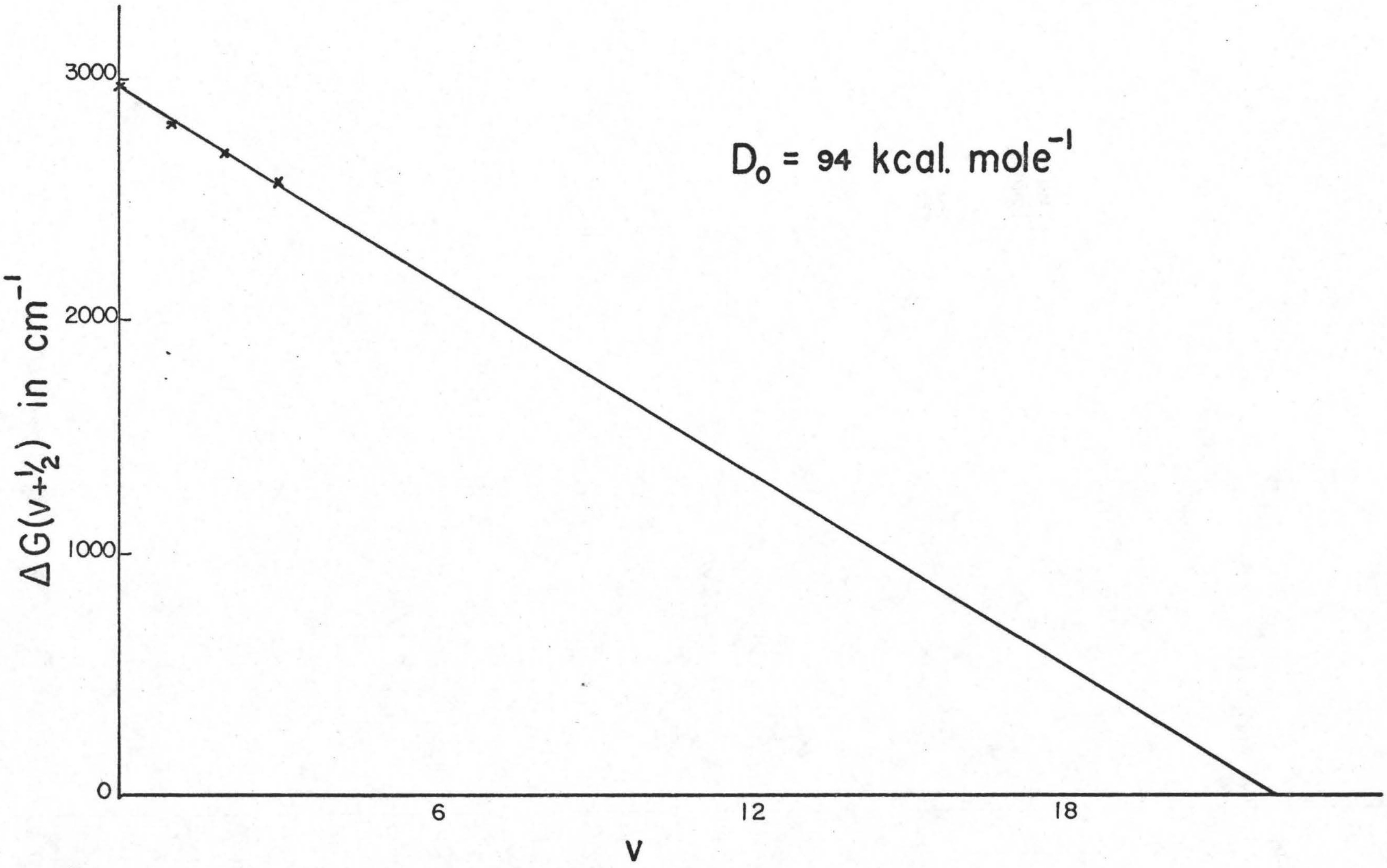

Figure 5·9 Birge-Sponer Extrapolation for the C–H Bond in Cyclopentanone.

It would be interesting to determine whether the decomposition by infrared radiation (see Section 4.2) proceeds by a similar mechanism.

TABLE 5.14

NEAR INFRARED FREQUENCIES AND ASSIGNMENTS FOR CPH8

Path Length cm.	Frequency cm^{-1}	Intensity	Assignment
10	11062	.4	4 ← 0 C-H
	10858		
	9852		
	9709	.2	
1	8489	.72	3 ← 0 C-H
	8368	sh .48	
	8299	sh .44	
	7262	.39	
	7117	.42 d	
	7013	.42	
	6711	vw	4 ← 0 C=O
	6431	vw	
	5420	1.17	
	5165	1.8	
0.1	5875	.53	
	5784	.44	2 ← 0 C-H

continued .....

TABLE 5.14
(continued)

Path Length cm.	Frequency cm^{-1}	Intensity	Assignment
	5727	.39	
	5656	.29	
	5165	.20	3 ← 0 C=O
	4715	.47	
	4646	.43	
0.03	4410	.26	
	4367	.31	
	4301	.31	
	4174	.27	3 ← 0 δCH_2
	4139	.27	
	4065	.24	

---

sh	shoulder
d	diffuse
vw	very weak

CHAPTER 6

ANALYSIS OF THE ULTRAVIOLET SPECTRUM

6.1 Identification of the n→π* Transition

In the near ultraviolet spectral region, the absorption spectrum of cyclopentanone extends from 2000 - 3500Å (see Figure 6.1). At long wavelengths, the absorption bands for the vapour phase are discrete and have very low intensity. The intensity and diffuseness of the bands rapidly increase as the wavelength decreases. The spectrum in the region 2500 - 3000Å appears at a pressure path of ∿ 0.1 m-atm. As the pressure path is increased to 6m - atm., additional bands in the region 3000 - 3500Å are observed. No discrete absorption bands are observed above 3500Å.

The absorption spectrum in the region 2500 - 3500Å shows a large number of bands spaced at intervals of ∿ 100 - 300 cm^{-1}. (See plate 6.1). The bands are very sharp above 3100Å; they resemble line-like doublets under medium resolution. Under high resolution, most of the bands show two intense heads separated by ∿ 5 to 10 cm^{-1}. A few of the bands show rotational fine structure extending ∿ 15 cm^{-1} to the high frequency side and ∿ 40 cm^{-1} to the low frequency side of the heads. The resolution of the fine structure is not high enough on the Ebert spectrograph to permit rotational analysis, but estimates of the excited state rotational constants could be made by comparison of the observed band contours with calculated contours.

For the liquid phase spectrum, the experimental oscillator strength of the absorption system over the range 2500 - 3500Å was determined from equation (3.5). The value obtained was $f = 6 \times 10^{-4}$. The customary value for a singlet-singlet n→π* transition is ∿ 10^{-4}; in formaldehyde, for example, $f = 2 \times 10^{-4}$.[103] The maximum molar extinction coefficient, ε_{max}, (measured at λ_{max}, the wavelength at which absorption intensity is highest) is usually ∿ 10 - 100 for this type of transition in carbonyl compounds, as shown in Table 6.1. For cyclopentanone, ε_{max} was ∿ 20.[104]

The effect of varying the solvent on the values of λ_{max} and ε_{max} in the n→π* transition in cyclic ketones has been studied.[105] This effect for cyclopentanone is illustrated in Table 6.2. According to Kasha,[70] a shift of λ_{max} to higher energies in acidic solvents is characteristic of an n→π* transition. The addition of a proton increases the binding energy of the lone pair (n electrons), and so the energy gap between the n and π* orbitals increases.

The characteristic f-value and solvent shift are evidence that the absorption spectrum of cyclopentanone in the 2500 - 3500Å region is caused by a singlet-singlet n→π* transition.

6.2 Previous Studies

Udvarhazi and El-Sayed[35] and Prugger and Dorr[36] studied the intense absorption spectrum of cyclopentanone vapour at wavelengths < 2500Å. An absorption system with diffuse vibrational structure was observed and a vibrational analysis was made. λ_{max} was at 1970Å and $\varepsilon_{max} \approx 3000$. Both sets of authors ascribed the system to an n→σ* transition. The configuration of the molecule was not discussed; apparently it was assumed to be C_{2v} planar in both upper and lower states. The theoretical oscillator strength for an n→σ* transition was calculated to be $f = 3.4 \times 10^{-2}$.[35] From the published data,[35] the experimental f-value can be estimated to be ∿ 6×10^{-2}. The n→σ* transition in cyclopentanone is a $B_2 \leftarrow A_1$ transition if the molecule is classified under the C_{2v} point group. The proximity of the B_2 electronic state to the A_2 electronic state determines the amount of vibronic interaction and hence the "intensity borrowing" (see section 3.4) by the n→π* transition.[106]

Rao, Rao and Rao[38] (hereafter referred to as RRR) photographed the spectrum of cyclopentanone (CPH8 only) vapour with a Hilger medium quartz spectrograph having a dispersion of 22.5Å/mm at 3400Å. The frequencies of 97 absorption bands in the region 2760 - 3470Å were reported. No rotational fine structure was observed. Their data for the sharp bands are accurate to ±15 cm^{-1}, but for the more diffuse bands below 2950Å larger uncertainties exist (probably as much as ±40 cm^{-1}). On the high frequency side of the band at 30,582 cm^{-1}, a regular pattern of band groups with an interval of 1227 cm^{-1} was observed. Because this pattern was not observed relative to any band at lower frequency than 30,582 cm^{-1}, RRR assigned 30,582 cm^{-1} as the 0,0 band of the electronic transition. Seventy-two bands were assigned somewhat arbitrarily, and seven fundamental frequencies in each of the upper and lower electronic states were identified. The transition was said to be an allowed one. The upper state configuration was not discussed; apparently, they expected no change from the assumed planar C_{2v} ground state.

Lestrade and Thouvenin[37] measured only 19 bands of the vapour

TABLE 6.1

n→π* TRANSITION OF CARBONYL COMPOUNDS[104] (SINGLET-SINGLET)

Compound	λ_{max} in Å		ϵ_{max}
	Iso-octane	MeOH	
CH_3CHO	2910		11
$(CH_3)_2CO$	2765		12
$CH_3C_2H_5CO$	2775		15
cyclobutanone	2810	2780	19.2
cyclopentanone	3000	2875	19.1
cyclohexanone	2900	2875	15.8
cycloheptanone	2920	2830	16.8

TABLE 6.2

EFFECT OF SOLVENT ON λ_{max} AND ϵ_{max} IN CYCLOPENTANONE[105]

Solvent	λ_{max} in Å	ϵ_{max}
H_2O	2801	21
MeOH	2870	18
acetonitrile	2943	17
iso-octane	2001	18

phase spectrum in the 3000Å region and presented a partial vibrational analysis. No rotational structure was observed. They observed a band pattern having an interval of 1225 cm^{-1}, and suggested 1225 cm^{-1} as the frequency of the carbonyl stretching mode in the excited state. Other frequency intervals that were observed were 130 cm^{-1} and 75 cm,$^{-1}$ attributed to excited state fundamentals, and 210 and 238 cm^{-1}, assigned to ground state fundamentals.

6.3 Temperature Dependence of Band Intensities

Calculation of Boltzmann population factors shows that the ratio of the intensity of a band originating on the v" = 1 level of a vibration with frequency 1770 cm^{-1} at 170°C, to the intensity of the same band at 25°C should be ∿ 13.7. For a vibrational frequency of 445 cm^{-1} this ratio should be ∿ 2.0 and for a frequency of 238 cm^{-1}, 1.44. The assignment of ground state fundamentals and of the 0,0 band is, in general, aided by the observation of "hot bands". Because of the difficulties encountered in the temperature study (see Chapter 4) only the region from 37,000 - 30,000 cm^{-1} could be effectively studied at high temperatures (up to 170°C). It was not possible to identify <u>positively</u> any "hot bands", that is, there was no observed increase in intensity at high temperature for any of the bands observed at frequencies from 40,000 cm^{-1} to 30,000 cm^{-1}. There is some indication that a temperature dependent continuum (probably the "hot band" end of the next highest system) underlies the discrete <u>n</u>→ π^* band system, and that the low frequency limit of observable banded absorption depends on the relative intensity of this continuum. As the temperature was increased from 25°C to 170°C the absorption bands at lower frequencies were gradually obscured. (The intensity of the continuous absorption increased and the bands were too weak relative to the continuous background to be observed.) The relative intensity of the observed continuum increased with pressure path as well as with temperature. At pressure paths of ∿ 7 - 8 m-atm., the entire absorption spectrum from 50,000 cm^{-1} to the low frequency limit at ∿ 28,400 cm^{-1} was continuous even at $25^{o}C$. At $170^{o}C$ no discrete absorption could be observed with pressure paths > ∿ 0.3 m-atm. Since the weak bands at frequencies below ∿ 30,000 cm^{-1} could be observed only if the pressure path was > ∿ 0.3 m-atm. (at $25^{o}C$), hot bands could not be identified in the region 30,000 - 28,400 cm^{-1}.

Some of the bands in the region 30,900 - 30,000 cm^{-1} were more intense, relative to adjacent bands, at $170^{o}C$ than they were at $25^{o}C$, while the band at 30,278 cm^{-1} was completely "washed out" at $170^{o}C$. All the bands have lower intensity relative to the continuum at high temperature than they do at low temperature, but the bands at 30,514, 30,442, 30,354 and 30,138 cm^{-1} whose intensity relative to the nearby bands at 30,592, and 30,278 cm^{-1} is greater at high temperatures than it is at low, may be identified tentatively as "hot bands".

6.4 Fluorescence of Cyclopentanone

The fluorescence spectrum of cyclopentanone vapour (excited by the 3130Å line of a Hanovia high pressure arc) was recorded by LaPaglia and Roquitte[34] with a Hilger and Watts quartz prism spectrograph (dispersion ∿ 160Å/mm at 4,000Å). The spectrum showed no vibrational structure; λ_{max} was at ∿ 4100Å. There was no evidence of phosphorescence emission from the vapour. According to the above authors, "fluorescence stabilization" does not occur in cyclopentanone; that is, the molecule in its excited electronic state is not vibrationally deactivated by collisions with molecules of an inert gas. Lack of fluorescence stabilization implies that fluorescence must compete with decomposition or radiationless loss of energy at every vibrational level. There may be some relationship between failure to undergo fluorescence stabilization and lack of vibrational structure in the emission spectrum.[34]

The continuous emission spectrum (published by La Paglia and Roquitte), when re-plotted on a wavenumber scale, exhibits an approximate mirror image relationship with the absorption spectrum, as illustrated in Figure 6.1. This type of mirror image symmetry is well known for other molecules, and it is commonly assumed that the absorption and fluorescence curves of a molecule cross at the approximate frequency of the 0,0 band.[107,108,109] If it is assumed that the intensity maxima in the absorption and fluorescence spectra correspond to the excitation of roughly the same number of quanta of the C=0 stretching vibration, ν_3, in the ground and excited electronic states, respectively, and if the drop in frequency of this vibration from $\nu_3'' = 1770$ cm^{-1} to $\nu_3' = 1225$ cm^{-1} is considered,[a] the wavenumber of the 0,0 band may be estimated to be in the region 30,260 - 30,290 cm^{-1}.

6.5 Analysis of the Spectra

Detailed analyses of the vibrational structure of the singlet-

---

[a] The definite assignment of $\nu_3 = 1227$ cm^{-1} will be discussed in the following section.

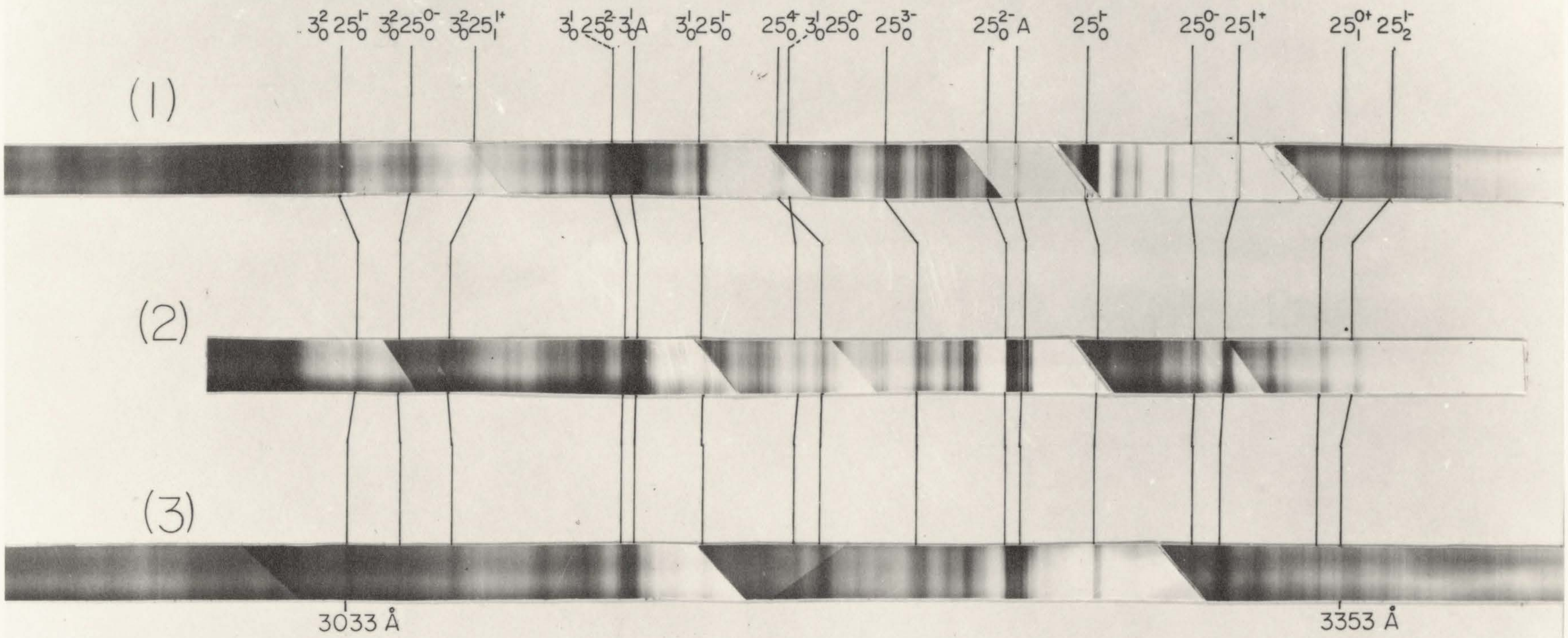

Plate 6·1 Spectrogram of the Absorption Bands of Cyclopentanone in the Region 3000-4000 Å.
(1) CPH8 (2) CPD4 (3) CPD8

singlet $\underline{n}\rightarrow\pi^*$ transitions of CPH8, CPD4, and CPD8 will be presented in the following sections. All of the intense bands are assigned, and in addition many of the weak bands are explained. Portions of the spectra (taken under medium resolution) of the three isotopic species are shown in Plate 6.1. The labelling convention of Brand and Watson[110] is used for vibrational bands in the electronic spectrum: transitions are labelled $m_b^a n_d^c$ ... where m, n, ... designate the normal modes of vibration by their numbers (see Table 5.1); the superscripts, a, c, and the subscripts, b, d, give the number of quanta of a vibration excited in the upper and lower electronic states, respectively. For example, successive members of an excited state progression in ν_3 are labelled 3_0^1, 3_0^2, 3_0^3 ... . (The band labelled A has an A-type band contour; it will be assigned to $18_0^1 25_0^{1-}$.)

(a) The Spectrum of CPH8

The predominant feature of the low resolution spectrum is a series of four or five intense bands with a spacing of 1227 cm^{-1}, at higher frequency than that of the assumed 0,0 band. These bands are undoubtedly a progression in the carbonyl bond stretching vibrational mode (ν_3'), as suggested by RRR and Lestrade and Thouvenin. The ground state frequency ν_3'' = 1770 cm^{-1} has been assigned from the infrared study (see Chapter 5), but the band 3_1^0 could not be identified in the ultraviolet spectrum. RRR assigned a band at 28,816 cm^{-1} as 0,0 - 1766 cm^{-1}. The band closest to this frequency observed in the present study is at 28,827 cm^{-1}. However, the present assignment of the 0,0 band differs from that of RRR (as is discussed later).

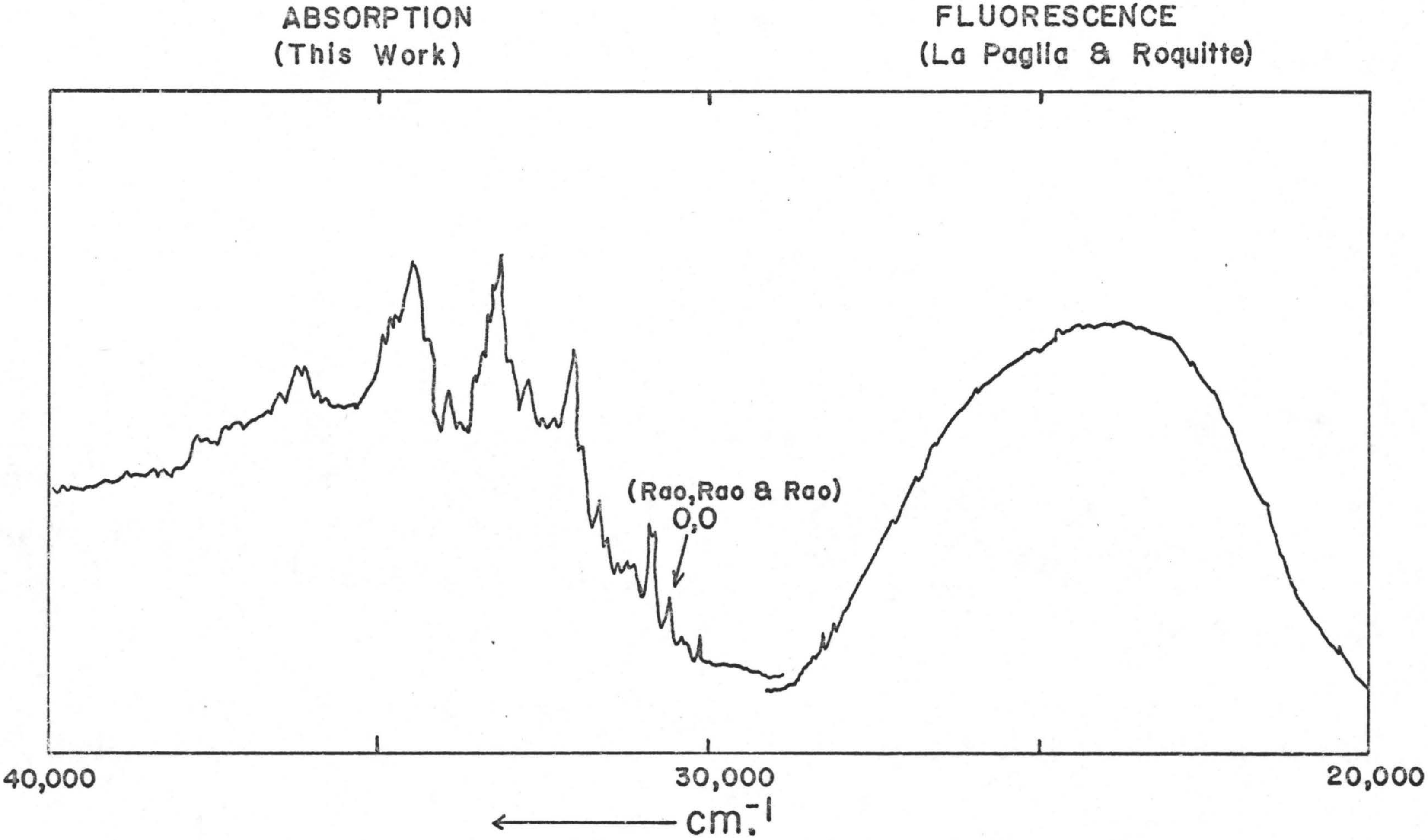

FIGURE 6·1 Low Resolution Spectra of Cyclopentanone Vapour.

The large difference in frequency of the C=O stretching mode in the ground and excited states agrees with the difference found in n→π* transitions of other carbonyl compounds, as illustrated in Table 6.3. The C=O bond length in the compounds in Table 6.3 increases by ∿ 0.1 in the excited state. According to simple MO theory, the n→π* promotion places the promoted electron in an orbital which is antibonding between carbon and oxygen, and results in redistribution of the π electron density such that the C=O bond is weakened. The geometry changes accompanying the electron promotion are an extension of the C=O bond and a possible change in the out-of-plane angle the C=O bond makes with the rest of the molecule -- as has been most completely confirmed for the formaldehyde molecule.[75] According to the Franck-Condon principle, the C=O stretching vibration should be active in forming long progressions when the C=O bond is lengthened in the excited state.

In the spectrum of cyclopentanone, the 1227 cm^{-1} pattern is observed relative to bands at lower frequencies than 30,583 cm^{-1}, contrary to the report of RRR. In the present assignment, three intense progressions in ν_3' based on different "origins" are observed. The "origin" of one of these progressions is the band at 30,278 cm^{-1}; this band was assigned as a hot band by RRR. The most intense progression in ν_3' has its first member at 30,884 cm^{-1}. The frequencies and assignments (results of the present study) for the bands in the low resolution spectra of all three isotopic species are listed together for comparison in Table 6.4. The intensities quoted are peak heights relative to the height of the band 25_0^{0-} (which will be later shown to be part of what

TABLE 6.3

SINGLET-SINGLET $\underline{n}\rightarrow\pi^*$ TRANSITIONS IN CARBONYL COMPOUNDS

Compound	0,0 band cm^{-1}	$\nu''_{C=O}$ cm^{-1}	$\nu'_{C=O}$ cm^{-1}	$r''_{C=O}$ Å	$r'_{C=O}$ Å	Reference
H_2CO	28,200	1738	1187	1.22	1.32	(75)
CH_3CHO	28,700 (or lower)	1743	1125			(108)
Propenal	25,861	1723	1265	1.22		(111)
HCOF		1837	1111	1.18	1.35-1.38	(112)

TABLE 6.4

BAND FREQUENCIES AND ASSIGNMENTS:

LOW RESOLUTION SPECTRA OF CPH8, CPD4 and CPD8

CPH8		CPD4		CPD8		Assignment
ν,cm^{-1}	I	ν,cm^{-1}	I	ν,cm^{-1}	I	
29,832		29,887		29,896		25^{0+}_{1}
30,045		30,039		30,080		$18^{0}_{1}25^{0-}_{0}$
30,139*		30,157		30,176		25^{1+}_{1}
30,285	1	30,258	1	30,267	1	25^{0-}_{0} "0,0 band"
				30,294		
				30,331		
				30,358		
30,359*	0.8	30,377		30,406		$18^{1}_{0}25^{1}_{1}$
30,446*		30,440		30,433		
30,514*						
30,586	8.4	30,554	10	30,554	2	25^{1-}_{0}
30,657	0.2	30,675	8			
30,713	0.6	30,731		30,751	3	
30,798	10	30,760	50	30,779	9.2	$18^{1}_{0}25^{1-}_{0}$
30,827	0.8			30,798	9.5	
30,884	7.5	30,817	60	30,817	10	25^{2-}_{0}
31,018	4.0	30,960	40	30,951	7	
31,076	2.5	31,008.4	25	31,008	6	

continued ......

Table 6.4 (continued)

CPH8		CPD4		CPD8		Assignment
ν,cm^{-1}	I	ν,cm^{-1}	I	ν,cm^{-1}	I	
31,202	3	31,105	30	31,095	6.5	25^{3-}_{0}
31,235	3	31,212	20	31,270	2.5	$3^{2}_{1}25^{1-}_{0}$
31,368		31,379		31,395		$3^{1}_{0}25^{1+}_{1}$
31,556	5.2	31,398	75			25^{4-}_{0}
31,503		31,477	70	31,497	7	$3^{1}_{0}25^{0-}_{0}$
31,566	5.2	31,596	50	31,596	8	$3^{1}_{0}18^{0}_{1}25^{1+}_{1}$
31,818	10	31,777	100	31,777	15	$3^{1}_{0}25^{1-}_{0}$
32,032	26	31,991	600			$3^{1}_{0}18^{1}_{0}$
32,104	4	32,011	600	32,011	30	$3^{1}_{0}25^{2-}_{0}$
32,186	4	32,135	500	32,166	27	$3^{3}_{1}25^{0-}_{0}$
32,448	vw	32,301	400	32,290	23	$3^{1}_{0}25^{3-}_{0}$
32,788	8	32,634	190	32,596	23	$3^{1}_{0}25^{4-}_{0}$
32,724	5	32,670	200	32,691	3	$3^{2}_{0}25^{0-}_{0}$
32,863	-	32,809	200	32,788	15	
33,037	7	32,961	200	32,961	20	$3^{2}_{0}25^{1-}_{0}$
33,268						$3^{2}_{0}18^{1}_{0}$
33,313	37	33,229	600	33,224	60	$3^{2}_{0}25^{2-}_{0}$
33,402	4	33,300	590	33,323		$3^{4}_{1}25^{0-}_{0}$
33,525	14	33,368	580	33,592		$3^{3}_{0}25^{0+}_{1}$
33,660	15	33,523		33,480	50	$3^{2}_{0}25^{3-}_{0}$
33,717	4			33,660		$3^{4}_{1}25^{1-}_{0}$

continued ......

Table 6.4 (continued)

CPH8		CPD4		CPD8		Assignment
νcm^{-1}	I	ν,cm^{-1}	I	ν,cm^{-1}	I	
33,785	10			33,808	210	$3^3_0 25^{1+}_1$
33,888	8	33,866	400	33,911	40	$3^3_0 25^{0-}_0$
34,248	4	34,141	400	34,143	40	$3^3_0 25^{1-}_0$
34,295	3	34,188				$3^4_1 25^{3-}_0$
34,473	w					$3^3_0 18^1_0 25^{1-}_0$
34,520	39	34,449	400	34,402	28	$3^3_0 25^{2-}_0$
34,760	w					$3^4_0 25^{0+}_1$
		34,544	450	34,544	20	$3^5_1 25^{0-}_0$
34,869	15	34,688	40	34,664	20	$3^3_0 25^{3-}_0$
		34,785	200	34,855	12	$3^5_1 25^{1-}_0$
35,160		35,066		35,137	15	$3^4_0 25^{0-}_0$
35,451	10	35,350	150	35,313	17	$3^4_0 25^{1-}_0$
35,729	20	35,564	150	35,677	w	$3^4_0 25^{2-}_0$
35,948	10					$3^5_0 25^{0+}_1$
36,114	30	36,232	w			$3^4_0 25^{3-}_0$
36,632		36,566	80	36,577	w	$3^5_0 25^{1-}_0$

is normally called the 0,0 band), measured from microdensitometer traces of the spectra.

The High Resolution Spectra

RRR interpreted all the bands observed by them below 30,582 cm^{-1} (their 0,0 band) in terms of the seven ground state fundamentals, 1766, 1022, 897, 573, 442, 300 and 238 cm^{-1}. According to their results, the system has many characteristics of an allowed transition. (A 0,0 band is observed and totally symmetric vibrations are active). They say: "A peculiar set of frequencies is given by 380 cm^{-1} (upper) and 442 cm^{-1} (lower) and 442 cm^{-1} in the Raman ($\rho = 0.9$). The presence of this non-totally symmetric type of fundamental does not, however, fit into the general pattern of the analysis".

It will be shown in the present analysis that this "peculiar frequency" provides the key to the interpretation of the spectrum.

The ground state fundamental at 442 cm^{-1} has been assigned as the oxygen-out-of-plane deformation vibration, ν_{25}, of species b_1 (see Table 5.12). According to the Franck-Condon principle (discussed in 3.6), if the oxygen is bent out of plane in the excited state configuration of the molecule, progressions in ν_{25} are expected to be observed.

All of the more intense bands (hereafter called "the main bands") of the high resolution spectrum (covering the region 31,600 - 28,000 cm^{-1}) can be assigned as members of progressions in ν_{25}. Some weaker bands at intervals of -238 cm^{-1} relative to the main bands can be interpreted as combinations of ν_{25} with a ring puckering frequency (241 cm^{-1} Raman, dp) in the ground state. It is not certain whether the ring mode observed is ν_{18} (a_2) or ν_{26} (b_1). The band frequencies and assignments for the bands photographed under high resolution are listed in Table 6.5 (a). The uncertainty in frequency is ± 0.1 cm^{-1} unless otherwise indicated. The intensities quoted are visual estimates only, because the rapid changes in intensity necessitated photographing each band under different conditions of pressure path and exposure time.

The proposed analysis postulates a pyramidal configuration about the carbon atom of the carbonyl group in the excited state configuration of the molecule, with a potential barrier between the two non-planar conformationsof the 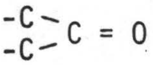 $\genfrac{}{}{0pt}{}{-\mathrm{C}\diagdown}{-\mathrm{C}\diagup}\mathrm{C} = 0$ group. This part of the molecule is assumed to be planar in the ground state. The ring is assumed, reasonably, to be puckered in the skew configuration in both states. Since the electronic excitation is primarily localized in the carbonyl group, and vibrational modes associated with this group are strongly active in the spectrum, the analysis gives information about changes in this part of the molecule. There will also be a potential barrier restricting interconversion of the two skew configurations of the methylene groups at the other end of the molecule, but no information about this barrier could be obtained from the spectrum. Tables 6.5(b) and (c) give the band frequencies and assignments for CPD4 and CPD8, respectively. The frequencies of all the band heads observed, including the weak, unassigned ones, are collected in Appendix III. For simplicity, the spectra of the three isotopic species, CPH8, CPD4 and CPD8 will be discussed separately at first, and they will be compared later. The frequencies reported in this section are for CPH8.

NOTES ON TABLES 6.5 (a),(b) and (c)

*	hot band
A	A-type Band
B	B-type Band
K str	K structure
doubl	doublet spacing ∿ 1 cm^{-1}
d	diffuse
w	weak
m	medium
s	strong
v	very
A_0,A_{-1},A_{-2} B_0,B_{-1},B_{-2} C_0,C_{-1},C_{-2} etc. for D,E,F	preliminary notation for members of progression in ν''_{25}
r.p.	ring puckering vibration
?	uncertain

TABLE 6.5 (a)

BAND FREQUENCIES AND ASSIGNMENTS FOR CPH8

ν cm^{-1} vacuum	Relative Intensity	Notation	Assignment	
31,808.6			$3^{1}_{0}25^{1-}_{0}$	
31,555		F_0	25^{4-}_{0}	
31,502.9			$3^{1}_{0}25^{0-}_{0}$	
31,365.0			$3^{1}_{0}25^{1+}_{1}$	
31,204.9		E_0	25^{3-}_{0}	
31,099.6	w	D_0+212		
31,008.2		B_0+2 r.p.		
30,924	w		25^{4+}_{1}	
30,887		B D_0	25^{2-}_{0}	
30,818.5		B		
30,798		A A_0	$18^{1}_{0}25^{1-}_{0}$	B_0+206
30,662.7	w		25^{4-}_{2}	F_0-891 = 30,664
30,645.3	w		$18^{0}_{1}25^{2-}_{0}$	D_0-242
30,619.6	vw		25^{3+}_{1}	
30,609	vw	doubl ∿ 1 cm^{-1}		
30,591.9	s	B B_0	K str. to ∿ 30,550	25^{1-}_{0}
30,582.8		underlies A? B_0		
30,514.2	w	*		
30,442.6	w	* doublet	C_0+164.5? D_{-1}	25^{2-}_{1} ? (forbidden)

continued ......

Table 6.5 (a)

ν cm^{-1} vacuum	Relative Intensity	Notations		Assignment	
30,418	vw		D_0-468	$25^{2-}_0 36^0_1$	
30,368	mw	doubl			
30,360.6	s	*		25^{2+}_1	
30,353.3	s	* A_{-1}			$\{$ B_0-238.6 A_0-444.7
30,329.0	s		(25^{2-}_0)-559	$11^0_1 25^{2-}_0$	
30,313.5	w			25^{3-}_2	
30,278.1		B Kstr to 30,250	C_0	25^{0-}_0	
30,237	w	doubl			D_{-1}-206
30,182.6	vw		D_0-705	25^{2-}_0-705	
30,139.6	vs	B* Kstr to 30,100 cm^{-1}	B_{-1}	25^{1+}_1	
30,115.9	s		B_0-2r.p.	$18^0_2 25^{1-}_0$	
30,110.0	w	doubl	d		
30,044.4	m		C_0-233		
30,033.6	mw			$\{$ 25^{4+}_3 $(25^{1-}_0$-559)	
30,006.9	m		D_{-2}	25^{2-}_2	
29,996.6	w	doubl	D_{-2}		C_{-1}+163.9 28,695+1300

continued ......

Table 6.5 (a)
(continued)

ν cm^{-1} vacuum	Relative Intensity	Notations		Assignment	
29,974.5	m			30,442-468	
29,969.9	mw			28,670+1300	
29,920.0	mw		A_2		A_0-878
29,888.9	vw		B_0-705	(25_0^{1-})-705	
29,885.0	vw		(30,442-559)	$18_1^0 25_0^{1-} 36_1^0$?	
29,832.7	s	B KStr to 29,800	C_1	25_1^{0+}	
29,808.7			C_0-2 r.p.	$18_2^0 25_0^{0-}$	
29,795.7	w d		B_0-238-559	$11_1^0 18_1^0 25_0^{1-}$	
29,790.1	w	doubl			
29,752.8	w d			(25_0^{0-})-515	
29,735.8				30,442-705	
29,728.2				25_3^{3+}	
29,701.0	s	B		B_{-2} 25_2^{1-}	
29,675.6	m s		B_{-1}-2r.p.	$18_2^0 25_1^{1+}$	
29,652.9	m w		B_0-238-705	$(18_1^0 25_0^{1-})$-705	
29,607.0			D_0-1272	(25_0^{2-})-1272	
29,598.4			C_1-r.p.	$18_1^0 25_1^{0+}$	25_1^{0+}-234.7
29,571.9	m		C_0-705	(25_0^{0-})-705	
29,477.9	m w		A_{-3}	25_3^{2+}	
29,453.2	m w		B_{-2}-r.p.		25_2^{1-}-247.8

continued ......

Table 6.5 (a)
(continued)

ν cm^{-1} vacuum	Relative Intensity		Notations	Assignment	
29,435.8	w		B_{-1}-3r.p.	$18^0_3 25^{1+}_1$	
29,387.2	ms	3 components	C_2	25^{0-}_2	
29,362.1			C_{-1}-2r.p.		(25^{0+}_1)-234.7-236.8
29.323.3	w		B_0-1272	(25^{1-}_0)-1272	
29,252.6	m		B_{-3}	25^{1+}_3	
29,225.3	w		B_{-2}-2r.p.	$18^0_2 25^{1-}_2$	25^{1-}_2(2x237.9)-475.7
29,153.3	w		C_{-2}-r.p.	$18^0_1 25^{0-}_2$	-233.9
29,136.6	vw				25^{1-}_0-1455 25^{2+}_1-1227
29,110.8	vw			25^{2-}_4	
29,057	vw				C_0-1221
28,978.0	w		B_{-2}-3r.p.	$18^0_3 25^{1-}_2$	(25^{1-}_2)-3(241)
28,951	m	doubl			
28,950.9					
28,941.5	m		C_{-3}	25^{0+}_3	
28,914	w		C_{-2}-2r.p.	$18^0_2 25^{0-}_2$	(25^{0-}_2)-233.9 (25^{1+}_1)-1228
28,878	w		B_{-1}-1272	(25^{1+}_1)-1272	
28,779.3	w		B_{-3}-2r.p.		25^{1+}_3- $(25^{2-}_2$-1227)
28,695.1	m	doubl			29,996.6-1302
28,676.3	m	doubl			29,945-1298
28,670.3	m				29,969.9-1300
28,601.1	mw				$(25^{0+}_1$-1222)

TABLE 6.5 (b)

BAND FREQUENCIES AND ASSIGNMENTS FOR CPD4

ν cm^{-1} vacuum	Relative Intensity	Notations	Assignment
31,560	m		$3^4_2 25^{0-}_0$ $3^5_3 25^{2-}_0$
31,475	w		$3^1_0 25^{0-}_0$
31,398.0	m	F_0	25^{4-}_0
31,302	w	d	$3^6_3 25^{1-}_0$
31,100.1	m	E_0	25^{3-}_0
31,095	w	C_{-1}+1207	$3^1_0 25^{0+}_1$
31,012	w		$3^5_3 25^{0-}_0$
30,835.7	w		25^{4+}_1
30,819.2	s	B D_0	25^{2-}_0
30,755.5	s	A B_0+206.1 A_0	
30,717	w		$3^1_0 25^{0-}_2$
30,642			25^{4-}_2
30,599	ms	D_0-220	$18^0_1 25^{2-}_0$ 25^{3+}_1
30,568.9	w		$18^0_1 25^{2+}_0$
30,555.7	s		
30,548.9	vs	B B_0	25^{1-}_0
30,440	mw	d	$3^6_4 25^{0-}_0$
30,428	mw	doubl	
30,411.3	w	doubl	
30,397	mw		25^{2+}_1
30,384	m		
30,377.6	m	A-1 or B_{-1}+r.p.	$18^1_0 25^{1+}_1$
30,297	mw	D_0-515	(25^{2-}_0)-515
30,267.2	mw	C_0	25^{0-}_0
30,205	w	~ D_0-624	(25^{2-}_0)-624
30,166.9	m	B_{-1}	25^{1+}_1
30,108.8	m	B_0- 2r.p.	$18^0_2 25^{1-}_0$

continued ......

TABLE 6.5 (b) continued

ν cm^{-1} vacuum	Relative Intensity	Notations	Assignment
30,064.0	m		
30,060.0	m	D_{-2}	25^{2-}_{2}
30,044.4	w	ν'_3 S-T?	28,744+1300
30,033.6	w		(25^{1-}_{0})-515
29,994.5	m	B_{-2}+204.8	$18^{1}_{0}25^{1-}_{2}$
29,945.7	w	B_{-1}-221.2	$18^{0}_{1}25^{1+}_{1}$
29,888.5	vs	K str to B29,860 C_{-1}	25^{0+}_{1}
29,839.9			25^{3+}_{3}
29,832.2		these 2 are assigned the same ?	$18^{0}_{2}25^{0-}_{0}$
29,808.6	nw		25^{3+}_{3}
29,796.5	s		
29,789.7	s	B B_{-2}	25^{1-}_{2}
29,765.3	w	D_0-1058	(25^{2-}_{0})-1058
29,749.4			(25^{0-}_{0})-517.6

ν cm^{-1} vacuum	Relative Intensity	Notations	Assignment
29,729.0	w	B_{-1}-2r.p. B_{-1}-438?	$18^{0}_{2}25^{1+}_{1}$ $25^{1+}_{1}36^{0}_{1}$?
29,716.0	w	D_0-1101 B_0-832	(25^{2-}_{0})-1101 25^{1-}_{0}-822
29,666.6	w	C_1-221.7	$18^{0}_{1}25^{0+}_{1}$
29,652	w		25^{1+}_{1}-515
29,638.2	vw		25^{2+}_{3}
29,625.7	mw	d	
29,618.3	m	A-3 d B_{-3}+213.1	$18^{1}_{0}25^{1+}_{3}$
29,607			(25^{2-}_{0})-1212
29,578	mw		? 25^{3-}_{4}
29,567	w	B_{-2}-221	$18^{0}_{1}25^{1-}_{2}$
29,508.0	s	C_{-2}	25^{0-}_{2}
29,448.9		B_0-1101 C_{-1}-438	(25^{1-}_{0})-1101 $25^{0+}_{1}36^{0}_{1}$?

continued ......

TABLE 6.5 (b)
(continued)

ν cm^{-1} vacuum	Relative Intensity	Notations	Assignment	ν cm^{-1} vacuum	Relative Intensity	Notations	Assignment
29,429.7		C_0-832	(25^{0-}_{0})-832	28,744.0		ν_3' S-T?	30,044-1300
29,405.2	ms	B_{-3}	25^{1+}_{3}	28,590.0		S-T?	
29,369.0	mw		(25^{1+}_{1})-515				
29,337	mw	B_0-1210? C_{-3}+210					
29,234.8	w	~B_0-220-1101	$(18^{0}_{1}25^{1-}_{0})$-1101				
29,204.3	w	C_0-1058	(25^{0-}_{0})-1058				
29,133							
29,127.1	m	C_{-3}	25^{0+}_{3}				
29,069.7		C_{-2}-438	$25^{0+}_{2}36^{0}_{1}$				
29,047.7	m	C_0-1219?	(25^{0-}_{0})-1219				
29,043							
28,956.1	w	B_0-1210	(25^{1-}_{0})-1210				
28,907.7	w	C_{-3}-219.3	$18^{0}_{1}25^{0+}_{3}$				
28,856.6	m		(25^{2-}_{2})-1206				

TABLE 6.5 (c)

BAND FREQUENCIES AND ASSIGNMENTS FOR CPD8

ν cm^{-1} vacuum	Relative Intensity	Notations	Assignment	ν cm^{-1} vacuum	Relative Intensity	Notations	Assignment
31,765.6	s d	B_0+1212	$3^1_0 25^{1-}_0$	30,619.6	vw	D_0-196.4	$18^0_1 25^{2-}_0$
31,483	m	C_0+1212	$3^1_0 25^{0-}_0$	30,590.8	mw		25^{3+}_1 ?
31,395	ms d	B_{-1}+1211	$3^1_0 25^{1+}_1$	30,553.7	vs B	K str to B_0 ∿30,520	25^{1-}_0
31,382.5		F_0	25^{4-}_0	30,463.2	mw	C_0+192	
31,120	w	C_{-1}+1215	$3^1_0 25^{0+}_1$	30,406.4			25^{2+}_1
31,088.3	ms	E_0	25^{3-}_0	30,384.8	vw	D_0-433	$25^2_0 36^0_1$
30,916	mw		$3^2_1 25^{0-}_0$	30,381.1	vw	B_{-1}+191.3	
30,886	w		$3^2_1 25^{1+}_1$	30,353.9	mw	(B_0-200) E_0-734.4)	25^{3-}_2
30,816.4	s	D_0	25^{2-}_0	30,342.5	mw	doubl	
30,772.2	m	A	25^{2+}_0 ?	30,335.2	mw	D_0-486	(25^{2-}_0)-486
30,749.1	mw	B_0+195.4		30,271.5	m	C_0	25^{0-}_0
30,740.1	mw	B_0+186.4		30,216.1	w	(25^{2+}_1)-190	$18^0_1 25^{2+}_1$
30,695.2	m		25^{4-}_2	30,183.6	vs	B(k str to B_{-1} ∿30,170)	25^{1+}_1
30,688	w		$3^3_2 25^{1-}_0$				
30,645.0	w	doubl	25^{4-}_2				

continued ....

TABLE 6.5 (c)
(continued)

ν cm^{-1} vacuum	Relative Intensity	Notations	Assignment	ν cm^{-1} vacuum	Relative Intensity	Notations	Assignment
30,168	mw		$18^0_2 25^{1-}_0$	29,818.5	ms	B_{-2}	25^{1-}_2
30,148	w	S-T ?	28,849+1300	29,786.0		C_0-486	25^{0-}_0-486
30,123.0	w		25^{4+}_3	29,746.5		B_{-1}-433	$25^{1+}_1 36^0_1$
30,118.0	w	B_0-433	$25^{1-}_0 36^0_1$	29,728.8		C_{-2}+192	$18^1_0 25^{0-}_2$
30,097.0	w	C_{-1}+193	$18^1_0 25^{0+}_1$	29,723			$3^1_1 25^{0-}_0$
30,081.8	mw		25^{2-}_2	29,708.2	m	C_{-1}-196.3	$18^0_1 25^{0+}_1$
30,073	mw	C_0-198.5	$18^0_1 25^{0-}_0$	29,637	vw	B_{-3}+193	$18^1_0 25^{1+}_3$
30,069.5	mw d	B_0-486	25^{1-}_0-486	29,623	vw		$3^1_1 25^{1+}_1$
29,999.5	w		$3^1_1 25^{1-}_0$	29,616.3	vw		25^{3-}_4
29,985.0	mw	B_1-198	$18^0_1 25^{1+}_1$	29,536.4	vw	C_{-2}	25^{0-}_2
29,970.5	mw	B_0-3 r.p.	$18^0_3 25^{1-}_0$	29,508	vw	C_{-1}-2 r.p.	$18^0_2 25^0_1$—
29,904.5	mw	C_{-1}	25^{0+}_1	29,478.0	w		
29,887.6	w	C_0-2 r.p.	$18^0_2 25^{0-}_0$	29,469.5	vw	C_{-1}-433	$25^{0+}_1 36^0_1$
29,862.3	vw		25^{3+}_3	29,456.2	w		$3^3_3 25^{3-}_0$
29,827	vw		$3^2_2 25^{2-}_0$	29,447.1	w	B_{-3}	25^{1+}_3

continued ....

TABLE 6.5 (c)
(continued)

ν cm^{-1} vacuum	Relative Intensity	Notations	Assignment
29,427.1	mw	B_{-2}-2 r.p.	$18^0_2 25^{1-}_2$
29,336	w	B_{-2}-486	(25^{1-}_2)-486
29,168.0	w	C_{-3}	25^{0+}_3
29,034	w		25^2_0-486
28,867	w		(25^{2-}_2)-1210

The band at 30,591.9 cm^{-1} is one of the more intense bands of the high resolution spectrum. Three bands at successive intervals of ∿ 445 cm^{-1} were observed on the low frequency side of 30,591.9 cm^{-1}. The intervals were found to be alternately larger and smaller than 445 cm^{-1}. This irregularity is commonly called "staggering", and it arises as follows: if there is a double potential minimum in the upper state, transitions originating in ground state vibrational levels terminate alternately in the upper and lower inversion components of the excited state vibrational levels. Figure 6.2 illustrates that the interval 25^0_0-25^{0+}_1 should be greater than ν''_{25}, the ground state fundamental frequency, by an amount equal to the inversion doubling splitting 0^+-0^- in the vibrationless upper state. The vibronic levels are alternately A_1, B_1, A_1, ... in the ground state and A_2, B_2, A_2 ... in the upper state (compare Figure 3.6).

A similar, but larger, staggering should be observed for transitions terminating on the 1^--1^+ levels and higher levels. The bands at 30,591.9, 30,139.6, 29,701.0 and 29,252.6 cm^{-1} are assigned as a progression in ν''_{25}, called the B progression. The intervals between successive members of this progression are 452.3, 438.6 and 448.4 cm^{-1}. From the first three members, ν''_{25} is calculated to be 445.45 cm^{-1} and the inversion splitting of the upper state vibrational levels (which will be shown to be the 1^+-1^- levels) is determined to be 6.9 cm^{-1}.

At the beginning of this research, it was assumed that the infrared band at 468 cm^{-1} could be identified as the oxygen out-of-plane deformation, $\nu_{C=O\perp}$. Such an assignment created the problem that the interval between the first two members of the progression in $\nu_{C=O\perp}$ was smaller than the ground state frequency, whereas Figure 6.2 shows that this interval must be larger. After the Raman study of the three molecules CPH8, CPD4 and CPD8 was completed and after the progression in ν''_{25} was identified in the ultraviolet spectra of CPD4 and CPD8, it became evident that the Raman band at 442 cm^{-1} should be assigned as ν''_{25} in CPH8.

As the levels drawn in Figure 6.2 illustrate, if a number of progressions in ν''_{25} are observed, the progression with its first member at the lowest energy and with the smallest staggering will be the progression in which transitions terminate on the 0^+-0^- levels. The only other obvious progression in ν''_{25} has its first member at 30,278.1 cm^{-1} and successive members at 29,832.7, 29,387.2 and 28,941.5 cm^{-1}. The intervals between these are 445.4, 445.5 and 445.7 cm^{-1} respectively. The staggering is not observed as it was in the B progression. The inversion splitting in the upper state vibrational levels (which will be shown to be the 0^+-0^- level) could not, therefore, be measured and is inferred to be very small (< 0.2 cm^{-1}). There is some indication of positive anharmonicity in ν''_{25}, although the observed increase in frequency of successive intervals is within the experimental error. It is concluded that the transitions of this second progression terminate on the 0^+-0^- levels, and that the inversion doublet 0^+-0^- is very closely spaced. The band at 30,278.1 cm^{-1} is assigned as 25^{0-}_{0}. The assignment of other members of the progression (called the C progression) follows:

29,832.7 ... 25^{0+}_{1}
29,387.2 ... 25^{0-}_{2}
29,941.5 ... 25^{0+}_{3}

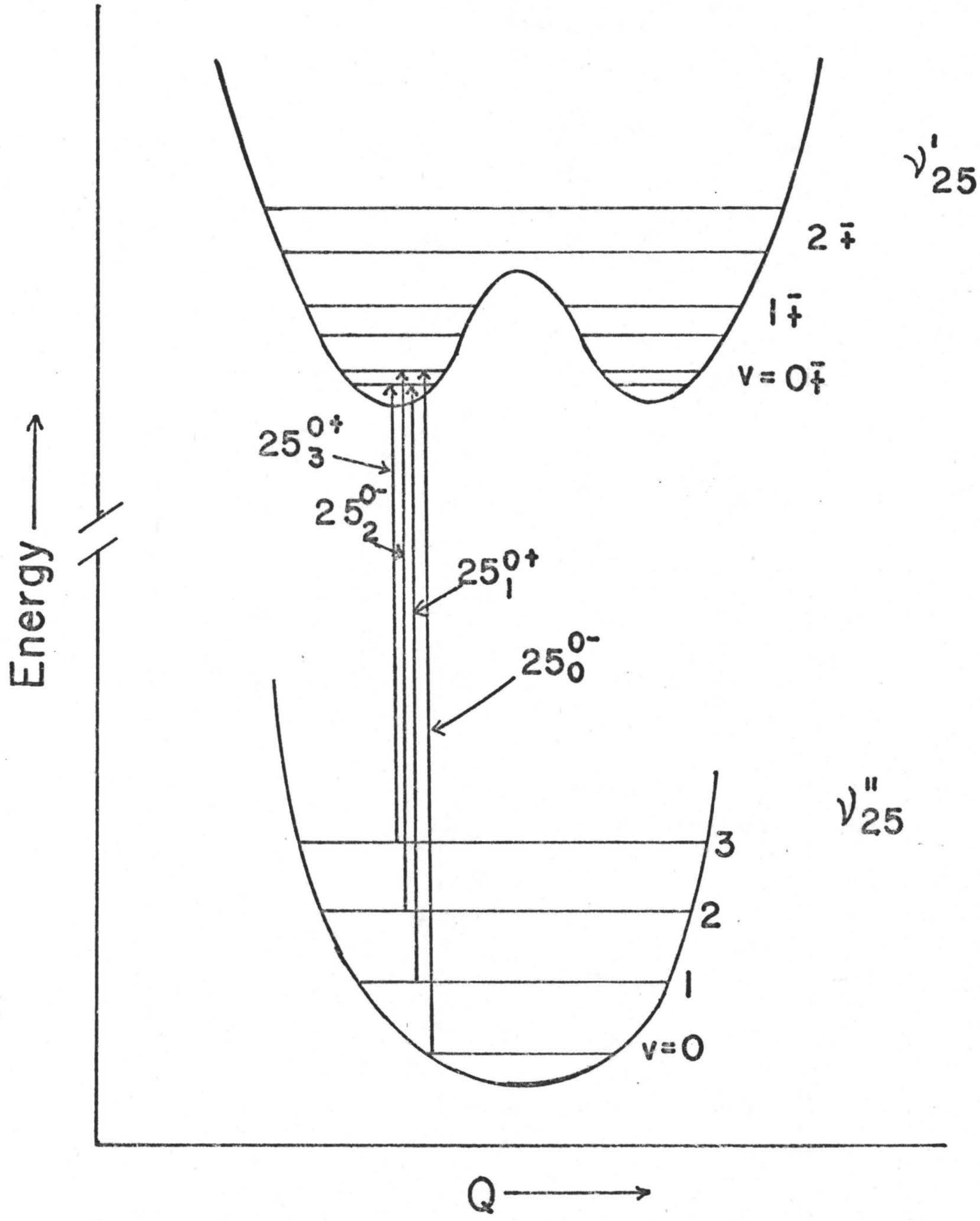

FIGURE 6·2 Staggering in the ν_{25} Progression.

The bands of the B progression arise from transitions terminating on the 1^+-1^- levels which have a separation of 6.9 cm^{-1}; they are assigned:

30,591.9 ... 25_0^{1-}
30,139.6 ... 25_1^{1+}
29,701.0 ... 25_2^{1-}
29,252.6 ... 25_3^{1+}

The band 25_1^{1+} was assigned tentatively as a hot band in section 6.3. Bands which originate on ground state levels differing by two quanta of ν''_{25} and terminate on the same upper level should show a constant separation of 890.9 cm^{-1}. Pairs of bands which are expected to show this constant difference, and the observed differences, are listed in Table 6.6. The discrepancy in the value 25_1^{1+}-25_3^{1+} may be because the band 25_3^{1+} is very weak (it is near the low frequency limit of the spectrum) and is difficult to measure to the same accuracy as the other bands. The wavenumber of the 25_0^{0-} band is 313 cm^{-1} less than that of the 25_0^{1-} band. The possibility that this 313 cm^{-1} interval is a ground state fundamental can be excluded since no such frequency is observed in the infrared and Raman spectra. Moreover, the interval 30,139.6 - 29,832.7 cm^{-1} would have to be equal to 313 cm^{-1} also, but it is only 306.9 cm^{-1}. In the present assignment, 313.8 cm^{-1} is the separation of the 1^- and 0^- levels of ν'_{25} and 306.9 cm^{-1} the separation of the 1^+ and 0^+ levels.

The calculation of a double minimum potential function and the inversion doublet separations will be discussed in detail in Section 6.6 The results will be referred to here in order to complete the discussion of the assignments.

Progressions in ν''_{25} formed by transitions terminating at higher excited state vibrational levels were looked for. The relatively intense bands at 30,887 cm^{-1}, 31,204.9 cm^{-1} and 31,555 cm^{-1} are assigned as 25^{2-}_{0}, 25^{3-}_{0}, and 25^{4-}_{0}, respectively. The intervals 2^{-}-0^{-}, 3^{-}-0^{-} and 4^{-}-0^{-} are therefore 609.1, 925.9 and 1276.9, respectively, in excellent agreement with the calculated values 605.8, 919.5 and 1279.2 cm^{-1} (see Table 6.9). Because the inversion splitting increases rapidly with successive vibrational quanta in the upper state, the staggering is expected to increase. Regular band intervals of close to 445 cm^{-1} are not observed for members of the ν''_{25} progressions terminating at higher levels, although the wavenumbers of alternate members should still exhibit a constant difference of 890.9 cm^{-1}. The bands caused by transitions to the upper state levels, $2^{\pm}$, $3^{\pm}$, and $4^{\pm}$ show increasing diffuseness, however, and the uncertainty in the differences is as much as ± 10 cm^{-1} for some pairs of bands. The splitting 2^{+}-2^{-} is calculated to be 72 cm^{-1}. The band 25^{2+}_{1} should occur at 30,887 - 445.5 - 72 cm^{-1} = 30,360 cm^{-1}. The band observed in this region has a complicated structure, possibly a consequence of the overlapping of two or more bands; the band head at 30,360.6 cm^{-1} is assigned as 25^{2+}_{1}. The tentative assignment of this band as a "hot band" (Section 6.3) is confirmed. The band at 30,006.9 cm^{-1} is assigned as the next member of the ground state progression, 25^{2-}_{2}. The calculated position of 25^{2+}_{3} is 29,483 cm^{-1}. There is a band at 29,478.0 cm^{-1} which is assigned as this. A very weak band at 29,110.8 is assigned as 25^{2-}_{4}. The wavenumbers of 25^{2-}_{2} and 25^{2-}_{4} show discrepancies of ∿ 10 cm^{-1} and 4 $cm.^{-1}$, respectively, from the wavenumbers calculated from combination differences.

The calculated inversion doublet splitting of the 3^+-3^- levels is 138.5 cm^{-1}. If a progression in ν''_{25} having 25_0^{3-} at 31,204.9 as vibronic origin is observed, bands should occur at frequencies 30,621 cm^{-1}, 30,314.0 cm^{-1} and 29,730.0 cm^{-1}. The weak bands at 30,619.6 cm^{-1}, 30,313.5 cm^{-1}, and 29,728.2 cm^{-1} are therefore assigned as 25_1^{3+}, 25_2^{3-}, and 25_3^{3+}, respectively.

The calculated splitting of the 4^+-4^- levels is 184.6 cm^{-1}. A progression in ν''_{25} with the diffuse band at 31,555 cm^{-1} (25_0^{4-}) as vibronic origin should have bands at 30,924.9 cm^{-1}, 30,664.1 cm^{-1} and 30,034.9 cm^{-1}. The very weak bands at 30,924 ± 2 cm^{-1}, 30,662.7 cm^{-1} and 30,033.6 cm^{-1} are assigned as 25_1^{4+}, 25_2^{4-}, and 25_3^{4+}, respectively.

A large number of very weak bands with no apparent rotational structure or sharp heads are observed. Two or three such bands can be picked out at intervals of ∿ 236 cm^{-1} to the low frequency side of each of the members of the ν''_{25} progressions. A Raman band at 238 cm^{-1} has been assigned as a ring puckering vibrational mode. The symmetry of this vibration has not been established. Cyclopentanone has two low frequency ring puckering vibrations, one of a_2 symmetry and the other of b_1 symmetry. (See Table 5.1). The absence of a band at 238 cm^{-1} in the infrared spectra may mean that the vibration of this frequency has symmetry $a_2(\nu_{18})$ or on the other hand, the b_1 vibration ν_{26} may produce only a very small change in dipole moment so that the resulting band is too weak to be observed. The symmetry species of the vibronic levels resulting from the excitation of either of these vibrations in combination with ν_{25} in the $A_2 \leftarrow A_1$ electronic transition are illustrated in Figure 6.3.

Some of the vibronically allowed transitions from levels in which ν''_{26} is excited in combination with ν''_{25} are shown in 6.3 (b). The transition $25^{1+}_{1}26^{0}_{2}$ should be less intense than $25^{1-}_{1}26^{0}_{1}$ because of the Boltzmann factor of ν''_{26}. (The relative population of the vibration levels $v_2=2$ to $v=1$ of ν''_{26} is ~ 0.3). Some of the allowed transitions in which ν_{18} is excited in combination with ν_{25} are shown in Figure 6.3(a). The vibronic selection rules $A_1 \leftrightarrow B_2$ and $B_1 \leftrightarrow A_2$ are fulfilled except for levels in which one quantum (or an odd number of quanta) of ν_{18} is excited. For example, the ground state levels in which ν''_{25} combines with one quantum of ν''_{18} have vibronic symmetry species A_2 or B_2. Both of these levels can combine with both A_2 and B_2 vibronic levels of upper state, but since the direct product species are A_1 and B_1, there can be no "intensity borrowing" through mixing with the higher B_2 electronic state. The transitions $18^{0}_{1}25^{1-}_{1}$ and $18^{0}_{1}25^{1+}_{1}$ are therefore expected to show two components, and to be weaker than the transition $26^{0}_{1}25^{1-}_{1}$. The transitions $18^{0}_{1}25^{1-}_{1}$ and $18^{0}_{1}25^{1+}_{1}$ may be weaker than $18^{0}_{2}25^{1+}_{1}$ if the Boltzmann population factor of the ν''_{18} levels is offset by a larger factor resulting from "intensity borrowing". The bands assigned as 25^{1+}_{1}, 25^{0+}_{1}, 25^{1-}_{2} and 25^{0-}_{2} (the "main bands") have weak band heads at -24 cm^{-1} which have the appearance of sequence bands. If there were sequence bands, they would be expected to accompany all the members of the ν''_{25} progression. None of the main bands in the ν''_{25} progressions of CPD4 and CPD8 show weaker heads of the same appearance. It is found that the position of the band at (25^{1+}_{1})-24 cm^{-1} coincides with the expected position of a band in which two quanta of a ground state vibration of frequency $\sim$ 236 cm^{-1} are excited in combination with 25^{0-}_{0}. Thus, possible assignments for the bands observed at (25^{0-}_{0}) - 233.5 and (25^{0-}_{0}) - 233.5 - 235.9, where the second band is more intense, are $18^{0}_{1}25^{0\mp}_{0}$ and $18^{0}_{2}25^{0-}_{0}$. As explained above, $18^{0}_{1}25^{0\mp}_{0}$ is expected to show two components, and they may be weaker than the band $18^{0}_{2}25^{0-}_{0}$. The expected relative intensities are observed, but the two components are not. The two components would be very close (< 1 cm^{-1}), however, and the band is very weak. For intervals of ∿ 235 cm^{-1} relative to the bands 25^{1-}_{0} and 25^{1+}_{1} it is possible to detect two weak components with the expected splitting of 6-7 cm^{-1}. There are, however, other weak bands in the regions near (25^{1-}_{0}) - 235 and 25^{1+}_{1}. Bands observed at the second interval of -235 cm^{-1} are again more intense and have apparently only one component. The indication is that the frequency 236 cm^{-1} should be assigned as ν_{18} (a_2), although the arguments are not considered to be conclusive.

A puzzling aspect of the 235 cm^{-1} interval is its occurrence at higher frequencies relative to all the main bands 25^{0-}_{0}, 25^{0+}_{1}, 25^{1-}_{0}, 25^{1+}_{1} and 25^{2-}_{2}. A possibility is that the excited state frequency does not change much from the ground state value. There is, however, a strong A-type band at (25^{1-}_{0}) + 206 cm^{-1} and the interval 206 cm^{-1} is assigned as ν'_{18}.

The wavenumbers of bands which would occur at intervals corresponding to all ground state fundamental frequencies relative to each of the main bands were calculated. A careful examination of the spectrum of CPH8 at the maximum obtainable pressure path failed to show any absorption at 28,508 cm^{-1}, the calculated wavenumber of $3^{0}_{1}25^{0-}_{0}$ -- (25^{0-}_{0} -

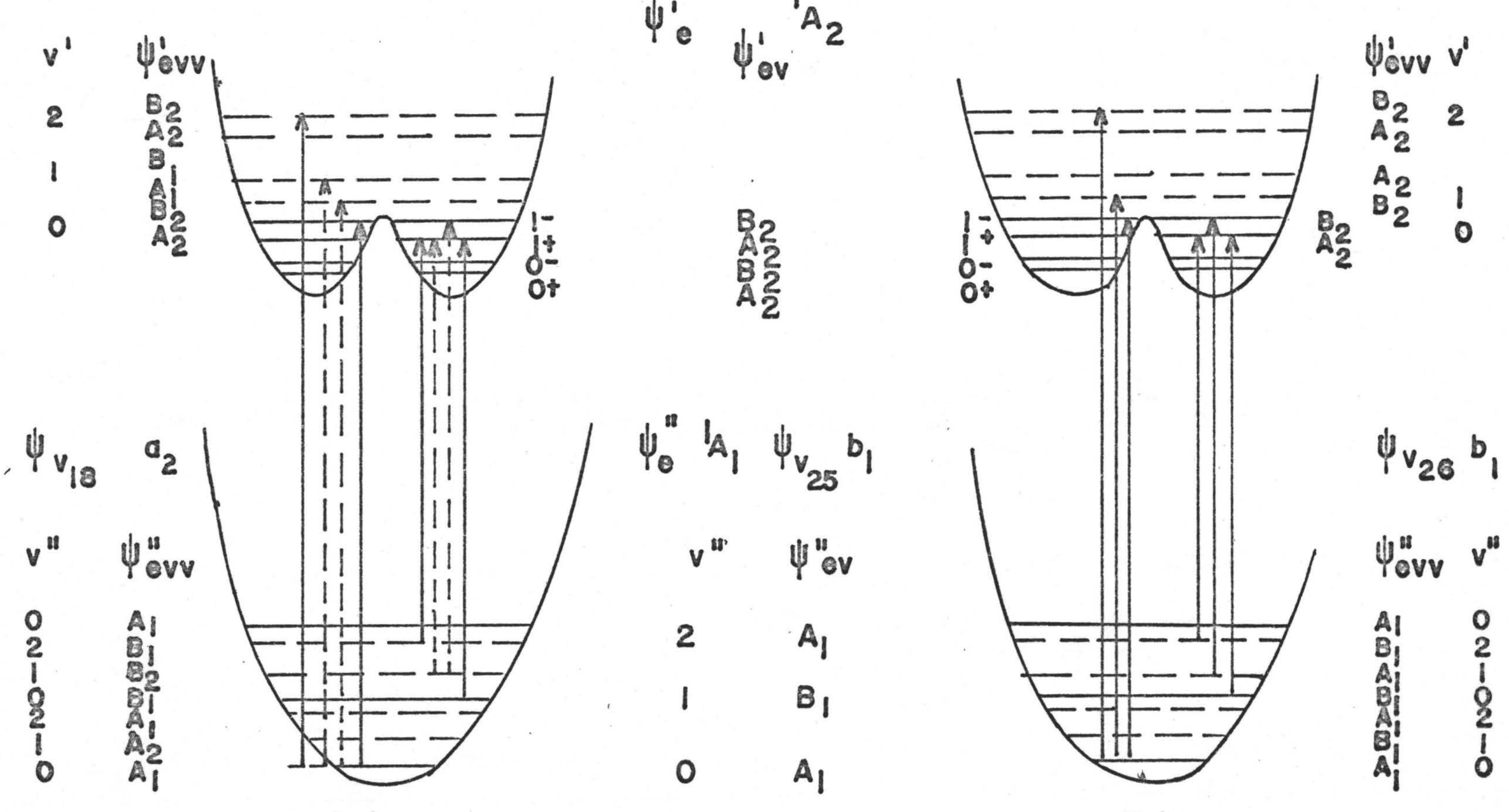

(a) (b)

FIGURE 6·3 Vibronic Species for $25^{v'}_{v''}18^{v'}_{v''}$ and $25^{v'}_{v''}26^{v'}_{v''}$

1770 cm^{-1}). The low Boltzmann population factor for ν_3 (v = 1 has a population at 20^{o}C of 0.0002 relative to v = 0) explains the absence of this band. Moreover, the interval 1770 cm^{-1} is approximately four quanta of ν''_{25} (4 x 445 = 1780) and so the assignment of 3^0_1,even if observed, would be ambiguous. The band at 28,827.4 cm^{-1} could be $3^0_1 25^{1-}_1$; however, it could also be 25^{0-}_0 - 1451 cm^{-1}. (The CH_2 deformation mode has a frequency of 1455 cm^{-1}).

Because cyclopentanone has thirty-six ground state fundamental frequencies, it is possible to calculate combinations of frequencies which will explain the wavenumbers of all the numerous weak bands. Therefore, only those prominent bands which occur consistently at ground state intervals relative to the main bands have been listed as positively assigned.

The band reported by RRR at 28,816 cm^{-1} was not observed in this study; the band reported by them at 0,0 - 897 (the frequency interval similar to the breathing mode, 888 cm^{-1}, Raman) is observed but is now assigned as 25^{1-}_2. The fundamental at 888 cm^{-1} is not observed in the ultraviolet spectrum.

The band at 30,009 cm^{-1} assigned by RRR as 0,0 - 573 is probably the band observed in the present study at 30,006.9 cm^{-1} and assigned as 25^{2-}_2. Only a very weak band at a frequency of 576 cm^{-1} is observed in the Raman spectrum. (Reitz[15] reported a Raman band at 578 cm^{-1}.) The band observed by RRR at 29,560 cm^{-1}, and assigned by them as 0,0 - 1022 is probably the same band that is assigned as 25^{2+}_3 in this work (29,566 cm^{-1}.)

Weak bands at intervals of 559 cm^{-1} and 468 cm^{-1} are observed at the low frequency side of all the main bands and these frequencies may be assigned to the ground state fundamentals, ν''_{11} and ν''_{36}, respectively. Other ground state intervals identified in at least four bands are 1458 cm^{-1}, 1272 cm^{-1} and 705 cm^{-1}. (See Table 6.7.). Assignment of excited state frequencies from other observed bands (apart from ν'_3, ν'_{25} and ν'_{18}) would be purely speculative and is not being attempted.

Bands at frequencies lower than the lowest wavenumber band reported by RRR are observed at 28,779.3, 28,772.8, 28,743.7, 28,733.7, 28,713.0, 28,695.1, 28,670.3 and 28,601.1 cm^{-1}. None of these "low frequency bands" form part of the main progressions, nor do they occur at ground state intervals relative to the main bands.

The possibility that some of these bands form part of the singlet-triplet $^3A_2 \leftarrow {}^1A_1$ system should be considered. A singlet-triplet (S-T) $\underline{n}\rightarrow\pi^*$ transition having 0,0 band at a wavenumber about 3,000 cm^{-1} lower than that of the singlet-singlet (S-S) 0,0 band is generally observed for carbonyl compounds. A S-T $\underline{n}\rightarrow\pi^*$ transition is much weaker than a S-S transition, the oscillator strengths being $\sim 10^{-6}$ and 10^{-4}, respectively.[113]

For H_2CO, eight bands of the S-T system at a pressure path of 2m - atm. were observed by Robinson and DiGorgio.[114] Hodges, Henderson and Coon[115] used absorbing paths of 5 - 120 m.-atm. for observation of 9 S-T bands. Robinson and DiGorgio noted that the C=O stretching fundamental in the excited triplet state was $\sim$ 75 cm^{-1} larger than in the excited singlet state. They say, "this difference is expected to remain fairly constant among aliphatic aldehydes and ketones, and it may provide a good check as to the multiplicity of the excited state when only the coarse structure of the spectrum can be resolved.[114] A similar effect was observed in the spectra of the oxalyl halides.[117(a)] Consequently, bands at intervals of ∿ 1300 cm^{-1} (1227+75) were looked for relative to the "low frequency bands" observed in this work; it was hoped that the C=0 stretching frequency in the $^3A_2$ state also obtained by $\underline{n}\rightarrow\pi^*$ promotion could be identified. Bands are observed at 29,995 and 29,970 cm^{-1}, intervals of + 1300 cm^{-1} relative to 28,695 and 28,670 cm^{-1}. The wavenumber + 1300 relative to the moderately intense band at 28,856 cm^{-1} would be 30,156 cm^{-1}. This frequency is too close to the intense band assigned as 25^{1+}_{1} for a separate band to be distinguished.

(b) The Spectra of the Deuterated Species

In vibrational structure and intensity distribution, the ultraviolet spectra of CPD4 and CPD8 resemble the spectrum of CPH8. Frequencies and assignments of the diffuse bands (photographed under low resolution) are given in Table 6.4, for comparison with those of CPH8. By analogy with CPH8, ν'_3 was identifed as 1212 cm^{-1} and 1208 cm^{-1} for CPD4 and CPD8, respectively.

The Spectrum of CPD4

The Raman frequency at 376 cm^{-1} was assigned as ν''_{25}, the oxygen-out-of-plane bending vibration (see Chapter 5). All of the intense bands in the region from 33,000 cm^{-1} to 28,400 cm^{-1} are members of progressions in ν''_{25}.

The bands at 30,548.9, 30,166.8, 29,789.7 and 29,405.2 cm^{-1}, with frequency separations 382.1, 377.1 and 384.5 cm^{-1}, are assigned as 25^{1-}_{0}, 25^{1+}_{1}, 25^{1-}_{2} and 25^{1+}_{3} respectively. From the observed staggering in the first three members, the splitting of the excited state inversion doublet is calculated to be 2.5 cm^{-1}, and ν''_{25} to be 379.6 cm^{-1}. The bands at 30,267.2, 29,888.5, 29,508.0 and 29,127.1 cm^{-1}, with separations of 378.7, 380.5 and 380.9 are assigned as 25_0^{0-}, 25_1^{0+}, 25_2^{0-} and 25_3^{0+}, respectively. Since the staggering is not observed, the splitting in the 0^+-0^- line must be very small.

The band at 30,819.2 cm^{-1} is assigned as 25_0^{2-}. From the potential barrier calculations, the splitting of the upper state levels 2^+-2^- is estimated to be 39.6 cm^{-1}. The bands at 30,397, 30,060.0 and 29,638.2 cm^{-1} are assigned as 25_1^{2+}, 25_2^{2-} and 25_3^{2+}, respectively (calculated positions, 30,400.1, 30,060, 29,640 cm^{-1}; errors, ± 3 cm^{-1}).

The band at 31,100.1 cm^{-1} is assigned as 25_0^{3-}. The excited state 3^+-3^- splitting is calculated to be 119.8 cm^{-1}. The bands at 30,599, 29,839.9 and 29,578 cm^{-1} are assigned as 25_1^{3+}, 25_3^{3+}, and 25_4^{3-}, respectively (calculated positions, 30,600.4, 29,841.8 and 29,582.1 cm^{-1}; errors ± 4 cm^{-1}). The band 25_2^{3-} should fall at 30,341.1 cm^{-1}, but the absorption in this region is extremely weak. Also, the wavenumber 30,599 cm^{-1} coincides with that calculated for (25_0^{2-}) - 220 cm^{-1} and so the assignment of the band at 30,599 cm^{-1} is tentative. The band at 31,398.0 is assigned as 25_0^{4-}. The calculated excited state splitting of 4^+-4^- is 154.2 cm^{-1}. The bands 30,835.7 and 30,642.0 cm^{-1} are assigned as 25_1^{4+} and 25_2^{4-} (deviations from calculated wavenumbers, -30 cm^{-1}, +4 cm^{-1}). Pairs of bands exhibiting constant combination differences are listed in Table 6.6.

A number of weak bands are observed at intervals of about -220 cm^{-1} relative to the main bands of the ν_{25}'' progression. By analogy with CPH8, these bands are assigned tentatively as combinations of ν_{25}'' with the ring puckering mode, ν_{18}'' (220 cm^{-1}, Raman, dp). An interval of +213 cm^{-1} was

TABLE 6.6

COMBINATION DIFFERENCES IN THE ν_{25} PROGRESSION*

Observed Band	CPH8	CPD4	CPD8
$25_0^{0-} - 25_2^{0-}$	890.9	759.2	735.2
$25_0^{1-} - 25_2^{1-}$	890.9	759.2	735.1
$25_1^{0+} - 25_3^{0+}$	891.2	761.4	736.5
$25_1^{1+} - 25_3^{1+}$	887.0	761.5	736.5
$25_0^{2-} - 25_2^{2-}$	880.1	759.2	734.6
$25_1^{2+} - 25_3^{2+}$	882.	758.8	-
$25_0^{3-} - 25_2^{3-}$	891.4	-	734.4
$25_1^{3+} - 25_3^{3+}$	891.4	759.1	728.5
$25_0^{4-} - 25_2^{4-}$		756	737.5
$25_1^{4+} - 25_3^{4+}$	890.4		

---

* in units of cm^{-1}

also observed and may possibly represent the upper state frequency ν'_{18}.

Other ground state frequencies identified are 1101, 1058, 832, and 438. (See Table 6.7).

A search for possible S-T bands was made, as for CPH8. The weak low frequency bands at 28,590 and 28,744 cm^{-1} do not fit in the vibrational analysis of the S-S transition. The hypothetical band at +1300 cm^{-1} relative to 28,590 cm^{-1} would underlie the intense band 25_1^{0+}. A band at ∿ +1300 cm^{-1} relative to 28,744 cm^{-1} is observed at 30,044 cm^{-1}.

The Spectrum of CPD8

The assignment of the "main bands" of CPD8 is completely analogous to the assignments already discussed for CPH8 and CPD4.

The Raman frequency 378 cm^{-1} has been assigned as ν''_{25}. A staggered progression in this frequency is observed in the ultra-violet spectrum. Analysis of the intervals in the progression yields the values $0^+ - 0^- < 0.2$ cm^{-1}, $1^+ - 1^- = 2.5$ cm^{-1}, and $\nu''_{25} = 367.6$ cm^{-1}.

The bands at 30,816.4, 31,088.3 and 31,382.5 cm^{-1} are assigned as 25_0^{2-}, 25_0^{3-} and 25_0^{4-}, respectively. From the potential functions calculations, the splitting of the $2^+ - 2^-$ doublet is 39.4 cm^{-1}. The bands at 30,406.4 and 30,081.8 cm^{-1} are assigned as 25_1^{2+} and 25_2^{2-} (calculated wavenumbers 30,404.5 cm^{-1} and 30,081.2 cm^{-1}, errors ± 2 cm^{-1}). 25_3^{2+} should occur at ∿ 29,674 cm^{-1}, but the absorption in the region 29,708 - 29,623 cm^{-1} is too weak and no band is observed.

The interval $3^+ - 3^-$ is calculated to be 119.3 cm^{-1}. Weak bands at 30,590.8, 30,353.9, 29,862.3 and 29,616.3 are assigned as 25_1^{3+}, 25_2^{3-}, 25_3^{3+} and 25_4^{3-}, respectively (calculated wavenumbers, 30,602.0, 30,353.1, 29,866.0

and 29,617.9; errors, +12 cm^{-1}, -1 cm^{-1}, +4 cm^{-1}, +2 cm^{-1}, respectively).

The interval 4^+-4^- is calculated to be 154.7 cm^{-1}. Bands at 30,695.0 cm^{-1} and 30,123.0 cm^{-1} are assigned as 25_2^{4-} and 25_3^{4+} (calculated 30,649.3, 30,124.7 cm^{-1}, respectively; errors ± 2 cm^{-1}). 25_1^{4+} should fall at 30,860.2 cm^{-1}; a band is not observed at or near this wavenumber. 25_4^{4-} should fall at 29,911.8, but no separate band is distinguishable near the intense band 25_1^{0+} at 29,94.5 cm^{-1}.

A number of weak bands are observed at ∿ -197 cm^{-1} relative to the "main bands". This interval is assigned tentatively as ν''_{18} (Raman 197 cm^{-1}, dp) by analogy with CPH8 and CPD4. Weak bands at an interval of +195 cm^{-1} relative to the "main bands" may represent ν'_{18}.

Apart from 367 cm^{-1} and 197 cm^{-1}, intervals corresponding to only two ground state fundamentals -- 486 cm^{-1} and 433 cm^{-1} -- were identified. (See Table 6.7).

A band was observed at 30,148 cm^{-1}, an interval of +1300 cm^{-1} relative to the low frequency band at 28,849 cm^{-1}. A similar band relative to 29,034 cm^{-1} was observed, at 30,340 cm^{-1}, but 29,034 coincides with (25_0^{2-}) -486, so that a definite assignment of 29,034 and 30,340 cm^{-1} (as bands of a $^3A_2 \leftarrow {}^1A_2$ system) cannot be made.

(c) Isotope Shifts

Brand et al.[116] have found that the chlorine vibrational isotope shift in progressions of the 5340Å band system of thiphosgene is a linear function of quantum number. The same has been found for oxalylchloride.[117(b)]

A similar isotope effect in the spectrum of cyclopentanone has confirmed the assignments of the ν_{25} progression. Deviations from linearity

TABLE 6.7

GROUND STATE FREQUENCIES

Mode		Infrared* Spectra	Raman (liquid)	Ultraviolet (vapour)
CPH8	ν_{11}		559	559
	ν_{18}	-	241	235
	ν_{25}		444	445.6
	ν_{36}	468 (B)		468
CPD4	ν_{11}		515	515
	ν_{18}		220	221
	ν_{25}		376	379.6
	ν_{36}	438 (B)		438
CPD8	ν_{11}		486	486
	ν_{18}		197	197
	ν_{25}		378	367.6
	ν_{36}	433 (B)		433

---

* Units of cm^{-1}

can be explained and a prediction of the barrier height of the double minimum potential function in the upper state can be made.

Figure 6.4 shows the observed isotope effect for cyclopentanone (in the ground electronic state) for the ν''_{25} progression originating at 25^{0-}_{0}. The shift in wavenumbers of the vibrational bands of CPD4 and CPD8 relative to wavenumbers of the corresponding bands of CPH8 are plotted against quantum number. The expected linear relationship is observed. Figure 6.5 shows a similar plot for the $25^{1\pm}_{v''}$ progression originating at 25^{1-}_{0}.

Both progressions show a negative isotope shift for v=0, but this shift is smaller for the 25^{0-}_{0} band than it is for the 25^{1-}_{0} band. A positive shift of the 0,0 band would be in accordance with the general model of a shallower potential well in the excited state.[118] Brand[75] reported the shift of the 0,0 band of D_2CO as +62 cm^{-1} relative to the 0,0 band of H_2CO. It is not possible to calculate the theoretical shift of the 0,0 band in cyclopentanone, however, since all the fundamental frequencies in both upper and lower states are not known. The contribution of ν_{25} towards the (total) isotope shift of the 0,0 band may be calculated by subtracting the difference in zero-point energies of the ground excited states for CPD4 from that difference for CPH8. The calculation is illustrated in Figure 6.6. If the zero point energy is assumed to be equal to one-half of the first vibrational quantum in the ground state and one-half the difference between the centres of the 0^+-0^- and 1^+-1^- doublets in the excited state, the calculated contribution of ν_{25} to the shift of the 0,0 band is +18 cm^{-1} for CPH8-CPD4, and +25 cm^{-1} for CPH8-CPD8. The observed negative shift may indicate that potential well is "steeper" in the

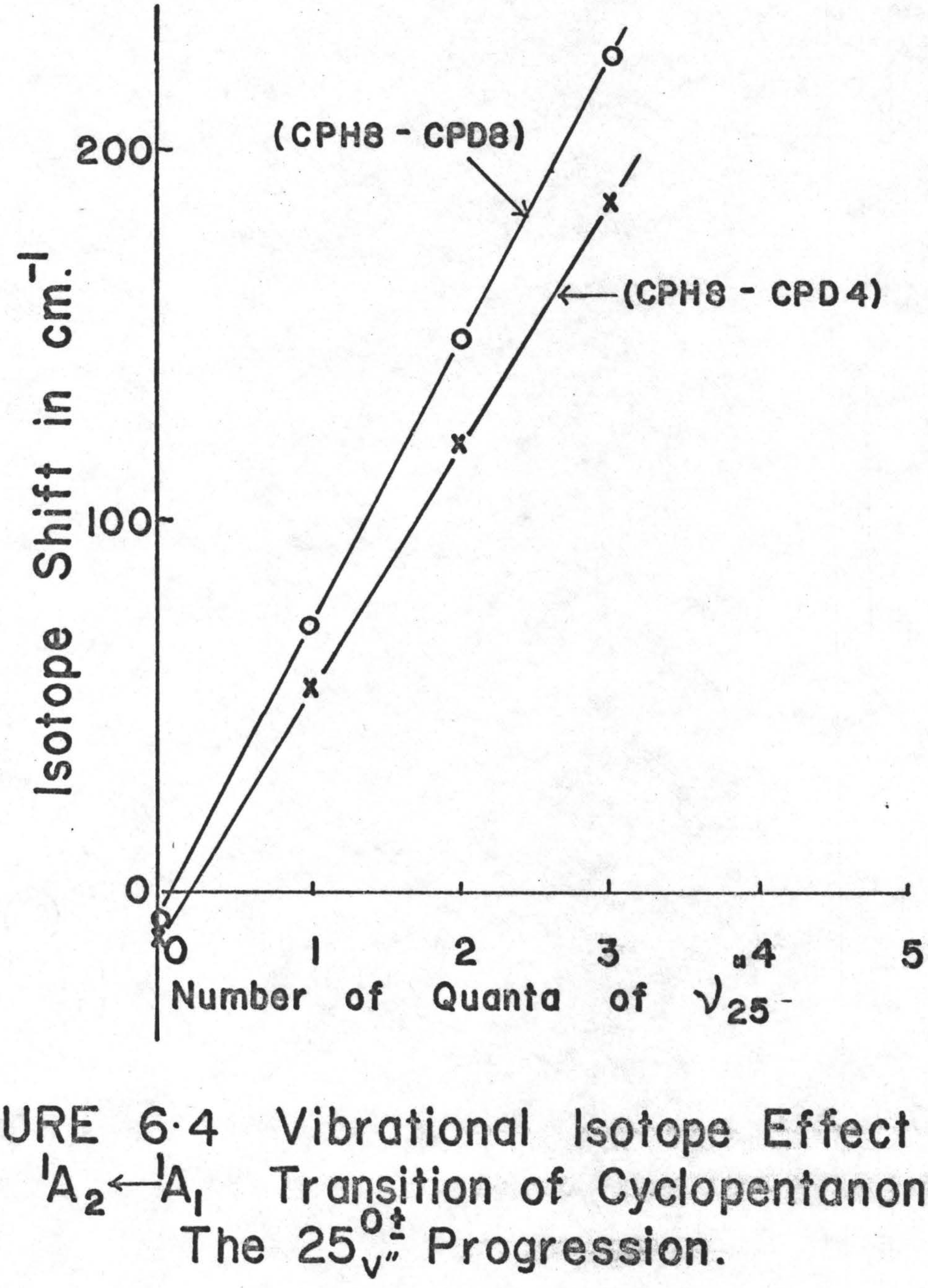

FIGURE 6·4 Vibrational Isotope Effect in the $^1A_2 \leftarrow {}^1A_1$ Transition of Cyclopentanone. The $25^{0\pm}_{v''}$ Progression.

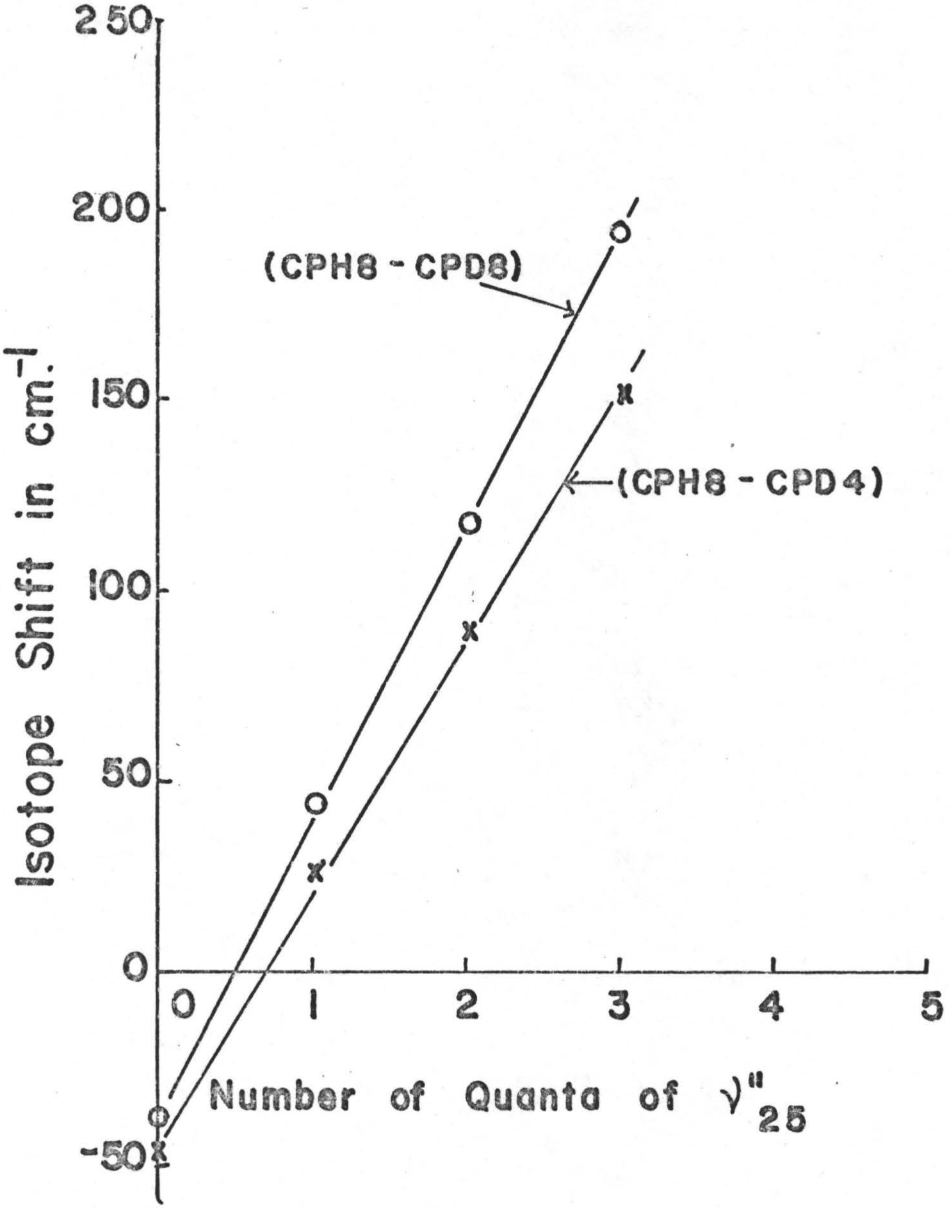

FIGURE 6·5 Vibrational Isotope Effect in the $^1A_2 \leftarrow {}^1A_1$ Transition of Cyclopentanone. The $25^{1+}_{v''}$ Progression.

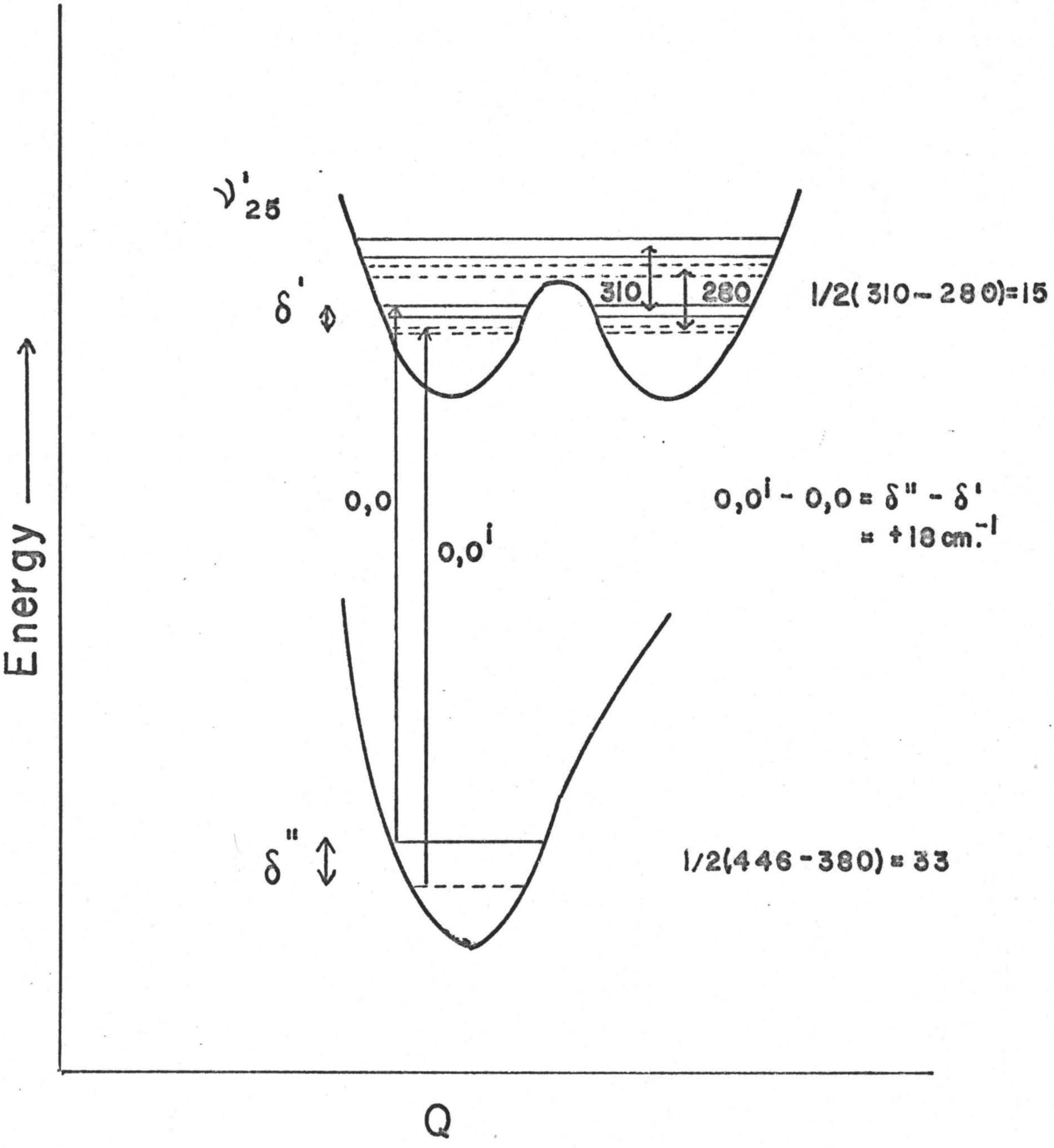

FIGURE 6·6 Contribution of ν''_{25} to 0,0 shift CPH8-CPD4 excited state. If the quanta of ν''_{25} were wrongly numbered, the curve in Figure 6.4 could be shifted to "the right" to give a positive shift for 25^{0-}_{0}. It is unlikely that the numbering given is wrong, however, since the double potential minimum in the upper state does give a steeper-sided curve than the ground state potential curve. The potential function calculations indicate that the upper state potential has positive anharmonicity; in the regions of the minima, however, the curve is nearly parabolic.

Figure 6.7 shows the experimental isotope effect (in the excited state) for the antisymmetric (minus) levels of the inversion doublets in the ν'_{25} progression. It is evident that the points do not lie on one straight line (the uncertainty in a given point is only $\sim$ 0.5 cm^{-1}, whereas the deviation from linearity is $\sim$ 10 cm^{-1}). The shifts for the levels 0^-, 1^- and 2^- fit one straight line. The shifts for the levels 3^- and 4^- fit a line of different slope. The two lines intersect in the region between the 2^- and 3^- levels, close to 2^-.

The linear relationship, as observed for the ground state progressions (see Figures 6.4 and 6.5) is expected only in the harmonic oscillator approximation. Deviations from linearity may be the result of anharmonicity. The first few successive - (minus) vibrational energy levels (or successive + levels) in the upper state will be approximately those of a harmonic oscillator. In the vicinity of the top of the barrier, however, large deviations from harmonic behaviour obtain. Above the barrier, the splitting between the symmetric and antisymmetric components rapidly approaches a constant value (equal to one-half the separation between the unperturbed vibrational frequency). It is suggested here that

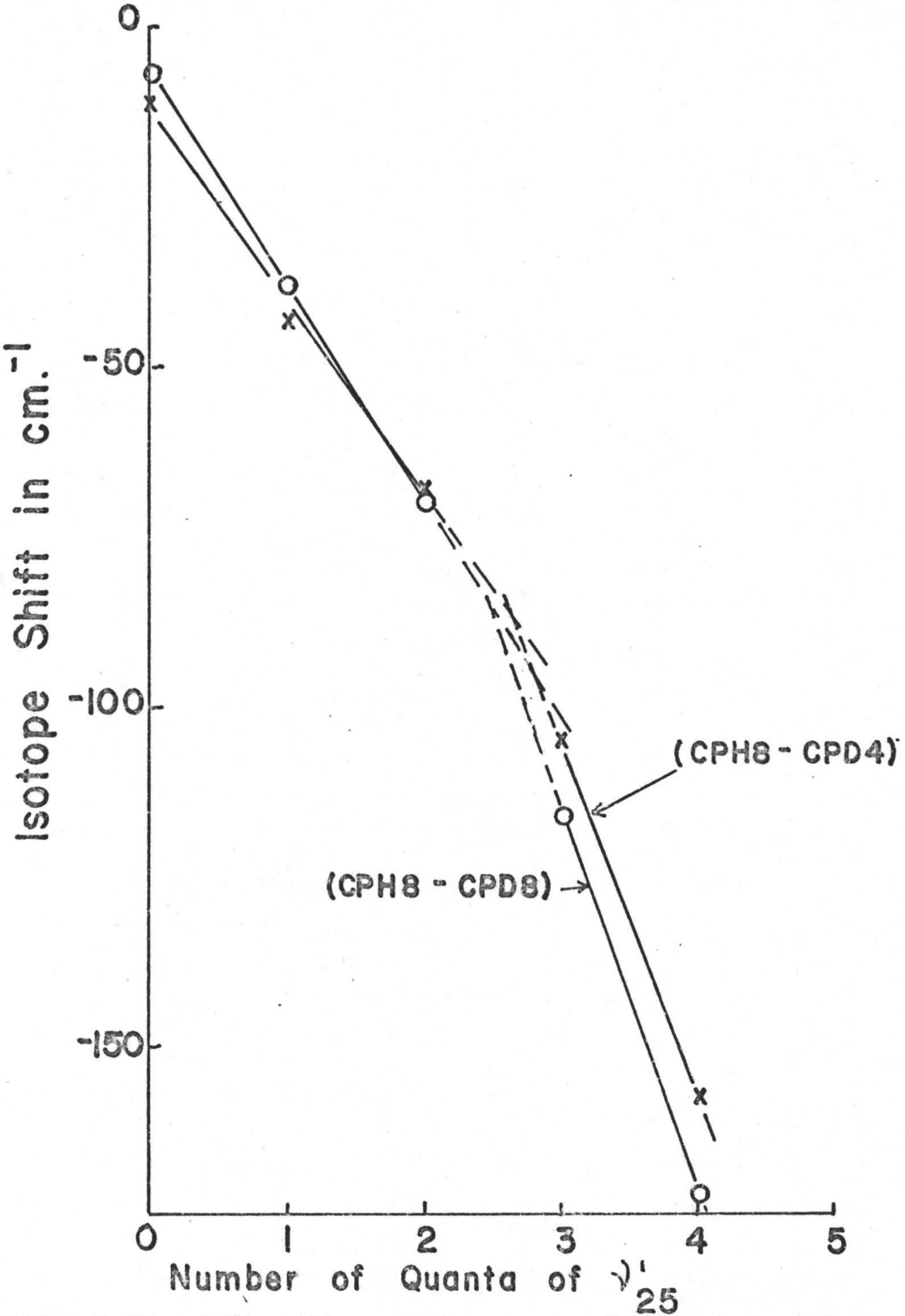

FIGURE 6·7 Vibrational Isotope Effect in the $^1A_2 \leftarrow {}^1A_1$ Transition of Cyclopentanone. The 25^{v-}_0 Progression.

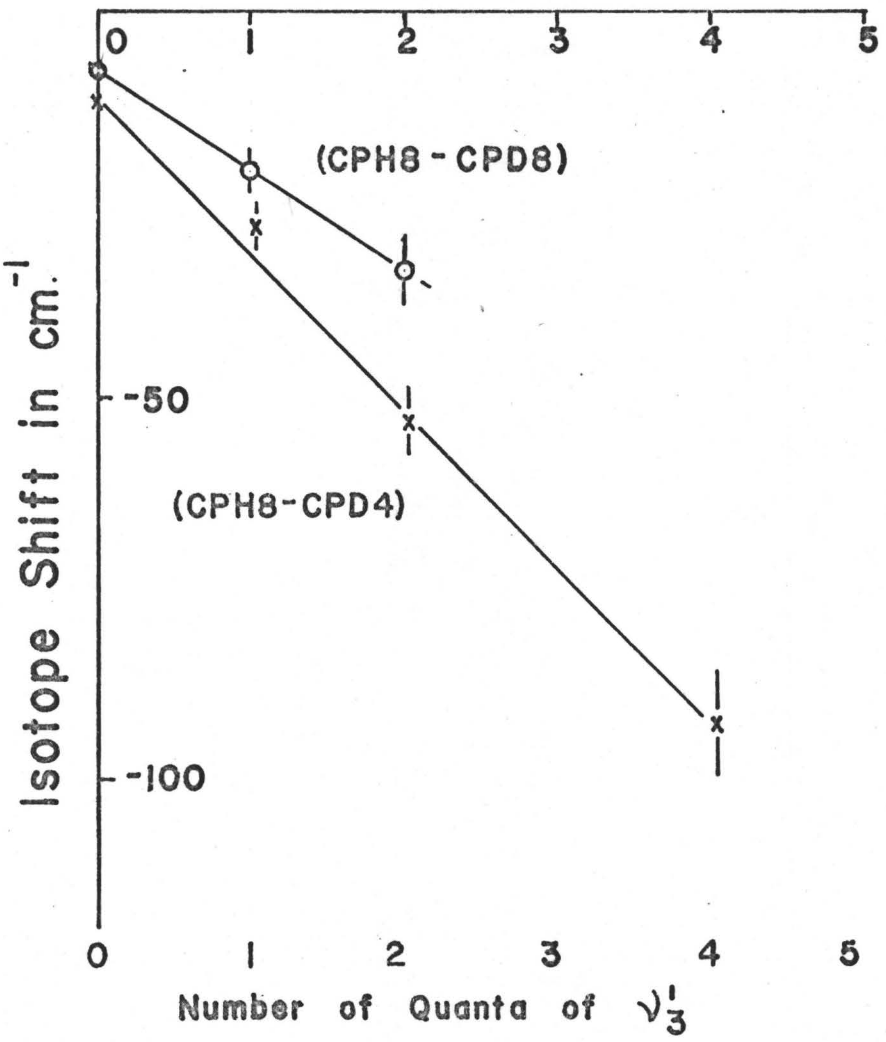

FIGURE 6·8 Vibrational Isotope Effect in the $^1A_2 \leftarrow {}^1A_1$ Transition of Cyclopentanone The ν_3' progression the point of intersection of the two plotted lines in Figure 6.7 occurs in the region of the top of the barrier. If this postulate is valid, the top of the barrier is just above the 2^- vibrational level. The results of the potential calculations confirm this idea (see Figures 6.10, 6.11, 6.12). The barrier is $\sim$ 705 cm^{-1} high and the 2^- levels are at 772 cm^{-1} (CPH8); 688.1 cm^{-1} (CPD4), and 689.4 cm^{-1} (CPD8), relative to the minima as zero.

Figure 6.8 shows the experimental isotope shift (in the excited state) for a progression in ν_3', originating on 25_0^{0-}. The shifts are approximately linear in quantum number. As in Figures 6.5 and 6.7, the lines do not extrapolate to the graphic origin; the first point in all three plots is the shift of the 25_0^{0-} band. The 0,0 band (that is, the 25_0^{0+} band, which is estimated to be within 0.2 cm^{-1} of the 25_0^{0-} band) shows a shift of -10.9 cm^{-1} for CPH8-CPD4 and -6.6 cm^{-1} for CPH8-CPD8. The negative shift is apparently anomalous (see above discussion), and the possibility that the true 0_0^{0+} band is displaced to low frequency by one quantum of ν_3' cannot be ruled out.

At -1227 cm^{-1} relative to 25_0^{0-} the absorption is very weak; the low frequency limit of observed bands is close. There are a few weak bands in this region which are still unassigned. Neither do they fit into the general pattern of the ν_{25}'' progression already identified, nor do they occur at intervals corresponding to ground state frequencies relative to the "main bands". (See Section 6, p.148).

The theoretical wavenumbers of bands displaced by one quantum of ν_3' to low frequency relative to some of the main bands are compared with the observed wavenumbers of low frequency bands in Table 6.8. Agreement between calculated and observed wavenumbers was obtained for 13 out of 21 possible bands down to the limit of observed absorption. Extrapolation of the line for CPD8-CPD4 in Figure 6.8 to the left of the graphic origin shows that a renumbering of the $3_0^{v'}$ progression would give an isotope shift of +10 cm^{-1} for v'=0. The absolute numbering cannot be assigned conclusively, however, because of the weakness and scarcity of the bands in the low frequency region of the spectrum. There is no obvious reason why the shifts for CPH8-CPD8 are smaller than those for CPH8-CPD4 in the ν_3' progression. Even if the shift for v'=0 in CPH8-CPD4 could be explained by a renumbering, the shift for CPH8-CPD8 would still be anomalous.

The band $3_0^3 25_0^{0-}$ was not observed in the spectrum of CPH8, but its wavenumber is predicted from the graph of Figure 6.8 to be ∿ 33,950 cm^{-1}. (RRR observed a band at ∿ 33,948 cm^{-1} which they could not assign). The assignments of the ν_3' progression in CPH8 (Tables 6.4 and 6.5) are based on the band at 30,278.1 cm^{-1} as 0_0^{0-} and the bands which are observed at intervals of -1227 cm^{-1} are indicated. This assignment of the 0_0^{0-} band is supported by the estimate made from the "mirror symmetry" of the absorption and fluorescence curves (see Section 6.4).

6.6 The Double Minimum Potential Function

The treatment of the double minimum potential function in this section follows that given in the paper of Coon, Naugle and McKenzie.[119] Double minimum potentials have explained the vibrational energy level spacings for a number of molecules in their electronic ground states; the classic example is ammonia; other examples are the puckered ring compounds discussed in Chapter 2 (see Table 2.3). There have been fewer applications of the theory to excited states of molecules; however,

TABLE 6.8

BANDS DISPLACED BY ONE QUANTUM OF ν_3' TO LOW FREQUENCY FROM "MAIN BANDS"

	CPH8 $\nu_3' = 1227$*		CPD4 $\nu_3' = 1212$		CPD8 $\nu_3' = 1208$	
Reference Band	Calc.	Obs.	Calc.	Obs.	Calc.	Obs.
25^{2-}_{0}	29,660		29,607.2	29,607	29,708	29,708
25^{1-}_{0}	29,364.9	29,362	29,336.9	29,337.1	29,341	29,346.7 vvw+
25^{0-}_{0}	29,051.1	29,057	29,055	29,047.7	29,059	
25^{2+}_{1}	29,140	29,136.6	29,188		29,194.4	
25^{1+}_{1}	28,912.6	28,914	28,954.8	28,956.1	28,971.6	
25^{0+}_{1}	28,605.7	28,601.1	28,669.5		28,692.5	
25^{2-}_{2}	28,779.7	28,779.3	28,850.0	28,856 str	28,873.8	28,867
	Beyond low frequency limit of observed absorption:					
25^{1-}_{2}	28,474		28,579.7			
25^{0-}_{2}	28,160		28,298			

---

* units of cm^{-1}

\+ v very

w weak

str strong

Brand et al,[116] using the method of this section, calculated a barrier of ∿ 600 cm^{-1} in the out-of-plane bending mode for Cl_2CS in its $^1A_2$ state. The $^1A_2$ and $^3A_2$ excited electronic states of H_2CO are known to have a double minimum potential with respect to the out-of-plane bending mode.[75] Using the energies of the 0^+, 0^-, 1^+ and 1^- levels known from the vibrational analysis (Brand[75], Robinson and DiGorgio[114]; Hodges, Henderson and Coon[115]), Coon et al[119] have calculated the barrier to be 350 cm^{-1} in the $^1A_2$ state and 783 cm^{-1} in the $^3A_2$ state.

A double minimum potential function, V(Q), is

$$V(Q) = \frac{1}{2}\lambda Q^2 + A \exp(-a^2Q^2) \qquad (6.1)$$

where Q is a mass weighted coordinate defined by $2T = \dot{Q}^2$ and λ, A and a^2 are three parameters.[b]

The minima of this function, located at $\pm Q_m$, are given by

$$Q_m{}^2 = \frac{1}{a^2} \ln \left(\frac{2a^2A}{\lambda}\right) \qquad (6.2)$$

(obtained from 6.1 by differentiating the expression for V(Q) and setting $\frac{\partial V(Q)}{\partial Q} = 0$). The parameters are redefined in a more convenient form: ρ is defined by the equation

$$a^2 = e^{\rho}\,\lambda/2A \qquad (6.3)$$

Substitution of equation (6.3) into equation (6.2) gives

$$Q_m{}^2 = \rho/a^2 \qquad (6.4)$$

---

[b] If V is in ergs, the dimensions of λ are sec^{-2};Q, g. cm^2; and A, ergs.

The parameter ν_0 (in cm^{-1}) is defined by the equation

$$\lambda = (2\pi c\nu_0)^2 \qquad (6.5)$$

and the dimensionless parameter B is defined so that the barrier height is $Bhc\nu_0$ (in ergs); that is, from equations (6.1), (6.2) and (6.3),[c]

$$Bhc\nu_0 = V(0) - V(Q_m) = A(e^\rho - \rho - 1)/e^\rho \qquad (6.6)$$

The barrier height in cm^{-1} is

$$b = B\nu_0 \qquad (6.7)$$

and the positions of the minima are given by [d]

$$Q_m{}^2 = \frac{2\rho}{e^\rho-\rho-1}\,\frac{h}{4\pi^2 c}\,\frac{B}{\nu_0} \qquad (6.8)$$

where $\frac{h}{4\pi^2 c} = 55.9810 \times 10^{-40}$ g. cm.

---

[c] From (6.1), (6.4), (6.3)

$$V(Q_m) = \frac{1}{2}\lambda\,\rho/a^2 + A\cdot 2a^2A/\lambda = A\rho/e^\rho + A\,e^{-\rho};\quad V(0) = A$$

[d]

$$Q_m{}^2 = \rho/a^2 = \rho 2A/e^{\rho\lambda};\quad \text{but } A/e^\rho = \frac{Bhc\nu_0}{e^\rho-\rho-1}$$

$$\therefore\ Q_m{}^2 = \frac{2\rho}{e^\rho-\rho-1}\,\frac{Bhc\nu_0}{\lambda} = \frac{2\rho}{e^\rho-\rho-1}\,\frac{h}{4\pi^2 c}\,\frac{B}{\nu_0}$$

The eigenvalues of equation (6.1) have been tabulated by Coon et al[119,120] for a wide range of the parameters, ρ, B and ν_0. They plotted the potential for ρ values of 0.6, 0.9, 1.2 and 1.5 with the quantities Q_m and $B\nu_0$ held fixed. Figure 6.9 (after Coon et al[119]) illustrates the effect of ρ on the shape of the function. For $\rho = 1.5$, the curve for each minimum is parabolic. For smaller ρ, the outer walls of the potential rise more steeply than the barrier.

If three energy levels of a double minimum potential function can be determined spectroscopically, a potential function having the same levels and the form of equation (6.1) may usually be calculated. For a given value of ρ the other two parameters may be determined from two known levels by use of one of the tables of energy levels. The same table gives the ten lowest levels of double minimum potential. If the calculation is then repeated for different ρ values, the final choice of ρ is the one which leads to best agreement between observed and calculated levels.

In Coon's tables 1(a) and 1(b),[119] the energy levels G/ν_0, relative to the potential minima as zero, are given as a function of the barrier height parameters B for $\rho = 0.6$. Let v_i designate the inversion doublet quantum numbers 0^+, 0^-, 1^+, 1^- .... The vibrational energy in wavenumbers, relative to the 0^- level, may be written

$$G_{0^-}(v_i) = G(v_i) - G(0^-) \qquad (6.9)$$

For CPH8, the level intervals $1^- - 1^+ = 6.9\ \mathrm{cm}^{-1}$ and $1^- - 0^- = 313.8\ \mathrm{cm}^{-1}$ were used in the calculation of the potential. (The interval $0^- - 0^+$ was not used because it is too small to be measured from the spectra). The

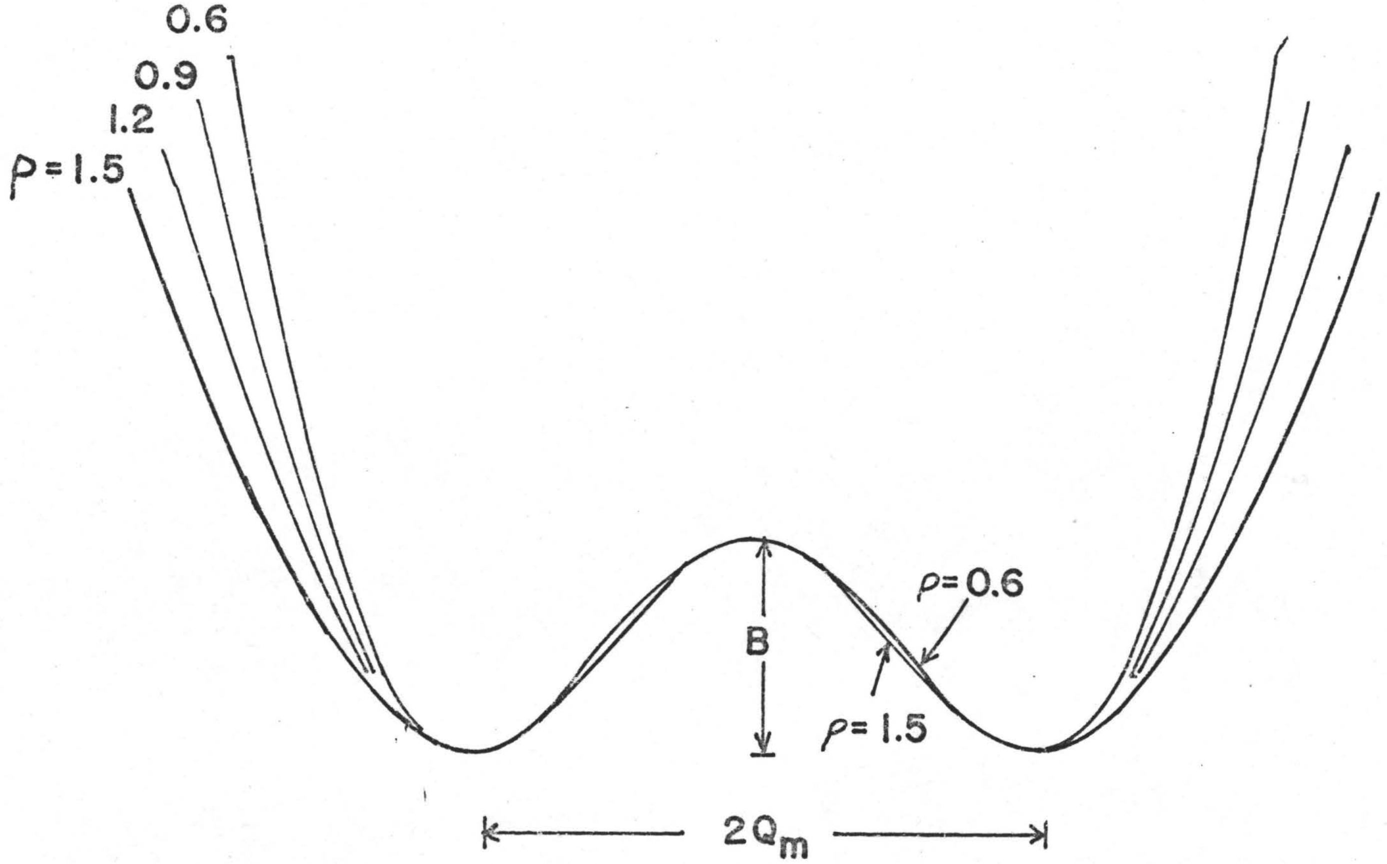

FIGURE 6·9 The effect of ρ on the shape of the double minimum potential function. (After Coon et al. J. Mol. Spectroscopy 20, 107, (1966).)

theoretical value of the ratio $\frac{G(1^-) - G(0^-)}{G(1^-) - G(1^+)}$ was calculated from tables 1(a) and 1(b)[119] and plotted as a function of B for $\rho = 0.6$. The experimental value of this ratio is $\frac{313.8}{6.9} = 45.478$. Graphical interpolation shows that 45.478 corresponds to a B value 2.242 for $\rho = 0.6$. The value of ν_0 may now be obtained from the identity

$$\nu_0 = [G(1^-) - G(0^-)] / [\frac{G(1^-)}{\nu_0} - \frac{G(0^-)}{\nu_0}] \qquad (6.10)$$

The numerator is 313.8 and denominator, 0.9972, is obtained from the tables by interpolation for B = 2.242. The result for CPH8 is $\nu_0 = 314.70$ cm^{-1}. The lowest ten levels are calculated from equation (6.9) in the form

$$G_{0^-}(v_i) = \left[\frac{G(v_i)}{\nu_0}\right] \nu_0 - G(0^-) \qquad (6.11)$$

The results for CPH8 together with the results of similar calculations for CPD4 and CPD8 are presented in Table 6.9. The observed levels are given for comparison. The energy levels are given with respect to 0^- because bands caused by transitions to the minus levels were assigned first, and these bands are the strongest in the high resolution spectrum. The splitting of the lowest inversion doublet 0^+-0^- is calculated to be 0.13 cm^{-1} for CPH8, and 0.033 cm^{-1} for both CPD4 and CPD8.

Calculations similar to the above were carried out for $\rho = 0.9$, 1.2 and 1.5. For these ρ values, the average deviations of the observed from the calculated levels were 6 cm^{-1}, 12 cm^{-1} and 20 cm^{-1}, respectively, for CPH8, whereas for $\rho = 0.6$, the deviation was 4 cm^{-1}. Similar calculations were carried out for CPD4 and CPD8 for the four ρ values.

TABLE 6.9

OBSERVED AND CALCULATED VALUES OF THE INVERSION LEVELS $G_0(v_i)$ IN CM^{-1}

v_i	CPH8 Obs.	CPH8 Calc.	CPD4 Obs.	CPD4 Calc.	CPD8 Obs.	CPD8 Calc.
0^+		0.13		0.033		0.033
0^-	0.00[a]	0.00	0.00[a]	0.00	0.00[a]	0.00
1^+	306.9[a]	306.9	279.2[a]	279.2	279.7[a]	279.7
1^-	313.8[a]	313.8	281.7[a]	281.7	282.2[a]	282.2
2^+	532[b]	533.8	511[b]	500.1	504[b]	501.0
2^-	609.1	605.8	522.0	539.5	544.9	540.4
3^+	787[b]	765.9	708[b]	684.4	690[b]	685.7
3^-	925.9	919.5	832.9	803.5	816.8	804.9
4^+	1091.7[b]	1094.1	947.2[b]	949.8	955[b]	951.4
4^-	1276.9	1279.2	1130.8	1104.0	1111.0	1106.1

---

[a] data on which calculations are based.

[b] data from bands assigned after the calculations.

As for CPH8, $\rho = 0.6$ gave the best agreement between observed and calculated levels; the average deviations were 23 cm^{-1} (CPD4) and 5 cm^{-1} (CPD8) for $\rho = 0.6$. There is no obvious reason why the deviation for CPD4 is relatively large, although, of course, there is always the possibility of Fermi resonances occurring in the excited state. The parameters ρ, B, and ν_0 are listed in Table 6.10. The same ρ value, 0.6, was used for the three species. The barrier height, b, was calculated from equation (6.7). Excellent agreement was obtained for the three isotopic species: the values are b = 705.6 (CPH8), 702.2 (CPD4), and 703.6 (CPD8). The double potential minimum functions and the vibrational energy levels in the $'A_2$ electronic state are drawn in Figures 6.10, 6.11 and 6.12 for CPH8, CPD4 and CPD8, respectively.

The positions $\pm Q_m$ were calculated from equation (6.8). For CPH8

$$Q_m^{\ 2} = 2.155 \times 10^{-40}\ g.\ cm^2$$

$$Q_m = \pm\ 1.468 \times 10^{-20}\ g^{\frac{1}{2}}\ cm.$$

Q_m may be related to a geometrical coordinate since Q is defined by $2T = \dot{Q}^2$. The desired coordinate is the oxygen out-of-plane bending angle, Θ_i; Θ_m is the angle when the potential is a minimum.

In a good approximation, the complete potential surfaces should be the same for molecules differing only by isotopic substitution, since the surfaces are determined by the electronic structure of the molecule. It is therefore assumed that b and Q_m are the same for CPH8, CPD4 and CPD8. It follows that

$$B\nu_0 = B^i \nu_0^{\ i} \qquad (6.12)$$

TABLE 6.10

THE DOUBLE MINIMUM POTENTIALS*

	CPH8	CPD4	CPD8
ρ	0.6	0.6	0.6
B	2.242	2.508	2.5085
ν_0	314.70 cm^{-1}	279.98 cm^{-1}	280.47 cm^{-1}
b	705.6 cm^{-1}	702.2 cm^{-1}	703.6 cm^{-1}
Q_m	1.468	(1.468)	(1.468)
Θ_m	35^o	(35^o)	(35^o)
$G(0^+)$	166.35	148.65	148.92

---

* $G(0^+)$, zero point energy; b, barrier height, Θ_m, oxygen out-of-plane angle when the potential is a minimum; units of Q_m are 10^{-20} $g^{\frac{1}{2}}cm$.

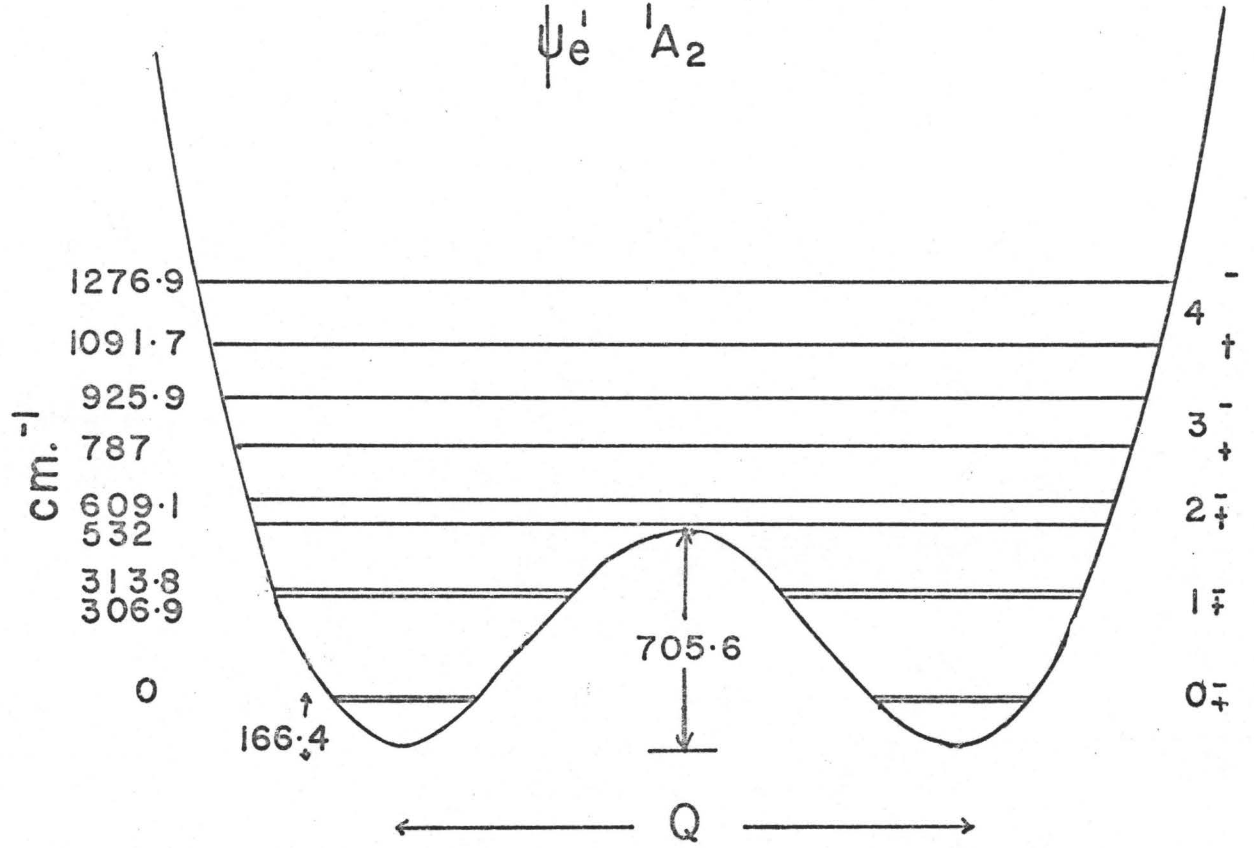

FIGURE 6·10 The Vibrational Levels of ν'_{25} for CPH8.

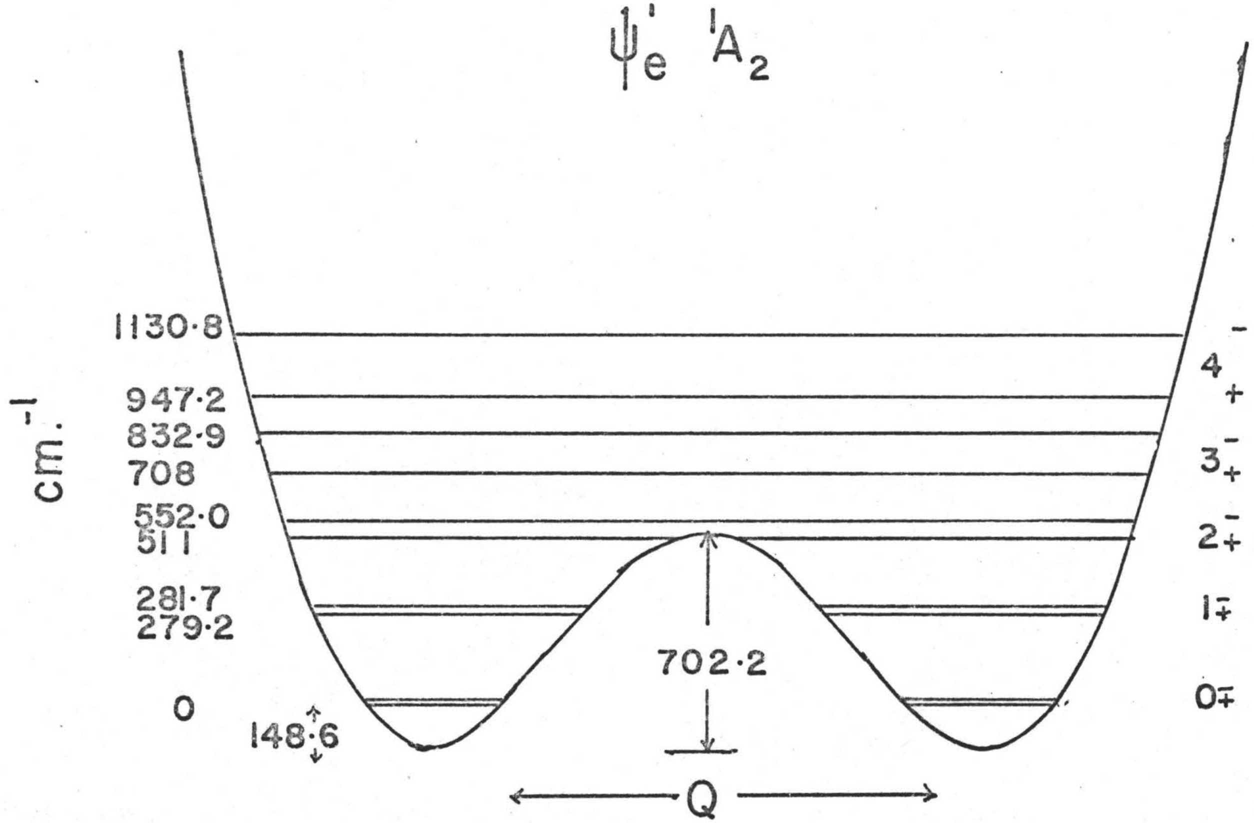

FIGURE 6·11 The Vibrational Energy Levels of CPD4

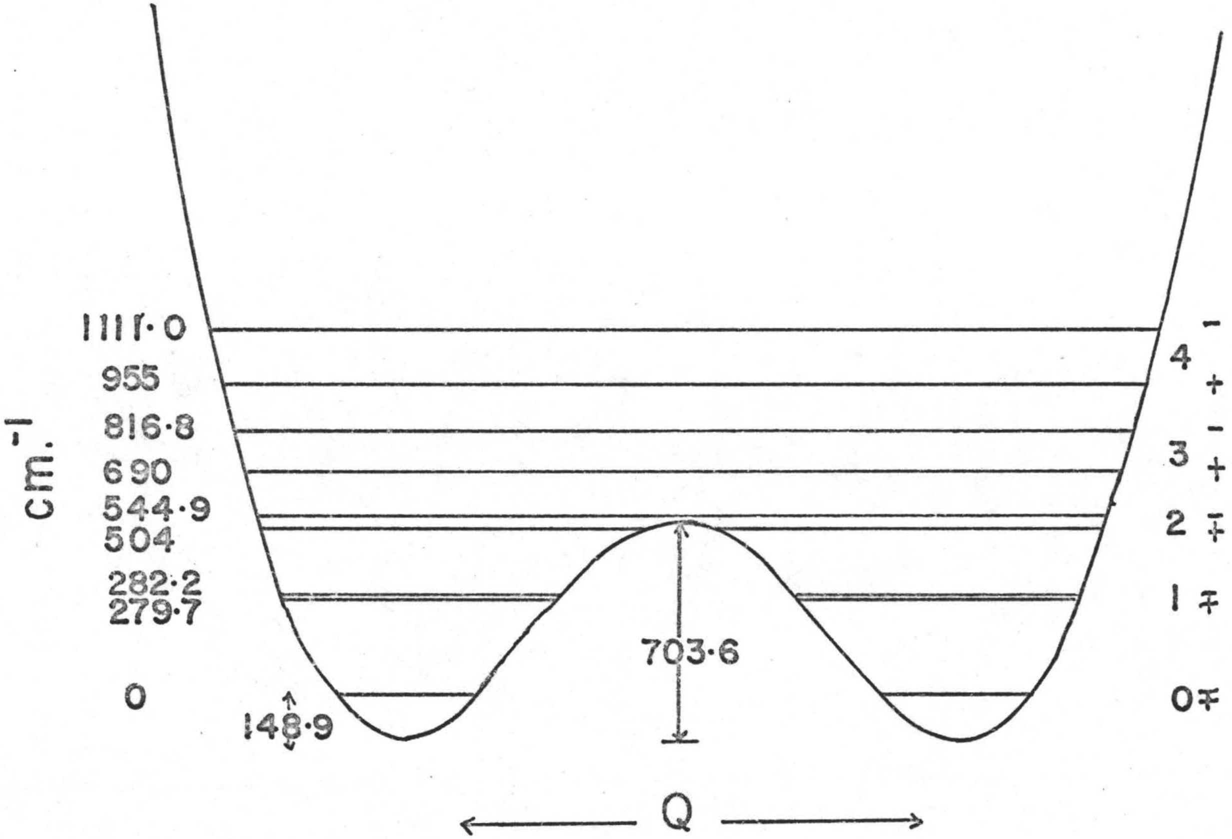

FIGURE 6·12 The Vibrational Energy Levels of CPD8.

$$\rho = \rho^{i} \tag{6.13}$$

$$Q_m = Q_m{}^{i} \tag{6.14}$$

where the superscript "i" designates the value for CPH8. The ratios $\frac{\nu^{i}}{\nu_0}$ and $\frac{B}{B^{i}}$ for CPD4 are 1.124; and 1.119, respectively. For CPD8 the same ratios are 1.122 and 1.119. The assumption that the potential functions are the same for the three isotopic species is justified.

Q_m and Θ_m are expected to be the same for the three species, and the calculation of these two quantities was carried out for CPH8 only.

An expression for the kinetic energy of the bending motion is required. A G matrix element for the bending motion was calculated, following the method of Wilson, Decius and Cross[56,p62]. The kinetic energy, T, in terms of velocities, is given by

$$2T = \sum_{tt'} (G^{-1})_{tt'} \dot{S}_t \dot{S}_{t'} \tag{6.15}$$

where S_t, $S_{t'}$ are internal coordinates. A vector $\overline{s}_{t\alpha}$ may be associated with each atom, α, and each internal coordinate, S_t. The direction of $\overline{s}_{t\alpha}$ is the direction in which a given displacement of atom α will produce the greatest increase in S_t. In terms of these $\overline{s}_{t\alpha}$ vectors, a set of quantities $G_{tt'}$ is given by

$$G_{tt'} = \sum_{\alpha=1}^{N} \mu_\alpha \, \overline{s}_{t\alpha} \cdot \overline{s}_{t'\alpha} \tag{6.16}$$

where μ_α is $1/m_\alpha$, the reciprocal of the mass of atom α. There will be one element, $G_{tt'}$, for each pair of internal coordinates, $S_t, S_{t'}$. The coefficients $(G^{-1})_{tt'}$ in equation (6.15) are related to the quantities

$G_{tt'}$ by the equations

$$\left.\begin{aligned} \sum_{t'} (G^{-1})_{tt'} G_{tt'} &= \delta_{tt'} \\ \sum_{t'} G_{tt'} (G^{-1})_{tt'} &= \delta_{tt'} \end{aligned}\right\} \qquad (6.17)$$

where $\delta_{tt'} = 1$ if $t=t'$ and is zero otherwise. In matrix language, G^{-1} is the inverse of the matrix G. The individual matrix element $(G^{-1})_{tt'}$ is not usually the reciprocal of the individual element $G_{tt'}$ -- these elements are reciprocals of each other only if the matrices are diagonal. However, $G_{tt'}=G_{t't}$. If the coordinate S_t happens to be orthogonal to $S_{t'}$ then $G_{tt'}=0$ (off-diagonal elements are zero); that is, if the internal coordinate, S_t, is assumed to be a normal coordinate, then the element $(G^{-1})_{tt}$ is equal to the reciprocal of the element G_{tt}.

Let S_t be the internal coordinate for the change in the oxygen out-of-plane angle, $\Delta\Theta$. The oxygen out-of-plane motion is represented by the upward motion of the carbonyl carbon atom and the simultaneous downward motions of the C=O bond and the two C-C bonds. $\Delta\Theta$ is the angle formed by the plane $C_1C_2C_5$ and the C=O bond.

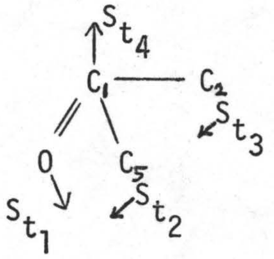

For this bending motion, Wilson, Decius and Cross have expressed the $\overline{s}_{t\alpha}$ vectors in terms of unit vectors $\overline{e}$ along the interatomic connecting lines. The derivation of the expression for $\sum_{tt'} G_{tt}$ is given in Appendix 1.

Equation (6.15) was used in the form

$$2T = \sum_{tt} G_{tt} (\Delta\Theta)^2 \tag{6.18}$$

Coupling between different frequencies, for example the oxygen out-of-plane bending and the ring puckering frequencies, was assumed to be zero for this calculation. Frei and Günthard [52] in a normal coordinate analysis of cyclobutanone, found that the oxygen out-of-plane bending frequency, ν_{26}, was only very weakly coupled to the out-of-plane ring vibration, ν_{27}. Since $2T = \dot{Q}^2$ and $Q_m{}^2 = 2.155 \times 10^{-40}$ g. cm^2, equation (6.18) gives

$$\dot{Q}^2 = \sum_{tt} G_{tt} (\Delta\Theta)^2 \tag{6.19}$$

$$\therefore \sum_{tt} G_{tt} \Theta_m^2 \approx Q_m{}^2 \tag{6.20}$$

Θ_m, the oxygen out-of-plane angle when the potential with respect to the bending coordinate is at a minimum, was obtained from the expression

$$\Theta_m = Q_m / [\sum_{tt} G_{tt}]^{\frac{1}{2}} \tag{6.21}$$

The factor $\sum_{tt} G_{tt}$ contains functions of Θ. By an iterative procedure, the final value of the out-of-plane angle obtained was $\Theta_m = 35^{\circ}$.

6.7 The Geometry of Cyclopentanone

6.7.1 Ground State

The moments of inertia and rotational constants are known from the microwave study.[11] The ring was reported to be puckered, but the calculated geometry (obtained by Erlandsson[11]) was based on an assumed planarity.

In the present work, the observed values of the rotational constants, A=0.22063, B=0.11169, and C=0.08033 cm^{-1} were used to determine an improved geometry. The large puckering angle, Θ_{11}, is needed to achieve the observed inertial defect, Δ, of -17 amu-Å^2. Although Erlandsson[11] reported that the hydrogen atoms would be expected to contribute $\sim$ 12 amu-Å^2 to Δ, the present calculation showed they contribute only 7.8 amu-Å^2. An IBM 7040 computer was programmed to calculate the moments of inertia and rotational constants from assumed geometries with puckering included. Parameters were varied until the calculated values of the moments of inertia showed least deivation from the known values. Figure 6.13 illustrates the numbering of the parameters used in the program. A few simplifying assumptions had to be made:

(i) there is a C_2 axis, that is, the skew configuration (Figure 2.3) is correct. It follows that only the coordinates of C(1), C(2), C(3), H(6), H(7), H(8), H(9) and O(14) need be calculated.

(ii) C(1), C(2) and C(5) and O(14) are coplanar. C(3) is displaced above the plane and C(4) below. The C(3)-C(4) bond makes a dihedral angle Θ_{11} with the plane of the rest of the ring; Θ_{11} can be zero.

(iii) All C-H bond lengths are equal and each $\mathrm{H}\underset{\mathrm{C}}{\diagdown\diagup}\mathrm{H}$ plane bisects the adjacent $\mathrm{C}\overset{\mathrm{C}}{\diagup\diagdown}\mathrm{C}$ angle. Likewise, the $\mathrm{C}\overset{\mathrm{C}}{\diagup\diagdown}\mathrm{C}$ plane bisects the adjacent $\mathrm{H}\underset{\mathrm{C}}{\diagdown\diagup}\mathrm{H}$ angle. The $\mathrm{H}\underset{\mathrm{C}}{\diagdown\diagup}\mathrm{H}$ angles are 109.5°.

The ring angles at C(1), C(2) and C(3), the dihedral angle Θ_{11}, and the bond lengths R(1), R(2) and R(3) were related by trigonometric expressions. These equations are given in Appendix II. Only two of these four angles, (Θ_2, Θ_3, Θ_4 and Θ_{11}) can be varied independently; Θ_7, Θ_9 and Θ_{12} depend on the above angles.

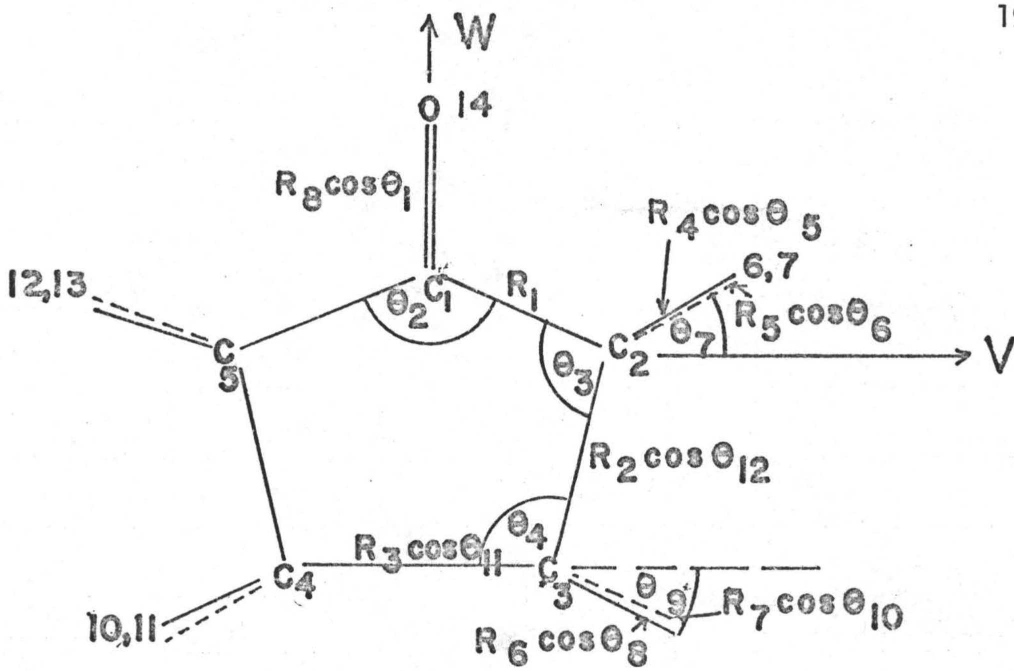

All Parameters Shown Refer To Distances And Angles Projected Onto The Plane VW Defined By Atoms C_5, C_1, C_2.

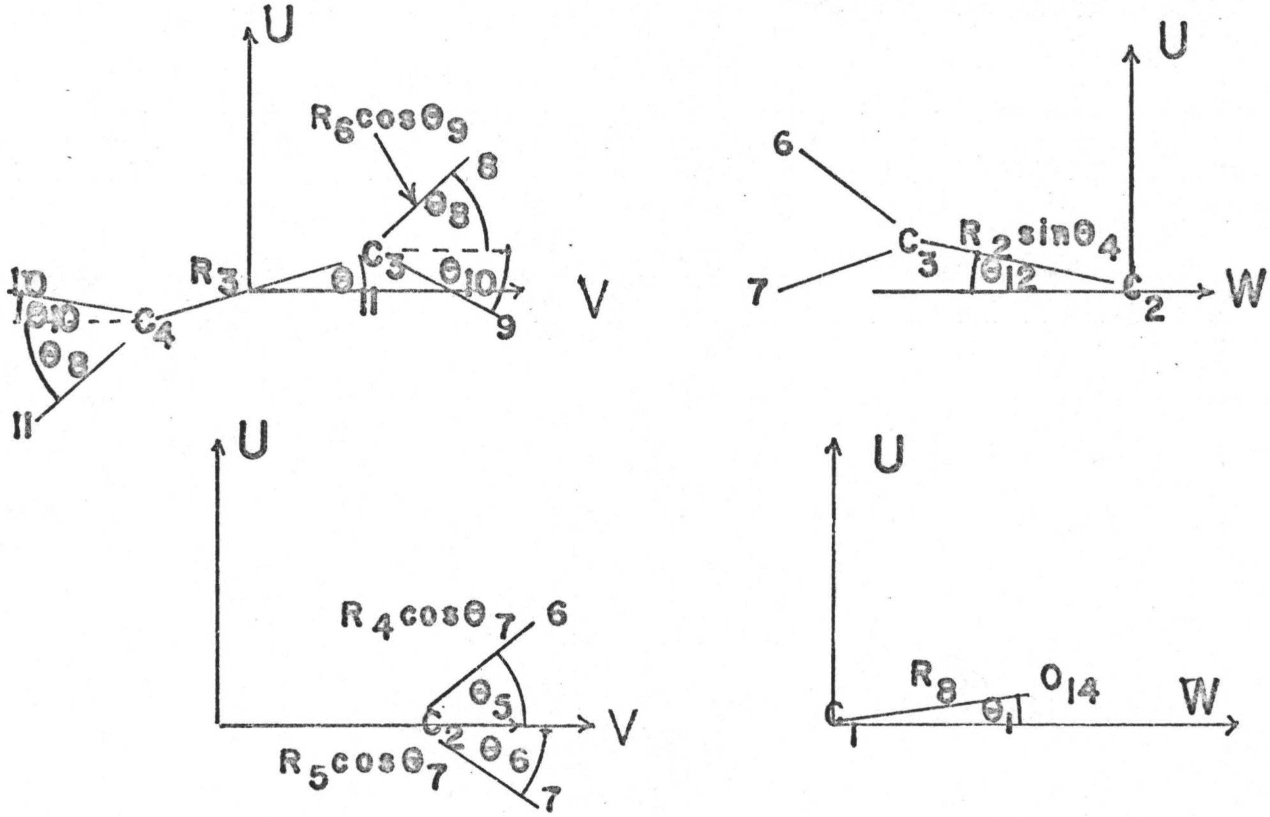

FIGURE 6·13 Parameters for Moment of Inertia Calculations.

The variables are R_1, R_2, R_3, R_4, R_8, Θ_2 and Θ_{11}. For the first calculation, the following values for the parameters were chosen:

C-C Bond Lengths

R(1), R(2), R(3) were chosen equal to 1.539Å. This is the value obtained by Almenningen et al.[121] for the C-C distances in cyclopentane by electron diffraction. In Interatomic Distances[122], the average C-C single bond length quoted is 1.537 ± 0.005 Å. In bicycloheptane the five-membered ring has a C-C bond length of 1.56 ± 0.01Å.[123]

C-H Bond Lengths

R_4, R_5, R_6 and R_7 were chosen equal to 1.095Å (as found in cyclopentane[121]). Costain and Stoicheff[124] reported values for -C-H of 1.092Å (methane) and 1.102Å (ethane).

C=O Bond Length

An average value for alkelydes and ketones, 1.215 ± 0.005,[122] was chosen.

Any two parameters could be simultaneously varied and the moments of inertia I_A, I_B, I_C (and rotational constants A, B, and C) calculated. The parameters which gave the least deviation of I_A, I_B and I_C from the known values were kept constant in the succeeding calculations, while other parameters were varied. When good agreement was obtained, the original two parameters were varied again to ensure that minimum deviation was still obtained. The best agreement (or "least minimum deviation") was observed for the geometrical configuration shown in Figure 1.2. The parameters differ only slightly from the ones chosen initially:

C-C Bond Lengths

R_1 at 1.56Å is longer than R_2 and R_3. However, a C-C bond of 1.55Å is reported for acetone[122] and 1.54Å for cyclohexanone.[125] 1.56Å is reported for tetramethylcyclobutane-1,3-dione.[126]

C-H Bond Length

All C-H bonds are assumed equal and the value is 1.106Å. This value is comparable to that for ethane (1.102Å),[124] bicyclo [3.2.0] heptane (1.10)[123] and cyclo-octane (1.100).[127]

C=O Bond

The C=O bond (1.24Å) is longer than the average, but the average value is obtained mostly from aldehydes.[122] Acetone has 1.24Å for C=O[122] as does cyclohexanone.[125]

Ring Angles

The angle Θ_2 at the carbonyl group is 109°, slightly larger than the value for a planar pentagonal ring (108°). The smallness of this angle compared to the corresponding angles in acetone and cyclohexanone (117°) is attributed to ring strain. Comparison with the puckering angles of other ring compounds (see Table 2.3), shows that the value 33° for cyclopentanone is reasonable.

In summary, the geometry calculated here is a reasonable one which gives good agreement with the known rotational constants. It would be interesting to compare the calculated geometry with one determined from a microwave study of several isotopic species, or from an electron diffraction study.

6.7.2 The Excited State

As for the ground state, enough parameters are not available for a determination of the complete geometry of the excited state. If suitable assumptions are made, it is possible to calculate at least some of the parameters with a fair degree of accuracy.

It is assumed (i) that C-C and C-H bond lengths and the ring puckering angle are the same as in the ground state; and (ii), that only the C=O bond length and oxygen out-of-plane angle differ from the ground state values. According to the Franck-Condon principle, this second assumption is justified, since the only progressions observed in the ultraviolet spectrum are in the vibrations ν_3 and ν_{25}.

Preliminary estimates of the C=O bond length $r'_{C=O}$ and the oxygen out-of-plane angle, Θ', in the upper state were made by means of the empirical relationships discussed in Chapter 3. The values are collected in Table 6.11.

6.7.3 Rotational Constants from Band Contours

Cyclopentanone (in the ground state) is an asymmetric top; $\kappa = -0.5529$.[11] This κ value is closer to that of the prolate top than to that of the oblate top. The rotational levels are therefore approximately given by equation 3.14.

The rotational constant A is large compared to B and C and sub-bands arising from transitions to different K levels should be separated, each sub-band having fine structure caused by accompanying changes in J. Because of the relative smallness of the rotational constants, even the coarse K structure (caused by changes in the quantum number K) (see

TABLE 6.11

CHANGE IN GEOMETRY BETWEEN GROUND AND UPPER STATE

	$r''_{C=O}$ Å	$r'_{C=O}$	Θ °	Θ'
Badger's Rule( )	1.24*	1.32	-	-
Douglas-Clark's Rule( )	1.24	1.40	-	-
Layton et al.( )	1.24	1.36-1.38	-	-
$\Delta E=\frac{1}{2}k(\Delta Q)^2$	$\Delta r=0.1-0.14$ Å		$\Delta\Theta=\sim30^{\circ}$	

* value assumed at ground state

TABLE 6.12

RESULTS OF BAND CONTOUR CALCULATIONS (TYPE-B)

Ba	A'	B' cm^{-1}	C'	$r'_{C=O}$ Å	Θ' in °	
25^{1-}_{0}-238	0.2133	0.1122	0.0812	1.34-1.36	33-35	(76)
25^{1+}_{1}	"	"	"	1.34-1.36	33-35	(77)
25^{0-}_{0}	0.2145	0.1114	0.0806	1.34-1.36	30-32	(78)

Section 3.8) is not sufficiently resolved in the spectrum of CPH8 to be measured. Asymmetric rotor band contour programs have been supplied to this research group by Dr. Parkin.[128] The programs were rewritten so that errors were removed and intensity integration procedures were improved; translation of the programs into Fortran IV for use on the IBM 7040 (32K) computer was made by Balfour.[129] The band contours for selected bands in the spectrum of CPH8 have been calculated for various values of A', B', C' and the known values of A", B", C". Good agreement between observed and calculated band contours was obtained for a B-type band (perpendicular) (transition moment directed along the b axis). The microdensitometer trace of the rotational fine structure of the 25_1^{1+} band and the computed contour drawn to the same scale as the trace are shown in Plate 6.2. Good agreement between the theoretical and observed profiles was obtained for the bands 25_0^{0-} and 25_1^{1+} if the oxygen out-of-plane angle was ∿ 2^o less for the 25_0^{0-} band . The upper state rotational constants and corresponding geometry changes are listed in Table 6.12. The changes in geometry were estimated, the rotational constants A', B' and C' calculated by the same type of program described for the ground state, and the band contours for these calculated constants were computed. The geometry was varied and the procedure repeated. When agreement between observed and computed contours was obtained for a given set of A', B' and C', the geometry which gave that set was assumed to be closest to the actual geometry. Within limits the band contour program is insensitive to changes in the rotational constants so that the geometry of the molecule in its two combining electronic states cannot be determined precisely. Bands computed for two sets of

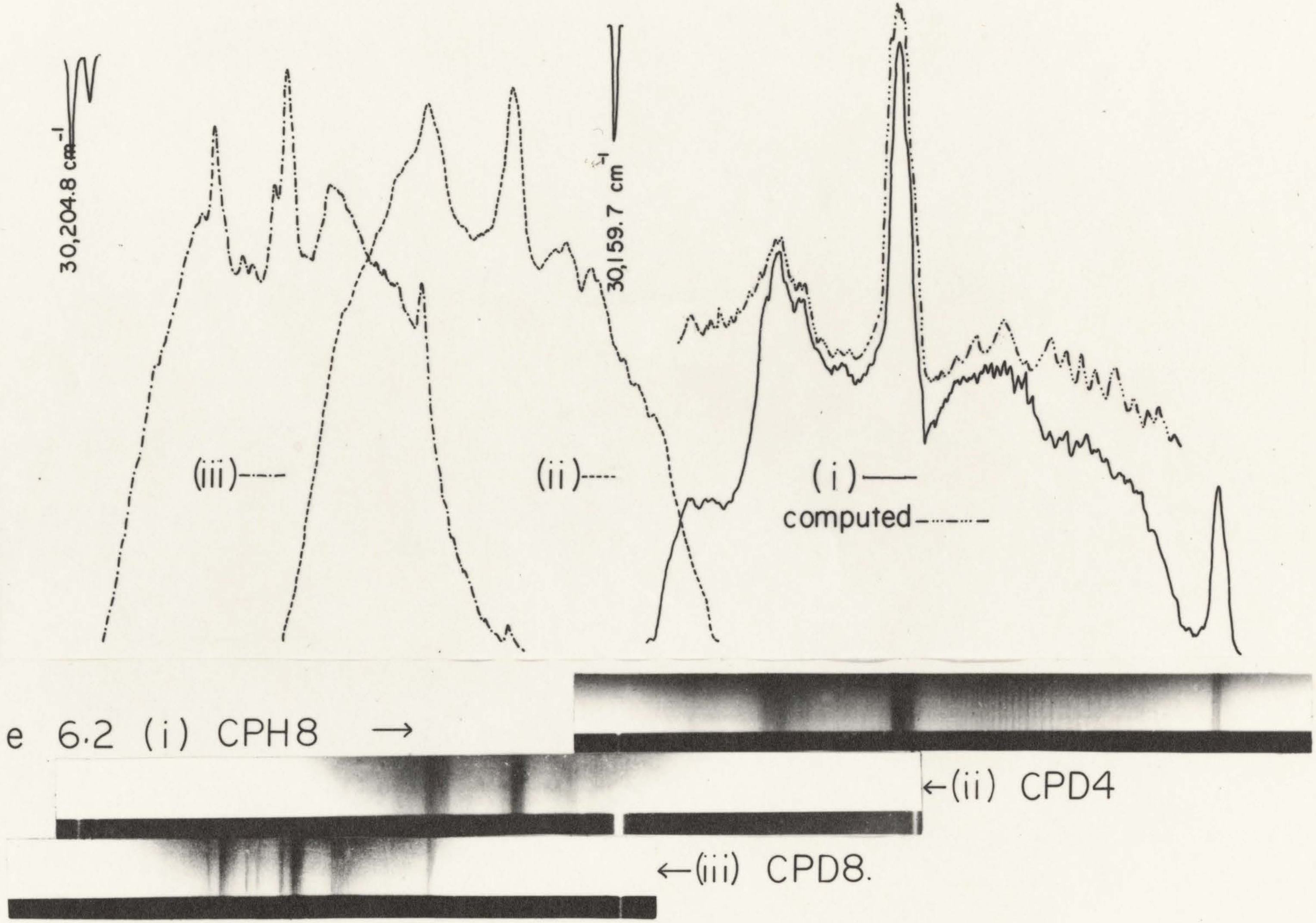

Plate 6.2

The 25_1^{1+} Band of the $^1A_2 \leftarrow {}^1A_1$ Transition in Cyclopentanone. (resolving power ≈ 300,000).

excited state rotational constants differing by

$$\Delta A' = 0.0001 \quad , \Delta B' = 0.0001 \text{ and } \Delta C' = 0.0002$$

gave essentially the same profiles. Type -A and Type -C bands were also computed; none of the "main bands" (in the ν_{25} progression) in the ultraviolet spectrum were found to be type -A or type -C; all were type B as expected. The only obvious type A band is the fairly strong band assigned $18^1_0 25^{1-}_0$. If the transition is from a vibronic level A_1 to a vibronic level A_1 (see Figure 6.3) a type A band would be expected.

Similar calculations were carried out for CPD4 and CPD8. No observed values of the ground state rotational constants were available for comparison with the calculated ones. Also, the rotational fine structure of the bands in the electronic spectrum is more poorly resolved for the deuterated molecules. Despite these handicaps, the 25^{1+}_1 B-type bands computed for the same ground state and assumed excited state geometries as for CPH8 showed good agreement with the observed band profiles.

CHAPTER 7

CONCLUSIONS

The infrared spectrum of cyclopentanone has been studied over the region 10,000 cm^{-1} to 30 cm^{-1} in the vapour and liquid phases, and the infrared spectra of cyclopentanone-α,α',α'-d_4 and cyclopentanone-d_8 over the region 4000 cm^{-1} - 30 cm^{-1} in the vapour and liquid phases. The Raman spectra of the three isotopic species in the liquid phase have been studied. Reasonable assignments are suggested for all the fundamentals except the low lying ring puckering mode ν_{26} (b_1), which could not be observed. Dissociation energies of 94 kcal $mole^{-1}$ and 152 kcal $mole^{-1}$ have been calculated for the C-H and C=O bonds, respectively, in cyclopentanone.

The high resolution ultraviolet spectrum of the three isotopic species in the vapour phase has been studied. The banded ultraviolet spectrum (2500-3500Å) is caused by the $'A_2 \leftarrow 'A_1$ electronic transition. The theory of non-rigid molecules has been applied to cyclopentanone and it has been shown that the molecule may be classified under a point group isomorphous with C_{2v} in both electronic states. The geometry of the molecule has been computed for both states. In the ground state, the molecule is in the skew conformation; the dihedral angle is 33^0. There must be a potential barrier to the ring puckering vibration which corresponds to inversion of the molecule between the two isodynamic configurations, but the height of the barrier could not be obtained from either the vibrational or the electronic spectrum.

The transition $'A_2 \leftarrow 'A_1$ is vibronically allowed with transition moment directed along the b axis of the molecule. This polarization of the electronic transition is confirmed by the following:

(i) Progressions in ν_{25}, the oxygen out-of-plane bending vibration of b_1 symmetry comprise the most intense bands in the high resolution electronic spectrum;

(ii) The rotational band profile analysis gives good agreement between the computed and observed band contours of these main bands only for B-type (perpendicular) bands;

As expected from the Franck-Condon principle, the oxygen atom is bent out of the plane of the three adjacent carbon atoms in the excited state conformation; the out-of-plane angle has been calculated to be $\sim 35^{\circ}$. The rotational band contours of the strong B-type bands are consistent with a C=O bond length of 1.35Å and an oxygen out-of-plane angle of $\sim 33^{\circ}$ in the excited state.

There is a barrier to inversion at the carbon atom of the carbonyl group of 705 cm^{-1} in the $^1A_2$ state. This barrier is essentially constant for three isotopic species. Its value lies between the value of 350 cm^{-1} found by Coon et al[119]. for formaldehyde and the value $\sim$ 1600 cm^{-1} found by Moule[53] for cyclobutanone.

Effects arising from interconversion of isodynamic configurations through a large amplitude ring puckering motion were not observed in the main bands of the spectrum.

The vibrational analysis of the $'A_2 \leftarrow 'A_1$ transition in cyclopentanone forms a striking analogy with Brand's[75] analysis of the corresponding electronic transition for the formaldehyde molecule.

The potential function discussed for the coordinate associated with ν_{25} may be regarded as a section from a 3N-6+1 dimensional surface with all other coordinates held fixed. If sections could be taken at different values of the coordinate associated with ν_3 (the carbonyl bond stretching vibration), the barrier height might well change. If "vertical" transitions from the ground state occur in accordance with the Franck-Condon principle, then transitions from the lower state levels in which, say, ν_3'' and ν_{25}'' are simultaneously excited may "hit" the upper potential surface at different points where the barrier with respect to ν_{25} has different heights.

The three parameter double minimum potential function is not a unique function, but it does give very good agreement with the experimental data.

APPENDIX I

$G_{tt'}$ -- G-MATRIX ELEMENT FOR OXYGEN OUT-OF-PLANE BENDING MOTION

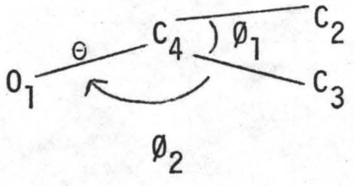

vector $s_{t\alpha}$ as given in W.D.C., p. 60, equation (19)

$G_{tt'}$ p. 61, equation (3).

$$S_{t1}\cdot S_{t1} = \frac{1}{r_{41}^2}\left(\frac{\bar{e}_{42}\times\bar{e}_{43}}{\cos\Theta\sin\emptyset_1} - \tan\bar{e}_{41}\right)\cdot\left(\frac{\bar{e}_{42}\times\bar{e}_{43}}{\cos\Theta\sin\emptyset_1} - \tan\Theta\,\bar{e}_{41}\right)$$

$$= \frac{1}{r_{41}^2}\left(\frac{1}{\cos^2\Theta} - \tan^2\Theta\right) = \frac{1}{r_{41}^2}$$

$$S_{t2}\cdot S_{t2} = \frac{1}{r_{42}^2}\left[\frac{\bar{e}_{43}\times\bar{e}_{41}}{\cos\Theta\sin\emptyset_1} - \frac{\tan\Theta}{\sin^2\emptyset_1}(\bar{e}_{42}-\cos\emptyset_1\,\bar{e}_{43})\right]\cdot$$

$$\left[\frac{\bar{e}_{43}\times\bar{e}_{41}}{\cos\Theta\sin\emptyset_1} - \frac{\tan\Theta}{\sin^2\emptyset_1}(\bar{e}_{42}-\cos\emptyset_1\,\bar{e}_{43})\right]$$

$$= \frac{1}{r_{42}^2}\left[\frac{\sin^2\emptyset_2}{\cos^2\Theta\sin^2\emptyset_1} - \frac{2\tan\Theta\sin\Theta}{\cos\Theta\sin^2\emptyset_1} + \frac{\tan^2\Theta}{\sin^4\emptyset_1}(1-\cos^2\emptyset_1)\right]$$

$$= \frac{1}{r_{42}^2}\left[\frac{\sin^2\emptyset_2}{\cos^2\Theta\sin^2\emptyset_1} - \frac{\sin^2\Theta}{\cos^2\Theta\sin^2\emptyset_1}\right]$$

$$= \frac{1}{r_{42}^{2}}\left[\frac{\sin^2\emptyset_2-\sin^2\Theta}{\cos^2\Theta\sin^2\emptyset_1}\right]$$

Substituting $\sin^2\emptyset_2 = 1-\cos^2\frac{\emptyset_1}{2}\cos^2\Theta$,

$$\rightarrow \frac{1}{r_{42}^{2}}\left[\frac{1-\cos^2\frac{\emptyset_1}{2}\cos^2\Theta-1+\cos^2\Theta}{\cos^2\Theta\sin^2\emptyset_1}\right]$$

$$= \frac{1}{r_{42}^{2}}\left[\frac{\sin^2\frac{\emptyset_1}{2}}{\sin^2\emptyset_1}\right] =$$

$$\frac{1}{r_{42}^{2}}\left[\frac{1}{4\cos^2\frac{\emptyset_1}{2}}\right]$$

$S_{t3}\cdot S_{t3} = S_{t2}\cdot S_{t2}$ by symmetry

$$S_{t4}\cdot S_{t4} = (-S_{t1}-S_{t2}-S_{t3})\cdot(-S_{t1}-S_{t2}-S_{t3})$$

$$= S_{t1}\cdot S_{t1}+S_{t2}\cdot S_{t2}+S_{t3}\cdot S_{t3}+2S_{t1}\cdot S_{t2}+2S_{t1}\cdot S_{t3}+2S_{t2}\cdot S_{t3}$$

$$= S_{t1}\cdot S_{t1}+4S_{t2}\cdot S_{t2}+4S_{t1}\cdot S_{t2}$$

$$= \frac{1}{r_{41}^{2}} + \frac{1}{r_{42}^{2}\cos^2\frac{\emptyset_1}{2}} + 4S_{t1}\cdot S_{t2}$$

$$S_{t1}\cdot S_{t2} = \frac{1}{r_{41}r_{42}}\left(\frac{\bar{e}_{42}\times\bar{e}_{43}}{\cos\Theta\sin\emptyset_1} - \tan\Theta\bar{e}_{41}\right)\cdot\left(\frac{\bar{e}_{43}\times\bar{e}_{41}}{\cos\Theta\sin\emptyset_1} - \frac{\tan\Theta}{\sin^2\emptyset_1}\left[\bar{e}_{42}-\cos\emptyset_1\bar{e}_{43}\right]\right)$$

$$= \frac{1}{r_{41}r_{42}}\left(\frac{\sin\emptyset_1\sin\emptyset_2\cos\Theta}{\cos^2\Theta\sin^2\emptyset_1} + \frac{\tan^2\Theta}{\sin^2\emptyset_1}\left[\cos\emptyset_2-\cos\emptyset_1\cos\emptyset_2\right]\right)$$

$$= \frac{1}{r_{41}r_{42}} \left(\frac{\sin\phi_1\cos\theta\sqrt{1-\cos^2\frac{\phi_1}{2}\cos^2\theta} + \sin^2\theta\cos\frac{\phi_1}{2}\cos\theta[\cos\phi_1-1]}{\cos^2\sin^2\phi} \right. \quad -$$

$$= \frac{1}{r_{41}r_{42}} \left(\frac{\sin\frac{\phi_1}{2}\cos\frac{\phi_1}{2}\sqrt{1-\cos^2\frac{\phi_1}{2}\cos^2\theta} - \sin^2\theta\cos\frac{\phi_1}{2}(\sin^2\frac{\phi_1}{2})}{\cos\theta 2\sin^2\frac{\phi_1}{2}\cos^2\frac{\phi_1}{2}} \right.$$

$$= \frac{1}{r_{41}r_{42}} \left(\frac{\sqrt{1-\cos^2\frac{\phi_1}{2}\cos^2\theta}-\sin^2\theta\sin\frac{\phi_1}{2}}{\cos\theta\sin\phi_1} \right.$$

Expressions used are:

$$\bar{e}_{42} \times \bar{e}_{43} = e_t\sin\phi_1$$

$$\bar{e}_{42} \times \frac{\bar{e}_{43}}{\sin\phi_1} \cdot \bar{e}_{41} = \sin\theta$$

$$\bar{e}_{43} \times \bar{e}_{41} \cdot \bar{e}_{43} = 0$$

$$\cos\phi_2 = -\cos\frac{\phi_1}{2}\cos\theta$$

$$\cos^2\phi_2 = \cos^2\phi_1\cos^2\theta$$

$$\sin^2\phi_2 = 1-\cos^2\frac{\phi_1}{2}\cos^2\theta$$

$$\sin\chi = 2\sin\frac{\chi}{2}\cos\frac{\chi}{2}$$

$$\bar{e}_{42} \times \bar{e}_{43} = \bar{e}_t\sin\phi_1$$

$$\bar{e}_{43} \times \bar{e}_{41} = \bar{e}_\chi\sin\phi_2$$

$$\bar{e}_t \cdot \bar{e}_\chi = \cos\theta$$

$$\bar{e}_{42} \times \bar{e}_{43} \cdot \bar{e}_{43} \times \bar{e}_{41} = \sin\phi_1\sin\phi_2\bar{e}_t \cdot \bar{e}_\chi = \sin\phi_1\sin\phi_2\cos\theta$$

APPENDIX II

RELATIONSHIPS BETWEEN GEOMETRICAL PARAMETERS IN CYCLOPENTANONE

$\frac{1}{2} R_3 \sin\Theta_{11} = R_2 \sin\Theta_{12}$

$\frac{\Theta_2}{2} + \Theta_3 + \Theta_4 = 270$ (angles projected in yz plane)

The bond angles are designated by ρ_1 ($=\Theta_2$), ρ_2 (at C_2) and ρ_3 (at C_3)

$$\Theta_3 = \text{arc cos} \left\{ \frac{\cos \rho_2}{\cos[\text{arc sin}(\frac{R_3}{2R_2} \sin\Theta_{11})]} \right\}$$

$$\Theta_4 = \text{arc cos} \left\{ \frac{R_2 \cos\rho_3 - \frac{R_3}{2} \sin^2\Theta_{11}}{R_2 \cos[\text{arc sin}(\frac{R_3}{2R_2} \sin\Theta_{11})]} \quad \cos\Theta_{11} \right\}$$

$$\cos\Theta_{11} = \frac{\frac{R_3}{2} - R_2 \cos\Theta_{13}}{R_1 \sin\frac{\Theta_2}{2}}$$

APPENDIX III

BAND HEAD FREQUENCIES AND INTENSITIES FROM THE HIGH RESOLUTION SPECTRA

	ν cm^{-1} vacuum	Intensity	ν cm^{-1} vacuum	Intensity
CPH8	31,808.6		30,924	w
	31,555		30,891	
	31,502.9		30,887	
	31,365.0		30,877	
	31,277.5		30,836.5	w
	31,204.9		30,831.5	w
	31,160		30,825.1	
	31,111.0		30,818.5	
	31,099.6	w	30,798	
	31,094.6	w	30,755.5	vvw
	31,086.6	w	30,749.6	vvw
	31,062.3		30,733	w
	31,040		30,715	w
	31,018		30,700	
	31,014		30,683	w
	31,008.2		30,662.7	w
	31,004		30,645.3	w
	30,930 30,940	} 4 bands vw	30,619.6	

continued ......

APPENDIX III

ν cm^{-1} vacuum	Intensity	ν cm^{-1} vacuum	Intensity
30,609	vw	30,329.0	s
30,591.9	s	30,322.1	w
30,582.8		30,313.5	w
30,537	vvw	30,305.4	w
30,514.2	w	30,300	w
30,465		30,278.1	
30,453	w	30,252	w d
30,442.6	w	30,241	w
30,418	vw	30,237	w
30,403	vw	30,228	vw d
30,396.7	w	30,221.0	mw
30,394.5	w	30,214.9	vw
30,388	w	30,210.0	vw
30,383	w	30,204.9	vw
30,379		30,182.6	vw
30,375		30,179.0	w
30,368	mw	30,172.8	mw
30,366	w	30,170.0	mw
30,360.6	s	30,168.4	
30,353.3	s	30,167.6	
30,337.5	s	30,163.6	

APPENDIX III
(continued)

ν cm^{-1} vacuum	Intensity	ν cm^{-1} vacuum	Intensity
30,154.4	ms	29,956.5	w
30,149.6	s	29,952.5	w
30,139.6	vs	29,947.4	w
30,115.9	s	29,935	w d
30,110.0	w	29,927	w d
30,084.0	w	29,928.2	mw
30,076	w	29,920.0	mw
30,068.5	m	29,904.6	vw
30,064.9	m	29,898.6	vw
30,044.4	m	29,894.6	vw
30,033.6	mw	29,888.9	vw
30,021.9	w	29,885.0	vw
30,019.9	w	29,876.7	vvw
30,014	w	29,834.7	m
30,011	w	29,832.7	s
30,006.9	m	29,808.7	
29,996.6	w	29,795.7	w d
29,974.5	m	29,790.1	w
29,969.9	mw	29,781.9	w
29,965.7	w	29,765.7	w
29,959.5	w	29,752.8	w d

continued ......

APPENDIX III
(continued)

ν cm^{-1} vacuum	Intensity	ν cm^{-1} vacuum	Intensity
29,743.8		29,453.2	mw
29,735.8		29,435.8	w
29,728.2		29,391.2	
29,706.6		29,387.2 }	ms
29,701.0	s	29,384	
29,675.6	ms	29,362.1	
29,665.9	mw	29,339	w
29,652.9	mw	29,323.3	w
29,641.9	mw	29,304	vw
29,625.9		29,300.9	w
29,622.9		29,258.3	w
29,607.0		29,252.6	m
29,598.4		29,231.7	w
29,582.3	w	29,225.3	w
29,580.4	w	29,221.7	w
29,571.9	m	29,247	w
29,566.3	ms	29,159.0	vvw
29,544	mw	29,153.3	w
29,439.5	w	29,136.6	vw
29,477.9	mw	29,110.8	vw
29,465.0	vw	29,057	vw

. continued ......

APPENDIX III
(continued)

ν cm^{-1} vacuum	Intensity	ν cm^{-1} vacuum	Intensity
28,978.0	w		
29,872	w		
28,951 28,950.9	m		
28,941.5	m		
28,914	w		
28,907	w		
28,905.5	w		
29,901	w		
28,878	w		
28,827.4	w		
28,779.3	w		
28,772.8	w		
28,743.7	w		
28,735.7	w		
28,713.0	w		
28,695.1	m		
28,676.3	m		
28,670.3	m		
28,601.1	mw		

continued ....

APPENDIX III (b)

	ν cm^{-1} vacuum	Intensity	ν cm^{-1} vacuum	Intensity
CPD4	31,782	m	31,017	vw
	31,775	m	30,014	w
	31,691	m	31,012	w
	31,560	m	31,009	w
	31,475	w	30,948	s
	31,398.0	m	30,835.7	w
	31,379	w	30,819.2	s
	31,365	w	30,817	ms
	31,302	w	30,796.2	m
	31,206	w	30,762.2	ms
	31,160	w	30,755.5	s
	31,119	w	30,731	w
	31,100.1	m	30,717	w
	31,095	w	30,706	w d
	31,072	w	30,702	w d
	31,069	w	30,696	mw d
	31,066	w	30,692	w
	31,057	w	30,675	mw
	31,051	w	30,655	w

continued ......

APPENDIX III
(continued)

ν cm^{-1} vacuum	Intensity	ν cm^{-1} vacuum	Intensity
30,642		30,395	w
30,599	ms	30,384	m
30,577.9	w	30,377.6	m
30,568.9	w	30,352	w
30,557.5	s	30,297	vw
30,548.9	s	30,267.2	mw
30,520.4	vw	30,205	w
30,487	w	30,166.9	m
30,481	w	30,129.6	w
30,465.6	vw	30,111.6	w
30,454		30,108.8	m
30,440	mw	30,103.0	w
30,438	mw	30,094.0	w
30,431	w	30,089.0	w
30,428	mw	30,085.0	w
30,426		30,064.0	m
30,419	w	30,060.0	m
30,415	mw	30,051.2	w
30,411.3	w	30,049.0	w
30,403	w	30,044.4	w
30,397	mw	30,039.4	w

continued ......

APPENDIX III
(continued)

ν cm^{-1} vacuum	Intensity	ν cm^{-1} vacuum	Intensity
30,033.6	w	29,796.5	s
30,027.2	w	29,789.7	s
30,023.6	w	29,765.3	w
30,009.6	vw	29,749.4	
30,005.6	m	29,729.0	w
30,001.5	m	29,716.0	w
29,994.5	m	29,708.4	w
29,986.9	w	29,666.6	w
29,970.9	w	29,656	w
29,967.4	w	29,652	w
29,962.4	w	29,638.2	vw
29,945.7	mw	29,634.2	vw
29,941.7	w	29,625.7	mw
29,936.5	mw	29,618.3	m
29,926		29,607	
29,888.5	vs	29,592.9	w
29,866.7		29,586.9	w
29,854.9		29,578	mw
29,839.9		29,567	w
29,832.2		29,508.0	s
29,808.6	mw	29,477.9	mw

continued ....

APPENDIX III
(continued)

ν cm^{-1} vacuum	Intensity		ν cm^{-1} vacuum	Intensity	
29,472.9	mw		28,865	w	
29,448.9			28,861	w	
29,429.7			28,856.6	m	
29,405.2	ms		28,824	w	
29,391.5	w		28,744.0		
29,388.2	w		28,590.0		
29,385.5	w	CPD8	31,765.6	s	d
29,369.0	mw		31,483	m	
29,362.0	mw		31,409		d
29,337	mw		31,401		d
29,234.8	w		31,395	ms	d
29,204.3	w		31,388	ms	d
21,133 }	m		31,382.5		
29,127			31,281.9	w	
29,069.7			31,120	w	
29,047.7 }	m		31,113.6	mw	
29,043			31,106	m	
28,956.1	w		31,096	m	
28,907.7	w		31,088.3	ms	
28,886	mw		31,082.2	m	
28,873	w		31,076.6	mw	

continued ......

APPENDIX III
(continued)

ν cm^{-1} vacuum	Intensity	ν cm^{-1} vacuum	Intensity
31,071.8	w	30,655.1	w d
31,058	vw	30,652.1	w
30,997.5	w	30,645.0	w
30,994.3	m	30,640.6	w
30,940	ms	30,627.6	mw
30,916	mw	30,622.6	vw
30,886	w	30,619.6	vw
30,816.4	s	30,590.8	mw
30,803	mw	30,553.7	vs
30,799	m	30,531.0	mw
30,781.3	ms	30,518.5	w
30,772.2	m	30,498.2	vw
30,749.1	mw	30,489.6	vw
30,740.1	mw	30,475.6	mw
30,716.1	w	30,471.3	w
30,710.3	w	30,463.2	mw
30,701.1	mw	30,458.7	mw
30,695.2	m	30,449.9	mw
30,688	w	30,430.4	m
30,664.1	w	30,428.7	m
30,660.5	w d	30,426.2	m

continued ......

APPENDIX III
(continued)

ν cm^{-1} vacuum	Intensity	ν cm^{-1} vacuum	Intensity
30,422.9	mw	30,216.1	w
30,418.4	mw	30,183.6	vs
30,411.5	mw	30,173	mw
30,406.4	ms	30,168	mw
30,394.6	vw	30,148	w
30,390.5	vw	30,139.6	w
30,384.8	vw	30,123.0	w
30,381.1	vw	30,118.0	w
30,377.9	mw	30,115.0	
30,375.0	w	30,110.0	w
30,370.5	w	30,097.0	w
30,360	w d	30,081.8	mw
30,353.9	mw	30,077	mw
30,342.5	mw	30,073	mw
30,339.7	w	30,069.5	mw
30,335.2	mw	30,066.9	mw
30,319	w	30,062.0	mw
30,315.5	vw	30,052.6	w
30,306.6	vw	29,999.5	w
30,296.8	m	29,992.5	w
30,271.5	m	29,985.0	mw

continued ......

APPENDIX III
(continued)

ν cm^{-1} vacuum	Intensity	ν cm^{-1} vacuum	Intensity
29,970.5	mw	29,616.3	vw
29,904.5	ms	29,578.8	w
29,887.6	w	29,571.3	w
29,862.3	vw	29,536.4	mw
29,827	vw	29,508	vw
29,818.5	ms	29,478.0	w
29,813.5	w	29,469.5	vw
29,811.5		29,456.2	w
29,806.5		29,447.1	w
29,801.5		29,427.1	mw
29,792.2		29,406	vw
29,790.3		29,336	w
29,786.0		29,168.0	w
29,753		29,034	w
29,746.5		28,867	w
29,728.8		28,863.6	w
29,723		28,849.6	m
29,712.6	m		
29,708.2	m		
29,637	vvw		
29,623	vvw		

BIBLIOGRAPHY

1. M. Born and R. Oppenheimer, Ann. Physik. 84, 457 (1927).
2. A. D. Liehr, Ann. Physics 1, 221 (1957).
3. Albert Messiah, "Quantum Mechanics", Vol. II. Amsterdam, North-Holland Publishing Co., 1962.
4. Michael Tinkham, "Group Theory and Quantum Mechanics". New York, McGraw-Hill Book Co. Inc., 1964.
5. Gerald W. King, "Spectroscopy and Molecular Structure". New York, Holt, Rinehart and Winston, Inc., 1964.
6. Gerhard Herzberg, "Molecular Spectra and Molecular Structure", Vol. I. New Jersey, D. Van Nostrand Co., Inc., 1950.
7. ibid., Vol. III, 1966.
8. NAS-NRC, J. Opt. Soc. Am. 54, 281 (1964).
9. G. Erlandsson, J. Chem. Phys. 22, 563 (1954).
10. J. H. Burkhalter, J. Chem. Phys. 23, 1172 (1955).
11. G. Erlandsson, Arkiv för Fysik, 9, 399 (1955).
12. P. G. Kökeritz and H. Selén, ibid., 16, 197 (1959).
13. F. S. Taboury and E. Gray, Compt. Rend. 234, 2181 (1952).
14. W. Suetaka, Gazz. Chim. Ital., 82, 768 (1952).
15. A. W. Reitz, Z. Physik. Chem., 35, 363 (1937); ibid., 38, 381 (1937-38).
16. A. Streitwieser, Jr., R. H. Jagow, R. C. Fahey and S. Suzuki, J. Amer. Chem. Soc. 80, 2326 (1958).

17. C. L. Angell, P. J. Krueger, R. Lauzon, L. C. Leitch, K. Noack, R. J. D. Smith and R. N. Jones, Spectrochimica Acta 15, 926 (1959).

18. J. E. Katon and F. F. Bentley, ibid., 19, 639-653 (1963).

19. M. Rey-Lafon and M. T. Forel, Bull. Soc. Chim. Fr., 4, 1145 (1967).

20. A. W. Baker, J. Phys. Chem. 60, 1660 (1956).

21. D. Biquard, Bull. Soc. Chim. Fr., 8, 55 (1941).

22. C. Castinel, G. Chiurdoglu, M.-L. Josien, J. Lascombe and E. Vanlanduyt, ibid., 807 (1958).

23. C. Cherrier, Compt. rend. 225, 930 (1947).

24. E. Gray and M. M. Bottreau, ibid., 240, 2134 (1955).

25. E. J. Hartwell, R. E. Richards and H. W. Thompson, J. Chem. Soc. (1948) 1436.

26. R. Srinivasan in "Advances in Photochemistry", Vol. I, edited by W. A. Noyes, Jr., G. S. Hammond and J. N. Pitts, Interscience, 1963, pp. 83-114.

27. P. F. Dunion, Diss. Abstr. B27, 775 (1966).

28. R. F. Klemm, D. N. Morrison, P. Gilderson and A. T. Blades. Can. J. Chem., 43, 1934 (1965).

29. E. K. C. Lee, J. Phys. Chem., 71, 2804 (1967).

30. F. A. L. Anet, Can. J. Chem. 39, 2317 (1961); J. Amer. Chem. Soc. 82 4071; ibid. 83, 1226 (1961).

31. H. Primas, K. Frei, and H. H. Günthard, Helv. Chim. Acta 41, 35 (1958); 44, 865 (1961).

32. J. B. Stothers and P. C. Lauterbur, Can. J. Chem., 42, 1563 (1964); J. Phys. Chem., 69, 3105 (1965); J. Org. Chem., 32, 353 (1967).

33. B. N. Figgis, R. G. Kidd and R. S. Nyholm, Proc. Roy. Soc. 62A, 269, 469.

34. S. R. LaPaglia and B. C. Roquitte. J. Phys. Chem. 66, 1739 (1962); Can. J. Chem., 41, 287 (1963).

35. A. Udvarhazi and M. A. El-Sayed, J. Chem. Phys. 42, 3335 (1965).

36. H. Prugger and F. Dorr, Z. Electrochem. 64, 425 (1960).

37. M. Lestrade and P. Thouvenin, Compt. rend., 234, 2183 (1952).

38. I. A. Rao, N. V. R. A. Rao and V. R. Rao, J. Sci. Industr. Res., 16B, 388 (1957).

39. C. J. Brown, Acta Cryst. 7, 92 (1954).

40. C. L. Angell, Trans. Faraday Soc. 52, 1178 (1956).

41. F. A. Miller and R. G. Inskeep, J. Chem. Phys. 18, 1519 (1950).

42. F. H. Kruse and D. W. Scott, J. Mol. Sp. 20, 276 (1966).

43. J. E. Kilpatrick, K. S. Pitzer and R. Spitzer, J. Amer. Chem. Soc., 69, 2483 (1947).

44. K. S. Pitzer and W. E. Donath, J. Amer. Chem. Soc., 81, 3213 (1959).

45. A. Almenningen, O. Bastiansen, and P. N. Skancke, Acta Chem. Scand. 15, 711 (1961).

46. H. Tschamler and H. Voetter, Monatsch. 83, 302 (1952).

47. J. H. Hand and R. H. Schwendeman, J. Chem. Phys. 45, 3349 (1966).

48. K. L. Dorris, J. E. Boggs, A. Danti and L. L. Altpeter, Jr., J. Chem. Phys. 46, 1191 (1967).

49. K. L. Dorris, C. O. Britt and J. E. Boggs, ibid., 44, 1352 (1966).

50. J. Laane and R. C. Lord, J. Chem. Phys. 47, 4941 (1967).

51. T. Ueda and T. Shimanouchi, ibid., 47, 5018 (1967).

52. K. Frei and H. H. Günthard, J. Mol. Sp. 5, 218 (1960).
53. D. C. Moule, private communication.
54. F. Albert Cotton, "Chemical Applications of Group Theory", New York, Interscience, 1963.
55. Gerhard Herzberg, "Molecular Spectra and Molecular Structure", Vol. II. New Jersey, D. Van Nostrand Co. Inc., 1945.
56. E. B. Wilson, Jr., J. C. Decius and P. C. Cross, "Molecular Vibrations". New York, McGraw-Hill Book Co. Inc., 1955.
57. R. T. Birge and H. Sponer, Phys. Rev. 28, 259 (1926).
58. H. J. Bernstein, Spectrochimica Acta 18, 161 (1962).
59. H. C. Longuet-Higgins, Mol. Phys., 6, 445 (1963).
60. J. K. G. Watson, Can. J. Phys., 43, 1996 (1965).
61. J. T. Hougen, ibid., 42 1920 (1964); ibid. 43 935 (1965).
62. B. J. Dalton, Mol. Phys. 11, 265 (1966).
63. S. L. Altmann, Proc. Roy Soc. (London) A298, 184 (1967).
64. S. L. Altmann, Rev. Mod. Phys. 35, 641 (1963).
65. S. L. Altmann, Phil. Trans. Roy. Soc. (London) A255, 216 (1963).
66. T. Ueda and T. Shimanouchi, J. Chem. Phys. 47, 4042 (1967).
67. J. R. Drurig and R. C. Lord, ibid. 45, 61 (1966).
68. J. Laane and R. C. Lord, ibid. 48, 1508 (1968).
69. D. Boone, C. Britt and J. Boggs, ibid. 43, 1190 (1965).
70. M. Kasha, Disc. Faraday Soc., 9, 14 (1950).
71. G. W. Robinson, in L. Marton: "Methods of Experimental Physics", Vol. III, section 2.4.5, Academic Press, New York, 1962.
72. S. L. Altmann, private communication.
73. J. M. Foster and S. F. Boys, Rev. Mod. Phys. 32, 303 (1960).

74. E. U. Condon, Phys. Rev. 32, 858 (1928).

75. J. C. D. Brand, J. Chem. Soc., 858 (1956).

76. R. M. Badger, J. Chem. Phys. 2, 128 (1934); ibid., 3, 710 (1935).

77. C. H. Douglas-Clark, Phys. Rev. 47, 238 (1938); Trans. Faraday Soc. 31, 1017 (1935).

78. E. M. Layton, R. D. Kross and V. A. Fassel, J. Chem. Phys. 25, 135 (1956).

79. S. W. Benson and G. B. Kistiakowsky, J. Amer. Chem. Soc. 64, 80 (1942).

80. A. Gero, J. Org. Chem., 26, 3156 (1961).

81. J. U. White, J. Opt. Soc. Am., 32, 285 (1942).

82. D. C. Moule, Ph.D. Thesis, McMaster University (1962).

83. Gerald W. King, J. Sci. Instr. 35, 11 (1958).

84. H. Bernstein and G. Herzberg, J. Chem. Phys. 16, 30 (1948).

85. G. R. Harrison, ed., "M. I. T. Wavelength Tables", Cambridge, Massachusetts, The M. I. T. Press, 1963.

86. B. Edlén, J. Opt. Soc. Amer. 43, 339 (1953).

87. N. R. C. Tables, donated by N.R.C., Ottawa, Ontario.

88. W. T. King and B. Crawford, Jr., J. Mol. Spectroscopy, 5, 421 (1960).

89. G. Herzberg, op. cit., Vol. II, p. 93.

90. N. B. Colthup, L. H. Daly and S. E. Wiberley, "Introduction to Infrared and Raman Spectroscopy", New York, Academic Press, 1964.

91. J. J. Fox and A. E. Martin, Proc. Roy. Soc. (London) A167, 257 (1938).

92. S. E. Wiberley, S. C. Bunce and W. H. Bauer, Anal. Chem., 32, 217 (1960).

93. S. A. Francis, J. Chem. Phys., 19, 942 (1951).

94. J. D. Roberts and V. C. Chambers, J. Amer. Chem. Soc., 73, 5030 (1951).

95. H. D. Noether, J. Chem. Phys., 11, 97 (1943).

96. N. Sheppard and G. B. B. M. Sutherland, Nature 159, 739 (1947).

97. G. B. B. M. Sutherland and A. Vallance Jones, ibid., 160, 567 (1948).

98. R. Mecke, R. Mecke and A. Lüttringhaus, Chem. Ber. 90, 975 (1957).

99. L. Piaux, C. R. Acad. Sci., Paris, 197, 1647 (1933).

100. P. Yates and L. L. Williams, J. Amer. Chem. Soc. 80, 5896 (1958).

100a. H. P. Figeys, Spectrochimica Acta 23A, 1281 (1967).

101b. G.J.Boobyer and A.P. Cox, J. Chem., Ed. 45, 18 (1968).

102. Linus Pauling, "The Nature of the Chemical Bond", Ithaca, Cornell University Press, 1945., p. 131.

103. J. A. Pople and J. W. Sidman, J. Chem. Phys. 27, 1270 (1951).

104. C. N. R. Rao, "Ultraviolet and Visible Spectroscopy", London, Butterworth and Co. Ltd., 1961, pp. 17,19.

105. E. M. Kosower and G. S. Wu, J. Amer. Chem. Soc. 83, 3142 (1961).

106. Gerhard Herzberg, op. cit. Vol. III, p. 139.

107. G. W. King and D. C. Moule, J. Mol. Spectroscopy, 20, 331-340 (1966).

108. K. K. Innes and L. E. Giddings, Jr., J. Mol. Spectroscopy 7, 435 (1961).

109. E. J. Bowen in "Advances in Photochemistry", Vol. I, ed. by W. A. Noyes, Jr., G. S. Hammond, and J. N. Pitts. Interscience, 1963, pp. 23-42.

110. J. C. D. Brand and J. K. G. Watson, quoted in J. H. Callomon and K. K. Innes, J. Mol. Spectroscopy, 10, 166 (1963).

111. J. C. D. Brand and D. G. Williamson, Disc. Faraday Soc., 35, 184 (1963).

112. K. K. Innes and L. E. Giddings, Jr., J. Mol. Spectroscopy 6, 528 (1961).

113. Gerald W. King, "Spectroscopy and Molecular Structure", op. cit., p.426.

114. G. W. Robinson and V. E. DiGiorgio, Can. J. Chem. 36, 31 (1958).

115. S. E. Hodges, J. R. Henderson and J. B. Coon, Air Force OSR, Technical Note, Document No. TR-59-206, December, 1959, p. 21.

116. J. C. D. Brand, J. H. Callomon, D. C. Moule, J. Tyrrel and T. H. Goodwin. Trans. Faraday Soc. 61, 2365 (1965).

117. (a) W. J. Balfour and G. W. King, J. Mol. Spectroscopy, 25, 131, (1968); (b) ibid., 26, 384 (1968).

118. V. A. Job and G. W. King, J. Mol. Spectroscopy, 19, 155 (1966).

119. J. B. Coon, N. W. Naugle and R. D. McKenzie, J. Mol. Spectroscopy 20, 107 (1966).

120. J. B. Coon, N. W. Naugle and R. D. McKenzie, Report Air Force OSR (contract AF49(638)-593), 1963, p. 27.

121. A. Almenningen, O. Bastiansen and P. N. Skancke, Acta Chem. Scand. 15, 711 (1961).

122. "Tables of Interatomic Distances", London, The Chemical Society, 1958.

123. J. F. Chiang and S. H. Bauer, J. Amer. Chem. Soc. 88, 420 (1966).

124. C. C. Costain and B. P. Stoicheff, J. Chem. Phys. 30, 777 (1959).

125. C. Romers, Rec. Trav. Chim., 75, 956, 331.

126. P. H. Friedlander and J. M. Robertson, J. Chem. Soc. 3083,(1956).

127. P. W. Allen, H. S. M. Bauer, L. E. Sutton and O. Bastiansen, Trans. Faraday Soc., 48, 991 (1952).

128. J. E. Parkin, J. Mol. Spectroscopy 15, 483 (1965).

129. W. J. Balfour, Ph.D. Thesis, McMaster University, 1967.

DISCUSSION AT THESIS DEFENCE

I'm going to take Dr. Preston at his word and not summarize the thesis, but rather try to show how this work fits into the general picture of things.

According to G. Wilse Robinson, in the book "Light and Life", the electronic structure of a large molecule is a superposition of the electronic structures of the small entities of which the large molecule is made up. Cyclopentanone is a small entity of certain members of a very important group of molecules, known as the steroids, which have the structure

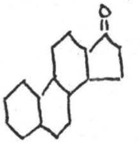

Other members of this group are certain sex hormones; for example, oestrone, which is derived from this general steroid structure. Biologically these

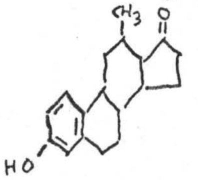

molecules are of great significance. This is one of the reasons why research into the structure of cyclopentanone is important. The chemical physicist may be likened to a brickmaker, producing bricks -- 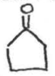 -- which the biochemist or biophysicist will build into houses.

But why are excited states important? The nature of bonding in molecules is getting to be pretty well understood in terms of present day models and in my opinion the next breakthrough in chemistry will come in the study of reaction mechanisms. There is evidence that, when chemical reactions take place, at some stage the reacting molecules assume the same configuration as they have in certain electronically excited states. Take acetylene. Acetylene was the first molecule for which a gross change in geometry upon electronic excitation was thoroughly established. In its ground electronic state it is linear H—C ≡ C— . In its lowest excited state it is trans bent 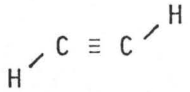 $\mathrm{{}^{}\!\!\diagup C \equiv C \diagup^{H}}$ and in another excited state it is cis bent 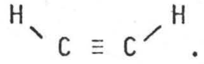 $\mathrm{{}^{H}\diagdown C \equiv C \diagup^{H}}$. In a <u>polymerization</u> reaction of acetylene, in which transition metals are used as catalysts, an intermediate has been isolated in which acetylene is bonded to the metal and has its cis configuration:

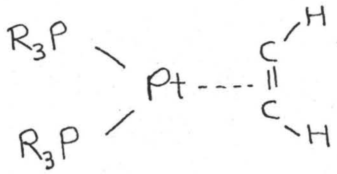

The reaction goes on to produce

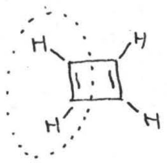

and

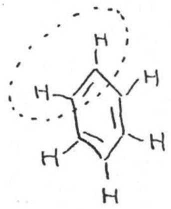

You can see that these molecules may be regarded as being composed of cis bent acetylene units. Knowledge of the excited state structures of other small molecules is therefore likely to be important in predicting how other reactions will go and what products will be formed. It is possible, in the same way, that knowledge of the excited state structure of cyclopentanone may be useful in studies of biologically important reactions.

We found that in the excited state of cyclopentanone the oxygen of the carbonyl group is bent out of the plane of the three adjacent carbon atoms by ~35°. The configuration at the carbonyl carbon atom is midway between planar and tetrahedral. As the configuration approaches tetrahedral it is likely that the carbon atom becomes an attack centre for the formation of a new bond.

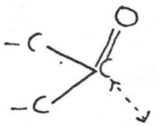

The work proved extremely interesting because apart from the conventional spectroscopy we had the problem of the isodynamic configurations of the moleucle. The transition from the ground state to the excited is complicated by the fact that there are four equivalent configurations in the excited state and two in the ground state, with a very small barrier between them. Group theory has been extended to cover cyclopentanone as a non-rigid molecule. The barrier between two of the excited state forms was found to be 703 cm^{-1}.

The study of excited states is a subject which has interested me for some time. What would be really exciting to do would be to study the properties of the molecule in its excited state directly. That is, if we could excite sufficient cyclopentanone molecules to the $'A_2$ state we might be able to observe the interconversion of the isodynamic configurations in the excited state directly (in a microwave experiment).

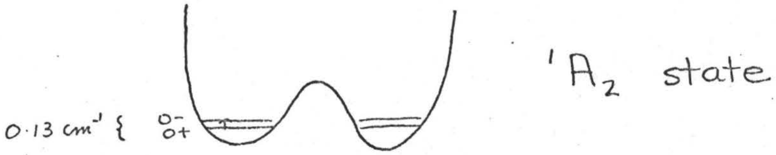

So far no satisfactory technique has been developed to do studies of this nature.

Certainly, further work is suggested by this research. A detailed microwave study of the ground state with three or four isotopic species should be made in order to determine the molecular parameters and the dihedral angle unambiguously. An electron diffraction study should be able to give the ground state parameters. Low temperature nmr work might help elucidate the equilibrium conformation by isolating one isodynamic configuration.

During the exploratory part of this research I looked at the UV spectra of a lot of molecules and I am suggesting that a very interesting molecule to study next would be 9-fluorenone:

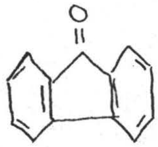

(a) It contains a cyclopentanone unit which we now know something about; and two benzene rings which a lot is known about spectroscopically. We can see whether the electronic spectrum of the whole is related to the sum of the parts.

(b) We can test two other effects: (1) how does increasing the conjugation affect the absorption spectrum? and (2) how does making the molecule more rigid affect the sharpness of the spectrum?

(c) We can possibly say more about the ring of cyclopentanone by a process of elimination since we can predict the ring will be held planar in 9-fluorenone. Study of the vapour phase at normal temperatures will require enormously long path lengths because of the low vapour pressure of 9-fluorenone. However, the spectrum taken in 10 cm heated cell on the Cary appeared to show discrete vibrational structure.

Some of the questions raised:

Dr. King: "Why can't you construct a group which covers all the different possible equilibrium configurations in the excited state - the boat, chair and skew?"

"Why don't you get any evidence of the barrier to ring puckering - and in what region would you expect to observe such an effect?"

Dr. Stager: "Going back to this problem of the Hamiltonians being different, why can't you construct one Hamiltonian for the molecule which will cover all possible states?"

"Are you suggesting that the spectrum of 9-fluorenone will consist of the spectrum of benzene plus the spectrum of cyclopentanone?"

Dr. Brown: (p. 11) " How did you obtain this geometry and what parameters did you vary? Presumably with three known moments of inertia you could vary three parameters."

"How do you know 9-fluorenone will be planar?"

Dr. Summers-Gill: (p. 62) "Is it fair to say the quantum number K is still defined for small asymmetry?"

(p. 68) "How does a grating polarize light?"

(p. 196) Plate 2. "The microdensitomer trace does not seem to represent the CPH8 spectrum."

Dr. Datars: "Can you explain what you mean by a hot band?"

"In what phase are you suggesting doing nmr work?"

Dr. McKandliss: Figure 5.9, p. 117. "Did you use a linear extrapolation or did you compute the dissociation energy from the points?"

"You don't seem to have put any limits to error on your Raman frequencies."